MED9, A MEDIATOR COMPLEX COMPONENT, AND ITS INTERACTING PROTEIN MORC1 BALANCE GROWTH AND DEFENSE IN ARABIDOPSIS

by

Ji Chul Nam, M.S.

A dissertation submitted to the Graduate Council of
Texas State University in partial fulfillment
of the requirements for the degree of
Doctor of Philosophy
with a Major in Aquatic Resources and Integrative Biology
December 2020

Committee Members:

Hong-Gu Kang, Chair

Nihal Dharmasiri

Sunethra Dharmasiri

Walter Gassmann

Keiko Yoshioka

FAIR USE AND AUTHOR'S PERMISSION STATEMENT

Fair Use

Duplication Permission

ACKNOWLEDGEMENTS

I would like to offer my sincerest praise and thanks to Dr. Hong Gu Kang for his excellent guidance with continued support and encouragement. Since I have joined the Dr. Kang's lab, I have learned from writing the lab note, designing the experiments, and interpreting the data to become a better researcher. I would like to thank committee members Dr. Nihal Dharmasiri, Dr. Sunethra Dharmasiri, Dr. Walter Gassmann, and Dr. Keiko Yoshioka for their patience, valuable time, and feedback on my research. I would also like to thank Dr. Sung Il Kim, Dinesh Pujara, Padam Bhatt, Jose Mayorga, Oluwadamilare Afolabi, Euna Kim and Dr. Yogendra Bordiya for their help during my experiments. I would like to thank Trina Guerra for help to sequence my RASL, and Angela Kang for checking/editing grammar. Also, I do appreciate to Ha Yang Kim, Claire Nam, and Emma Nam for supporting me of intense research.

TABLE OF CONTENTS

Page

LIST OF TABLES

Table **Page**

LIST OF FIGURES

Figure **Page**

LIST OF ABBREVIATIONS

Abbreviation	Description
AH109	A yeast strain of mating type a (MATa)
AT	3-Amino-1,2,4-triazole, a chemical that acts as a competitive inhibitor of the product of the HIS3 gene.
ATP	Adenosine triphosphate, a high energy source for cells
AvrPst	Avirulent *Pseudomonas syringae* pv. tomato
CFU/ml	Colony forming units per milliliter
Co-IP	Co-immunoprecipitation, a molecular technique to identify protein-protein interactions *in vitro*
Col-0	Columbia ecotype of Arabidopsis thaliana
CRT1	Compromised Recognition to TCV-CP 1
DNA	Deoxyribonucleic acid, the double helix containing anti-parallel strands of hereditary information constructed of nucleotides and a sugar-phosphate backbone
Dpi	Days post infection
EDS	Enhanced Disease Susceptibility
ETI	Effector-triggered immunity, a robust immune response in plants that leads to HR
ETS	Effector Triggered Susceptibility
FLAG-tag	A protein tag with the sequence motif DYKDDDDK

FLS2	FLAGELLIN-SENSITIVE 2, a leucine-rich repeat transmembrane receptor kinase, one of many pattern-recognition-receptors (PRRs) responsible for the detection of bacterial flagellin (flg22)
Gal4 AD or BD	A transcription factor gene that produces either an activating domain or a binding domain protein required for the transcription of a reporter gene in a yeast two-hybrid screening
GAs	Gibberellins
GFP	Green fluorescent protein, which emits green fluorescence when illuminated with light in the blue to ultraviolet range
GO	Gene Ontology
GV2260	A strain of *Agrobacterium tumefaciens*
HA	A protein tag with the sequence motif YPYDVPDYA
His	The amino acid histidine
HIS3	A yeast two-hybrid reporter gene encoding imidazoleglycerol-phosphate dehydratase, the product of which encodes an enzyme required for the synthesis of histidine
HR	Hypersensitive response, a plant immune response initiated as a result of ETI to induce programmed cell death around the infection site
HRT	Hypersensitive Response to TCV
kDa	Kilodalton, an atomic mass unit used here to describe the molecular weight of proteins

L40	A yeast strain of the mating type a (MATa)
LexA BD or AD	A transcription factor gene that produces either an activating domain or a binding domain protein required for the transcription of a reporter gene in a yeast two=hybrid screening
luxCDABE	A luminescent reporter gene cloned into the bacteria, *Pseudomonas syringae* pv. *tomato DC3000*
MAP	Mitogen-Activated Protein
MED	Mediator
MIP	MORC1-interacting protein
MORC1	MICROCHIDIA 1, also known as COMPROMISED RECOGNITION OF TURNIP CRINKLE VIRUS 1 (CRT1), required for optimum levels of plant immunity
mRNA	Messenger RNA, the product of gene transcription and the template for protein synthesis
Myc-tag	A protein tag with the sequence motif EQKLISEEDL
PAMP	Pathogen-associated molecular pattern
pB27	Bait plasmid for yeast two-hybrid screenings
PCR	Polymerase chain reaction
PIF	Phytochrome-interacting factors
pP6	Prey plasmid for yeast two hybrid screenings
PR	Pathogenesis Related

PRR	Pattern recognition receptor
Pst	*Pseudomonas syringae* pv. *tomato DC3000*
PTI	PAMP-triggered immunity
qRT PCR	Quantitative reverse transcription-polmerase chain reaction
R-proteins	Resistance proteins, which detect the presence of effector molecules emitted by pathogens
RdDM	RNA-directed DNA methylation
RNA	Ribonucleic acid, single stranded product of DNA transcription
RPM1	RESISTANCE TO PSEUDOMONAS SYRINGAE PV MACULICOLA 1, R-protein
SAIL	Syngenta Arabidopsis Insertion Library, a naming system for mutant seeds produced
SALK	A seed-naming system for seeds produced at the Salk Institute
SDS-PAGE	Sodium dodecyl sulfate-polyacrylamide gel electrophoresis, a method for separating proteins by size
SMC1	Structural maintenance of chromosomes1. Cohesin complex that is essential for viability and sister chromatid alignment.
T-DNA	Transfer DNA, transferred from bacteria to a host with the purpose of rendering a host protein nonfunctional
TAIR	The Arabidopsis Information Resource, a database of genetic and molecular biology data for *Arabidopsis thaliana*

Tip41	Tap42-interacting protein of 41 kDa, a housekeeping gene
UTR	Untranslated region of DNA
WRKY	A transcription factor that regulates transcriptional reprogramming in response to plant stress responses
WT	Wild-type ecotype, in this sense it refers to Col-0
VirPst	Virulent *Pseudomonas syringae* pv. tomato
Y187	A yeast strain of the mating type α (MATα)
Y2H	Yeast two-hybrid, a technique used to identify protein-protein interactions *in vivo*

ABSTRACT

Arabidopsis MORC1 (*Microrchidia*) is required for multiple levels of immunity, including effector-triggered immunity and basal resistance. MORC1 is also a topoisomerase that tightens chromatin/DNA supercoiling. I identified 14 MORC1-interacting proteins (MIPs) *via* yeast 2-hybrid screening, eight of which have putative nuclear-associated functions. While a few loss-of-function mutants for these *MIPs* displayed altered bacterial resistance in Arabidopsis, MIP13 was highly unusual. MIP13's single mutant was susceptible to *Pseudomonas syringae*, but when combined with *morc1/2* in which MORC1 and its closest homolog were knocked-out, it regained wild-type level resistance; note that *morc1/2* is also susceptible to the same pathogen. *MIP13* encodes MED9, a mediator complex component that interfaces with RNA polymerase II and transcriptional factors to reprogram transcriptional activities. Transcription dynamics assessments at multiple-time points of defense genes, up- and down-regulated, reacting to avirulent *P. syringae* revealed that *med9 morc1/2* expressed some defense genes in a slow but sustained manner, unlike its low-ordered mutants. This expression pattern may explain the restored resistance but raised concerns that the absence of MORC1/2 and MED9 might incur fitness costs from the prolonged defense responses. Indeed, repeated challenges with avirulent *P. syringae* triggered significant growth and reproduction decline in *med9 morc1/2*, suggesting that an optimum growth-defense balance requires MED9 and its interacting partner MORC1. Interestingly, down-regulated defense genes were substantially associated with photosynthesis, and

many of them had the canonical G-box in their promoter, linking photosynthesis to defense responses. PIF3, as a G-box-binding factor and a known negative photosynthetic regulator, was positioned to be a strong candidate for negatively regulating photosynthesis. Overexpression of PIF3, consistent with the prospect, led to enhanced resistance to *avirulent P. syringae,* perhaps by channeling energy from growth to defense responses. Moreover, nuclear PIF3 was significantly increased under ETI, suggesting its suppressive function in photosynthesis aiding defense responses. In summary, my thesis research i) established MORC1, MED9, and PIF3 as important regulators in balancing growth and defense, and ii) laid an insightful mechanical groundwork to achieve optimum resistance for maximum yield in plants.

1. INTRODUCTION: BALANCE BETWEEN IMMUNITY AND GROWTH

1.1 *Plant Immunity*

Plants have evolved an innate immune system against a wide range of pathogens (Chisholm et al., 2006, Jones & Dangl, 2006). Its simplified schematic representation is presented in Figure 1. The first line of defense starts with the perception of pathogen-associated molecular patterns (PAMPs), including flagellin (Zipfel & Felix, 2005, Jones & Dangl, 2006), to induce PAMP-triggered immunity (PTI). For instance, flagellin, a mobility component required for some pathogens, is directly recognized by the transmembrane leucine-rich repeat (LRR)-receptor kinase FLS2 (Zipfel & Felix, 2005). This recognition leads to the activation of PTI accompanied by activation of MAP (mitogen-activated protein) kinase cascades, the production of reactive oxygen species (ROS), nitric oxides, callose deposition, and the opening of ion channels (Jones & Dangl, 2006, Asai et al., 2002, Ausubel, 2005). Pathogens counter plant immune responses, including PTI, by delivering effector proteins to host plants to promote disease development; these phenomena are collectively known as effector-triggered susceptibility (ETS). For instance, *Pseudomonas syringae* pv. *tomato* (*Pst*) delivers approximately 28 effectors through the type III secretion system (TTSS) into host plants to induce PAMP-triggered immunity (PTI) (Chisholm et al., 2006, Jones & Dangl, 2006, Zipfel & Felix, 2005, Lindeberg et al., 2012). When unable to fight these effectors, susceptible plants display mostly basal resistance. As a counter to ETS, plant resistance (R) proteins directly or indirectly recognize the effectors to trigger one of the most potent defense responses, known as effector-triggered immunity (ETI). This robust defense response frequently involves a form of programmed cell death known as the hypersensitive

response (HR), a rapid calcium flux, an extracellular oxidative burst, and a massive transcriptional reprogramming within the infection sites (Hammond-Kosack & Jones, 1996). Many R proteins feature nucleotide-binding sites (NB) and a series of leucine-rich repeats (LRR) domains and, thus, are also known as NB-LRR proteins(Chisholm et al., 2006, Jones & Dangl, 2006, Hammond-Kosack & Jones, 1996, da Cunha et al., 2006). Interestingly, while ETI is known to be much stronger than PTI, the difference is mostly quantitative rather than qualitative (Tao et al., 2003, Tsuda et al., 2009), involving largely the same set of defense genes. This surprising observation suggests that an R protein, upon recognizing a corresponding effector, function to amplify the defense signaling common to ETI and PTI.

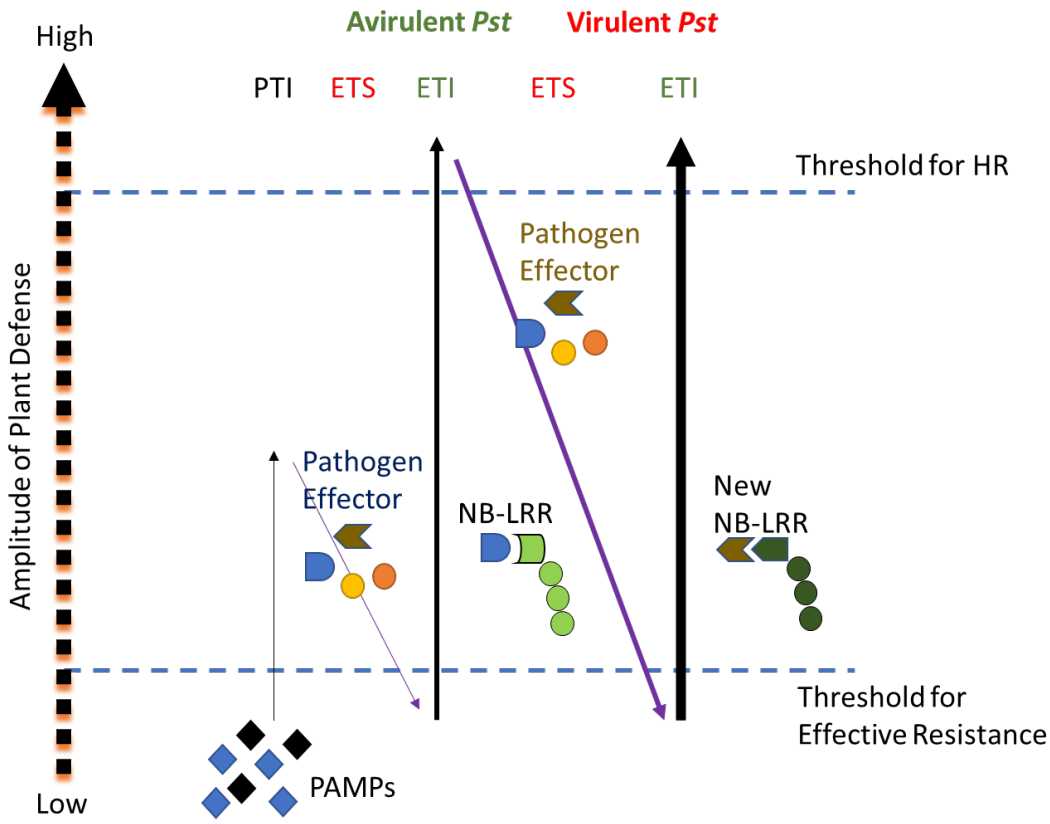

Figure 1. The zigzag model in plant immunity. The model describes multiple layers of innate immunity in plants and captures a sequential development process of immunity. The recognition of the pathogen-associated molecular patterns (PAMPs) initiates PTI (PAMP triggered immunity). This basal immunity is countered by pathogens via effectors, resulting in effector-triggered susceptibility (ETS). Pathogen-encoded effectors, when recognized by NB-LRR proteins, activate effector-triggered immunity (ETI).

1.2 *MORC1 is an epigenetic factor that functions in plant immunity*

Most ecotypes of *Arabidopsis thaliana* are susceptible to *Turnip crinkle virus* (TCV) except for Di-17 (Dempsey et al., 1997). The Di-17 ecotype develops HR in response to infection by TCV via an NB-LRR protein, termed HRT (Hypersensitive Response to TCV). CRT1 (Compromised Recognition to TCV-CP 1) was identified by a genetic screen for mutants that fail to develop HR against the coat protein of TCV (Kang et al., 2008). CRT1 was recently renamed as MORC1 since it was later found to resemble microchidia (MORC) proteins in animals (Kang et al., 2010, Moissiard et al., 2012a). MORC1 and its homolog, MORC6, were identified in two independent screens for mutants defective for gene silencing (Lorkovic et al., 2012, Moissiard et al., 2012a). The de-repression of silenced reporter genes and TEs (transposable elements) in *morc1* and *morc6* mutants suggests that these proteins are required for epigenetic gene silencing (Moissiard et al., 2012a, Lorkovic et al., 2012, Brabbs et al., 2013).

In addition to viral resistance to TCV, MORC1 and its closest homolog, MORC2, were shown to be required for PTI, ETI, basal resistance, non-host resistance, and systemic acquired resistance (Kang et al., 2008, Kang et al., 2010, Kang et al., 2012). MORC1 is one of the very few proteins known to date that physically associates with a large number of immune components, including at least twelve R proteins and the PAMP recognition receptor FLS2. Interestingly, a sub-cellular study revealed that MORC1 increases in the nucleus upon the activation of PTI and ETI, suggesting that the nuclear function of MORC1 may be important in defense responses (Kang et al., 2012).

MORC1 is also a chromatin remodeling factor. MORC1 contains the GHKL ATPase domain and the CW histone recognition domain (Iyer et al., 2008, Hoppmann et

al., 2011), which are found in topoisomerases and histone methyltransferases, respectively. MORC1 binds nucleic acids and exhibits Mn^{2+}-dependent endonuclease and ATPase activity (Kang et al., 2008, Kang et al., 2012). A recent report found that MORC1 regulates the compaction of chromatin and directly compacts DNA (Kim et al., 2019b), in line with the notion that it is essential in heterochromatin maintenance. In addition, this topology-associated function explains why MORC1 is required to suppress hypermethylated genes and TEs (Moissiard et al., 2012b) and to modulate physical accessibility to TEs near many defense-related genes (Bordiya et al., 2016a). When and how this physical topology becomes important in defense genes, however, is currently unknown (Kim et al., 2019b).

1.3 *The mediator complex*

The mediator complex is a large and multi-subunit RNA polymerase II-associated transcriptional regulator. This complex, first identified in *Saccharomyces cerevisiae*, coordinates recruitment of RNA polymerase II, phosphorylation of the C-terminal domain of RNA polymerase II, enhancer-loop formation, and a post-transcription initiation event (Buendía-Monreal & Gillmor, 2016, Conaway & Conaway, 2011, Kelleher et al., 1990, Samanta & Thakur, 2015a). It also has a role as a docking site for a wide range of nuclear machineries, such as cohesion proteins and chromatin-modifying factors (An & Mou, 2013b). The mediator complex in yeast has 25 subunits. The counterparts in mammals and plants have 31 and 34 subunits (Figure 2), respectively, although it is possible that additional subunits conditionally associate with the complex (Buendía-Monreal & Gillmor, 2016, Samanta & Thakur, 2015b, Allen & Taatjes, 2015b). Structural studies of the mediator complex have shown four distinct modules: head,

middle, tail, and cyclin-dependent kinase. The head module is responsible for initial interactions with RNA polymerase II, and contains a multipartite TBP (TATA-box binding protein)-binding site that can be modulated by transcriptional activators (Larivière et al., 2006, Borggrefe & Yue, 2011). The middle module, important in maintaining the structural integrity of the whole complex, conveys the transcription signal from the head to the tail. The tail module interacts with the gene-specific and *cis*-element bound transcription factors (Samanta & Thakur, 2015c, Buendía-Monreal & Gillmor, 2016, Yang et al., 2015). The role of the cyclin-dependent kinase module remains poorly known, although it was shown to be involved in repressing transcription (Yang et al., 2015). In Arabidopsis, the mediator complex has been shown to be involved in the development of embryonic, flower, and root cells, and the modulation of biotic and abiotic stresses. Due to the lack of specialized immune cells, plant cells mostly recognize pathogens autonomously (Spoel & Dong, 2012) and activate defense responses via massive reprogramming of transcription activities (Maleck et al., 2000). During the reprogramming process, the mediator complex has been proposed to play an essential role in coordinating transcription factors and RNA polymerase II (An & Mou, 2013a, Yang et al., 2015).

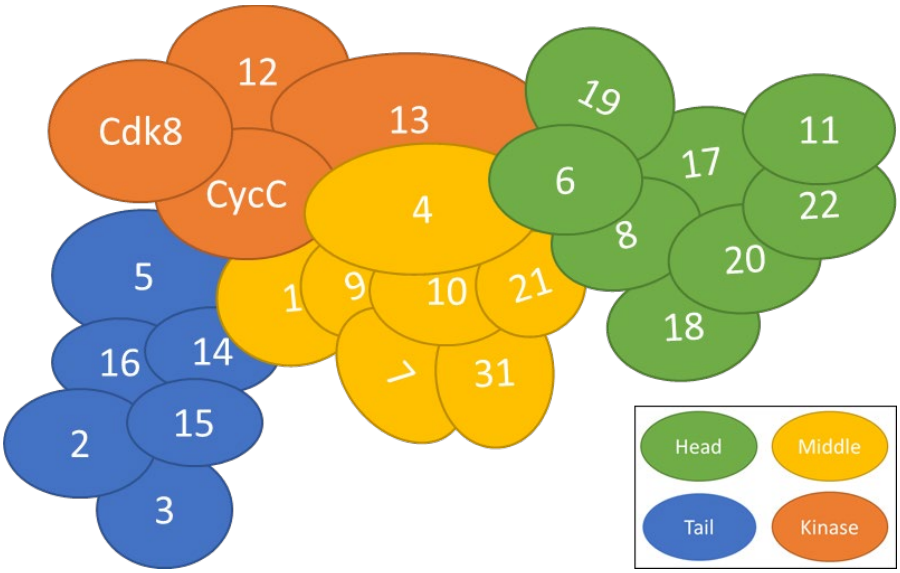

Figure 2. The composition of plant-specific Mediator subunits. Subunits located in the head, middle, tail, and CDK modules were highlighted in green, yellow, blue, and orange, respectively.

Extensive evidence has demonstrated that the mediator complex is important in plant resistance to a wide array of pathogens, although it is difficult to synthesize what has been reported to shed light on how these complex components contribute to resistance. In general, genetic mutants displaying compromised resistance and/or changes in associated marker genes appear to be a recurrent way to establish the defense role of the mediator complex. Following are some of the observations related to mediator components functioning in resistance: Disruption of the mediator complex subunits MED5a (also known as REF4) and MED5b (also known as RFR1) activated phenylpropanoid pathways led to the hyperaccumulation of many phenylpropanoids and stunted growth (Bonawitz et al., 2014). The level of many UV absorbing compounds, such as phenyalanine, was increased in *med5a med5b* plants relative to wild type (WT) plants in high-performance liquid chromatography analysis (Bonawitz et al., 2014). MED8 functions in JA and SA-dependent defense responses. For example, the *med8* mutants display increased resistance against *Fusarium oxysporum*, but are more susceptible to *Alternaria brassicicola* and *Pst*. (Kidd et al., 2009, Zhang et al., 2012). A mutation in *MED14*, known as *rgr1*, blocks *PR1* gene expression induced by NAD^+ and suppresses defense responses induced by SA (Zhang et al., 2013). Mutation of *AtMED14* showed higher susceptibility to avirulent *Pst* (Zhang et al., 2013). The *med15* (*nrb4*) mutants showed compromised SA-induced resistance (Canet et al., 2012). MED16 has been shown to be a key component of basal resistance against a necrotrophic fungal pathogen, *Sclerotinia sclerotiorum* (Wang et al., 2015). The *med18* mutant showed enhanced susceptibility to necrotrophic fungi *Alternaria brassicicola* and *Botrytis cinerea* (Zhang et al., 2012). The Arabidopsis *PEPTIDE TRANSPORTER3* (*PTR3*) gene is

implicated in plant defense against wounding and infection by necrotrophic bacterial pathogens (Karim et al., 2007) and its expression was significantly reduced while the *PDF1.2* gene was elevated in the *med18* mutant when infected with *Botrytis cinerea* relative to WT, suggesting that MED18 is involved in the regulation of JA/ET signaling (Fallath et al., 2017). HaRxL44, from the Arabidopsis downy mildew pathogen *Hyaloperonospora arabidopsidis* (*Hpa*), interacts with and degrades MED19; JA responsive genes such as *PDF1*, *LOX2*, and *OPR3* in the *med19* mutant are elevated after infection with *Hpa* (Caillaud et al., 2013). A knock-down line of *MED21* showed enhanced susceptibility to *Alternaria brassicicola* and *Botrytis cinerea* (Dhawan et al., 2009). A *med25* mutant, also known as *pft1*, exhibited delayed flowering and reduced induction of jasmonate responsive genes such as *PDF1.2*. The *med25* mutant displays increased susceptibility to *Alternaria brassicicola* and *Botrytis cinerea*, while increased resistance to *Fusarium oxysporum* (Kidd et al., 2009). MED25 has been found to interact with 19 transcription factors, such as MYB, MYC2 and ZFHD, and regulates JA-responsive defense gene expression such as *PDF1.2*, *ORA59*, and herbivore genes such as *VSP1* and *MYC2* (Chen et al., 2012). Together, these observations show that the mediator complex plays an important role in biotic stress, and that these characterized components are distributed to all the modules except for the CDK module (Figure 2).

Mediator subunits are also important for plant development. MED25, which regulates JA-responsive genes, is involved in lateral root formation and sugar-dependent cell elongation (Backstrom et al., 2007, Chen et al., 2012, Raya-González et al., 2014). MED8 is required for the expression of genes encoding cell wall components and sugar responsive growth (Seguela-Arnaud et al., 2015). The mutation of MED15 and MED8

subunits suppressed the sugar-hypersensitive hypocotyl elongation 2 (Raya-González et al., 2014). MED12 and MED13, acting as a pair in the Arabidopsis CDK8 kinase module, are required for plant development from embryogenesis to flowering and floral morphogenesis(Chen et al., 2012, Backstrom et al., 2007, Imura et al., 2012, Raya-González et al., 2014).

1.4 *Growth and immunity trade-offs*

Mounting a defense response comes with the fitness cost, which often manifests as a reduction in growth and reproduction. This fitness penalty in biotic stress carries critical implications for agricultural populations (Karasov et al., 2017) (Figure 3). Growth-defense trade-offs were shown to be decoupled under a specific condition, raising the intriguing possibility that the fitness cost can be minimized while maintaining adequate defense responses (Campos et al., 2016, Burdon & Thrall, 2003, van Hulten et al., 2006). In particular, crop yield has been intensely studied for the past decade, especially pertaining to identifying the best balance point between fitness cost and appropriate resistance.

Hormones have been shown to be a critical player in balancing growth and immunity. Gibberellins (GAs) are involved in multiple areas of plant development, including breaking seed dormancy, seed development, and vegetative/floral growth (Daviere & Achard, 2013). GAs degrade a class of growth-suppressing-proteins, DELLA, which promotes growth. When immunity is activated, these DELLA proteins are stabilized, thereby suppressing growth (Navarro et al., 2008). *Pst* infection inhibits plant growth by preventing the GA-triggered degradation of DELLA proteins in a partially EDS1-dependent fashion (Li et al., 2019). In addition to GA, two well-known defense

hormones, SA and JA, are shown to suppress auxin biogenesis (Wang et al., 2015) and its transport (Sun et al., 2011, Burdon & Thrall, 2003, Tian et al., 2003, van Hulten et al., 2006, Gangappa et al., 2017), demonstrating a complex hormonal network modulating the growth-immunity balance.

The regulation of photosynthesis and growth is tightly coupled (Krahmer et al., 2018). Plants have multiple groups of photoreceptors that respond to a wide range of the light spectrum, including phytochromes, cryptochromes, and phototropins (Galvao & Fankhauser, 2015). These light receptors, when activated, are shown to directly interact with transcription factors. For instance, phytochromes in the cytosol activated by red light are translocated to the nucleus, which target PIFs (Phytochrome Interacting Factors), basic helix-loop-helix (bHLH) transcription factors. This targeting often results in ubiquitin-mediated degradation(Krahmer et al., 2018, Galvao & Fankhauser, 2015, Sheerin et al., 2015, Park et al., 2012), which, in turn, derepresses photomorphogenesis and its associated photosynthetic apparatus. Phytochrome mutants, as a result, have substantially less biomass than WT, suggesting that regulation of photosynthesis is critical in growth (Yang et al., 2016, Kharshiing & Sinha, 2016). Pathogen infection negatively impacts photosynthesis, loss of photosynthetic tissue, and/or disruption of the vasculature affecting water and sugar transport (Aldea et al., 2005, Zou et al., 2005, Nabity et al., 2009, Kerchev et al., 2012). Suppression of photosynthesis-related genes under biotic stress has also been reported (Jung et al., 2007, Zou et al., 2005). However, whether suppression of photosynthesis is a programmed part of the defense response or simply a by-product remains to be characterized (Zou et al., 2005, Borges et al., 2013,

Guo et al., 2012, Gohre et al., 2012, Chen et al., 2011, Sugano et al., 2010, Bilgin et al., 2010, Ishiga et al., 2009).

The Arabidopsis PIF transcription factors bind to the conserved G-box sequence motif (Huq & Quail, 2002, Leivar et al., 2008, Leivar & Quail, 2011b). PIFs are known to transduce light signals, repress seed germination, and promote seedling skotomorphogenesis (Leivar & Quail, 2011b, Leivar & Monte, 2014). PIFs are degraded upon binding to phytochrome photoreceptors (Leivar & Monte, 2014, Leivar et al., 2008, Leivar & Quail, 2011b, Park et al., 2018). PIFs are phosphorylated either by Phytochrome or Photoregulatory Protein Kinases (PPKs) upon exposure to light (Leivar & Monte, 2014, Leivar et al., 2008, Leivar & Quail, 2011b, Park et al., 2018, Al-Sady et al., 2006, Shin et al., 2016). Emerging evidence also points to PIFs being a signaling hub in integrating multiple signaling pathways by interfacing diverse groups of factors to optimize growth and development in addition to a role as transcription factors modulating the target genes (Paik et al., 2017). A recent study reported that PIFs negatively modulate plant defense against *Botrytis cinerea* (Xiang et al., 2020), suggesting a function in defense responses. PIF4 coordinates thermosensory growth and immunity, acting as a negative regulator of defense responses and modulating temperature sensitivity of disease resistance (Gangappa et al., 2017). Thus, this type of transcription factor may act as a master regulator directly controlling growth as a part of the defense response in plants. Regardless of PIFs being the master regulator, learning the underlying molecular mechanism on how growth is coordinated with defense responses will provide insightful groundwork in which a resistance trait would be tailored to protect plants from diseases without causing significant fitness penalty.

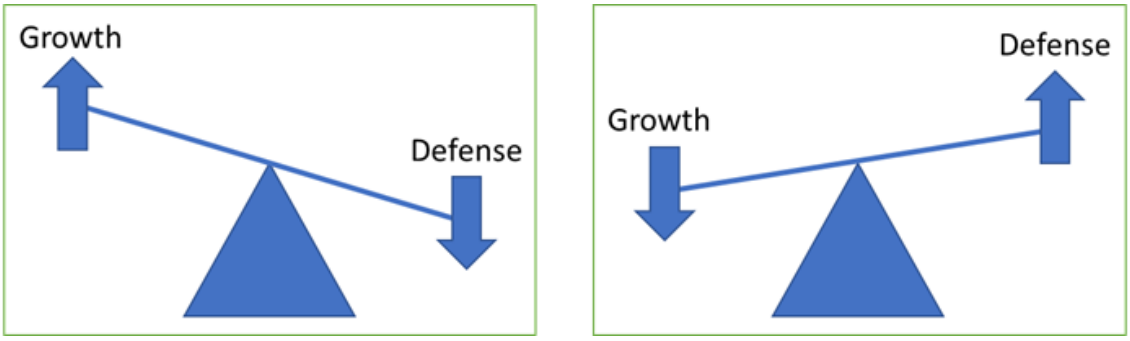

Figure 3. Growth and defense are balancing acts. Plants balance growth and stress to maximize the survival chance and minimize the fitness cost.

2. CHARACTERIZATION OF MORC1 INTERACTING PROTEINS

2.1 *A yeast-2-hybrid screening identified 14 MORC1 interaction proteins*

The Hybrigenics service (www.hybrigenics-services.com) performed a conventional yeast two-hybrid (Y2H) screening for MORC1 as bait by using 87 million prey clones. This commercial service provided 14 confirmed clones that interacted with the bait, which is listed in Table 1. To confirm the physical interaction and also characterize the interactions among MORC1-interacting proteins (MIPs), I generated the prey and the bait vector for MORC1 as well as all 14 MIPs, and performed a targeted Y2H assay (Figure 4). MORC1, when used as bait, interacted with all the MIP clones identified in the screen, confirming the outcome provided by Hybrigenics. MORC1 showed a weak interaction with itself, suggesting homodimerization. MORC1, when switched to prey, interacted with a subset of the MIPs: MIP2, MIP3, MIP6, MIP7, MIP11, MIP12, MIP13. When a transcription-activating domain is present in a bait vector, it generally activates without a prey vector. This transactivation was observed with MIP6 and MIP13, and to a lesser degree, with MIP7, suggesting that these MIP proteins may carry a transactivation domain. MIP13 is a mediator complex that interfaces a transcription factor with RNA polymerase II (Kidd et al., 2011, Allen & Taatjes, 2015a, Buendía-Monreal & Gillmor, 2016). Thus, MIP13, when used as bait, appears to function as a coactivator and to bring in a factor(s) with transactivation activity.

There were several interactions among MIPs. MIP11, sorting nexin (Phan et al., 2008), interacted with the highest number of MIPs, including MIP2, MIP11, MIP12, MIP13, and MIP14 (Figure 4). MIP3 is a MORC1 homolog, MORC6. The interaction between MORC1 and MORC6 was previously reported (Liu et al., 2014), and their

heterodimer was shown to maintains heterochromatin (Moissiard et al., 2012a). Interestingly, MORC6 did not interact with any of the MIPs, suggesting that the MIPs are likely specific to MORC1. The Hybrigenics screening used an Arabidopsis cDNA library (RP1). As a result, all the MIP clones only contained part of the corresponding genes. Thus, I constructed the bait and the prey plasmids carrying the full-length clone of all 14 *MIP* genes. In contrast to the outcomes obtained from the partial MIPs (Figure 4), only a minority of the MIPs, MIP3 and MIP13, displayed measurable interaction with MORC1 (Figure 5). This reduction in the number of interactions suggests that some of these MIPs may form a structure in which the interacting region becomes inaccessible in a full-length context. Alternatively, some of these interactions in Y2H (Figure 4) may be an artifact in which a peptide from a partial clone forms an unnatural structure that allowed interaction with MORC1.

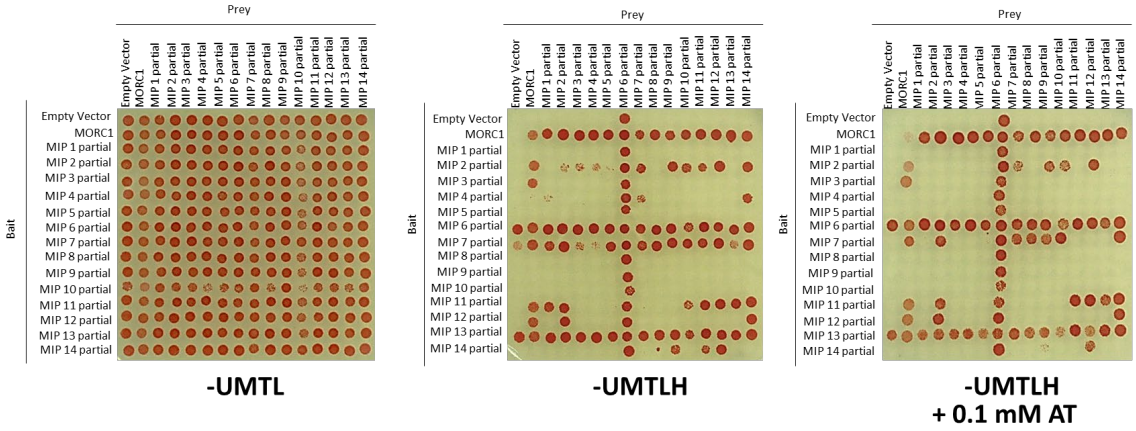

Figure 4. Interaction of MORC1 and MIPs in yeast 2-hybrids assay. MORC1 and 14 MIP clones identified from the yeast 2-hybrids screening were reconfirmed by a targeted yeast 2-hybrids assay. pB27 plasmid with a LexA DNA binding domain (Y187) and pP6 plasmid with a GAL4 activating domain (L40) were used as a bait and a prey vector, respectively. The plasmids were transformed into *S. cerevisiae* carrying the *HIS3* reporter genes under the control of the LexA DNA binding sites. Transformants were plated onto minimal media; -Ura/-Met/-Trp/-Leu (-UMTL) and -Ura/-Met/-Trp/-Leu/-His (-UMTLH) +/– 0.1 mM 3-AT.

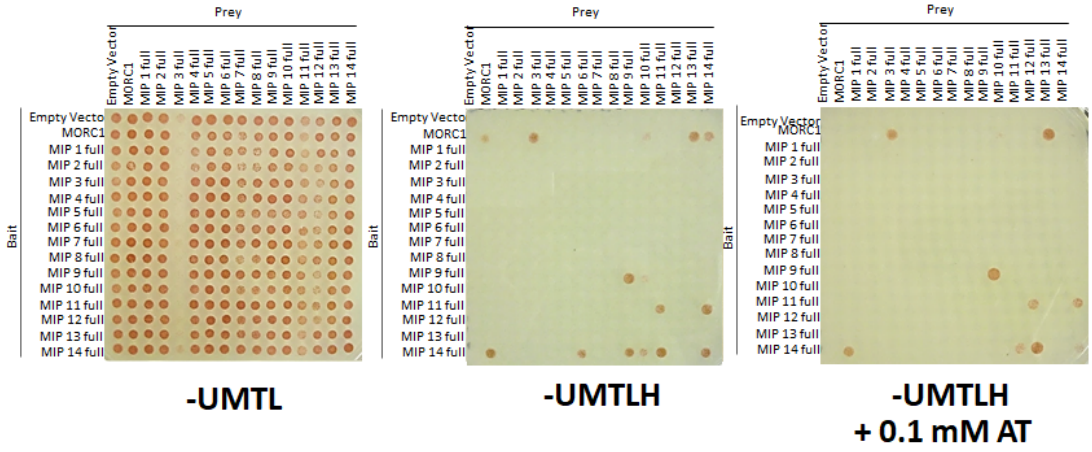

Figure 5. Interaction of MORC1 and full-length MIPs in yeast 2-hybrids assay. The full-length 14 *MIPs* were cloned into pB27 and pP6. The plasmids were transformed into *S. cerevisiae* (Y187 and L40) carrying the HIS3 reporter genes under the control of the LexA DNA binding sites. Transformants were plated onto minimal media; -Ura/-Met/-Trp/-Leu (-UMTL) and -Ura/-Met/-Trp/-Leu/-His (-UMTLH) +/– 0.1 mM 3-AT.

2.2 *Confirmation of MIPs in a co-IP experiment using a* **Nicotiana benthamiana** *transient expression system*

The MIP proteins were further examined to determine if the interaction occurs with MORC1 *in planta*. To this end, I transiently co-expressed MIPs and MORC1 tagged with HA and Myc, respectively, in *Nicotiana benthamiana*. The expressed proteins were subject to a co-IP (immunoprecipitation) experiment in which an αHA antibody immunoprecipitated MIP proteins, and its co-precipitation of MORC1 was monitored by western analysis with an αMyc antibody. MIP4, MIP6, MIP7, MIP8, and MIP12 were not detectable via an HA immunoblotting analysis (Figure 6). MIP3 and MIP13 co-IPed significantly more MORC1 than other weak interactors, such as MIP9, MIP10, and MIP11 (Figure 6), confirming the physical interaction shown in the Y2H analysis (Figures 4 and 5).

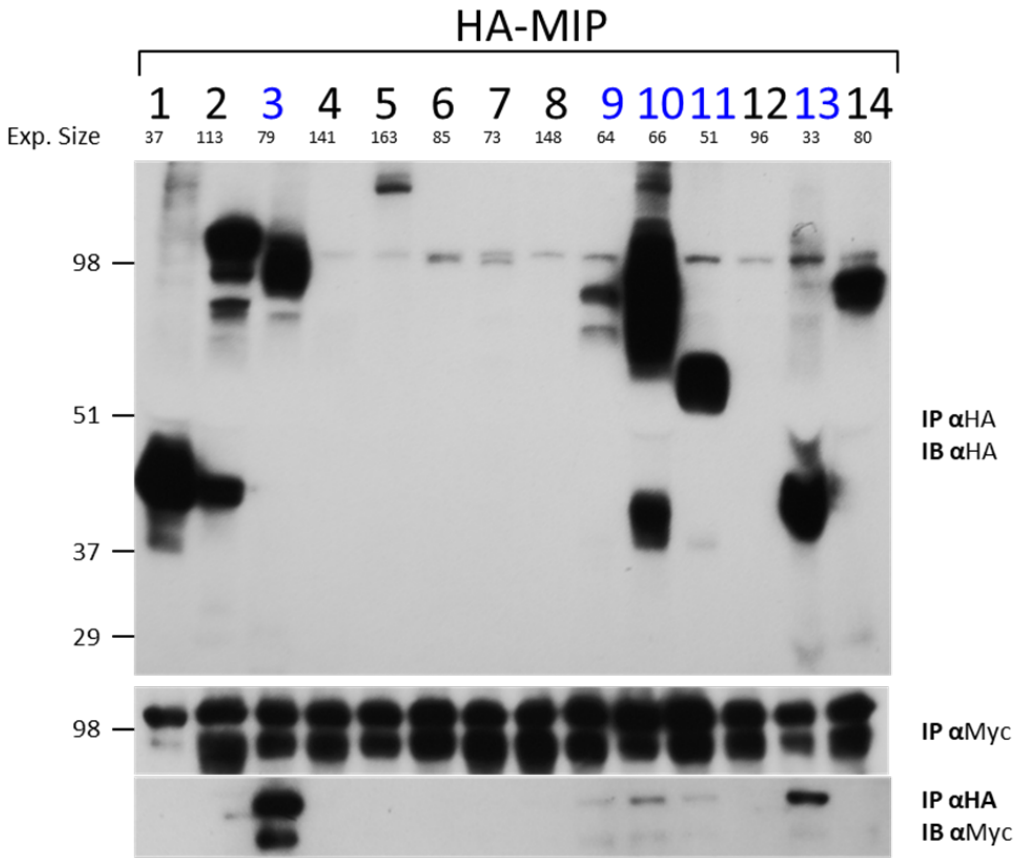

Figure 6. Interaction of MORC1 with MIPs *in planta*. Physical interaction of MORC1 and MIPs were tested in *Nicotiana benthamiana* plants transiently expressing *35S-Myc-MORC1* and *35s-HA-MIPs*. Proteins extracted were immunoprecipitated with αHA antibody. Expression of *Myc-MORC1* and *HA-MIPs* were examined by western analysis with αMyc and αHA antibodies, respectively. Co-immunoprecipitated proteins were detected by western analysis with αMyc antibody.

2.3 *Resistance phenotypes of MIPs with a putative nuclear-related function*

MORC1 maintains heterochromatin, physically contacts DNA, and displays topoisomerase activity (Weiser et al., 2017, Kim et al., 2019b, Manohar et al., 2017). Consistent with these nuclear functions, the presence of MORC1 in the nucleus was visually confirmed by transmission electron microscopy and subcellular fractionation (Kang et al., 2010, Moissiard et al., 2012a). Moreover, MORC1 increases in the nucleus by the activation of ETI and PTI (Kang et al., 2012). Thus, to further characterize the nuclear function of MORC1 by using MIPs, I chose eight MIPs with putative nuclear function for resistance analysis as follows: MIP3 is MORC6 that is involved in DNA methylation (Liu et al., 2016). MIP4 is CPL3, regulating the activity of RNA polymerase II (Koiwa et al., 2002). MIP5 is a WAVE protein that modulates actin polymerization and gene expression in the nucleus (Verboon et al., 2015). MIP8 is SMC1, a regulator in chromatin architecture (Schubert, 2009). MIP9 is a SANT domain protein associated with the chromatin remodeling factor ISWI (Horton et al., 2007). MIP10 is a putative bZIP transcription factor (Jakoby et al., 2002). MIP12 is a protein with a mobile domain involved in TE silencing and genome stability (Nicolau et al., 2020). MIP13 is a subunit of the mediator complex that connects transcription factors and RNA polymerases II (Table 1).

Table 1. MORC1 Interacting Protein (MIP) identified in the yeast-2-hybrids screening. The annotation and locus of 14 MIPs were based on Arabidopsis TAIR 10. MIPs with a putative nuclear-associated function were highlighted in red. Resistance phenotypes to *Pst* presented in Figures 7 and 8 were summarized in the last three columns. The strength of immunity is indicated as the number of + (resistance) and – (susceptibility), respectively.

	LOCUS	Annotation	Pst DC3000		
			Single *mip* mutant	*mip morc1/2* mutant	overexpression
MIP1	AT3G56190	Intracellular protein transport; αSNAP2			
MIP2	AT5G15450	chloroplast-targeted HSP101 homologue			
MIP3	AT1G19100	MORC6	No	No	No
MIP4	AT2G33540	CPL3	+++	++	No
MIP5	AT2G35110	NAPP/WAVE	--	--	+
MIP6	AT5G51600	Mitotic microtubule organizer			
MIP7	AT4G27500	Regulates proton transport			
MIP8	AT3G54670	SMC1 – cohesion during DNA replication	No	N/A	--
MIP9	AT3G10030	SANT – chromatin remodeling factor	--	--	No
MIP10	AT4G38900	bZIP transcription factor	--	--	-
MIP11	AT5G06140	SORTING NEXIN 1			
MIP12	AT1G50750	WRKY transcription factors, Mobile domain	--	--	-
MIP13	AT1G55080	Mediator9 complex protein	---	--	+++
MIP14	AT1G31780	COG6 (Golgi retrograde transport)			

Resistance		Susceptibility	
+++	Strong	---	Strong
++	Medium	--	Medium
+	Weak	-	Weak

T-DNA insertion mutants for eight select *MIPs* were obtained from TAIR. *mip8*, however, due to a homozygous lethality, was not further characterized. I used virulent and avirulent *Pst* for infection, which provided the resistance phenotypes for basal resistance and ETI, respectively (Figure 7). *mip10* and *mip13* were susceptible against *VirPst* (virulent *Pst),* while *mip4* was resistant. When *AvrPst* (avirulent *Pst*) challenged the plants, only *mip3, mip10,* and *mip13* became susceptible. The resistance traits of a higher-order mutant in which *morc1/2* was crossed with a single *mip* mutant (Figure 8) were characterized. Note that *morc1/2* displayed compromised basal resistance and ETI against *Pst* (Kang et al., 2010). Surprisingly, *mip3* and *mip13* regained the WT-level resistance to *VirPst* (Figure 8) when *morc1/2* was introduced. In contrast, *mip4* lost its resistance to *VirPst* when combined with *morc1/2*, suggesting a complicated genetic interaction between some MIPs and MORC1/2. *mip5* and *mip10* showed little difference in their higher-order mutant backgrounds. Note that an image-based resistance assay involving *Pst* carrying the luminescent *luxCDABE* reporter gene (Fan et al., 2008) was used to analyze the disease resistance phenotypes in a large number of lines. While this system is efficient in assessing a large sample number, we noted that its resolution and sensitivity were generally lower than a leaf-disc-based conventional assay (Shah et al., 1997). Therefore, the real difference between the lines is likely underestimated in this imaging-based tool presented in Figure 8.

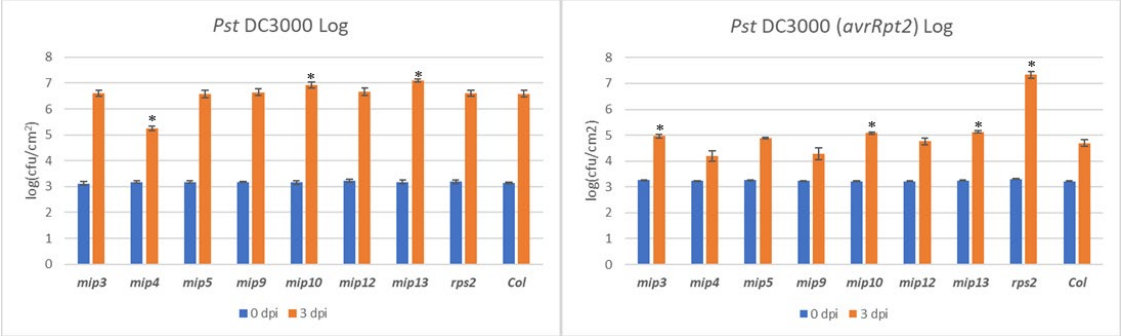

Figure 7. Resistance phenotypes of MIPs. Bacterial growth of *Pseudomonas syringae* pv. *tomato* DC3000 (*Pst*) with and without *AvrRpt2* was measured in WT(Col-0) and indicated mutants at 0 and 3 dpi (day post-infection); the mean ± SD (n = 3) is presented. The starting inoculum was at 10^5 cfu/ml. Statistical difference from WT is indicated: *P<0.05 (Student's *t*-test).

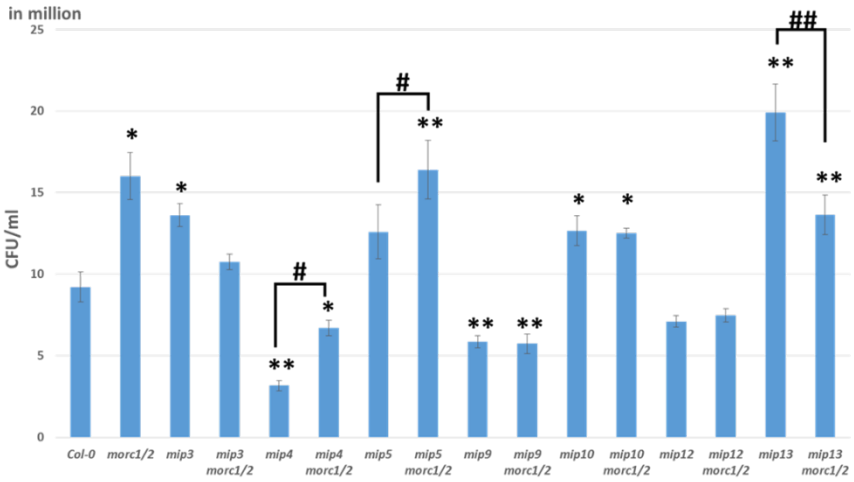

Figure 8. Resistance phenotypes of higher-order backgrounds combining *morc1/2* and each *mip*. Bacterial growth of *Pst* carrying a luminescent *luxCDABE* reporter gene was measured at 2 dpi with the indicated backgrounds; initial inoculum was at $1x10^5$ cfu/ml. The luminescence was monitored by an EMCCD camera to indirectly measure the bacterial concentration. the mean ± SD (n = 4) is presented. Statistical difference from WT is indicated: *P < 0.05, **P<0.01 (*t*-test). Statistical difference of each *mip* mutant between with and without *morc1/2* is indicated; $^{\#}$P < 0.05 (*t*-test).

2.4 *Identification of a domain in SMC1 interacting with MORC1*

MIP8 is SMC1. An earlier report showed that Defective in Meristem Silencing3 (DMS3), an SMC homolog, indirectly interacts with MORC6 (Lorkovic et al., 2012). Given both DMS3 and MORC1/6 are known regulators in chromatin topology, I tested if DMS3 and an additional homolog, SMC2, physically interact with MORC1 and found little MORC1 interaction in Y2H assay (Figure 9), suggesting that SMC1, among the SMC family, is the only physical interactor with MORC1.

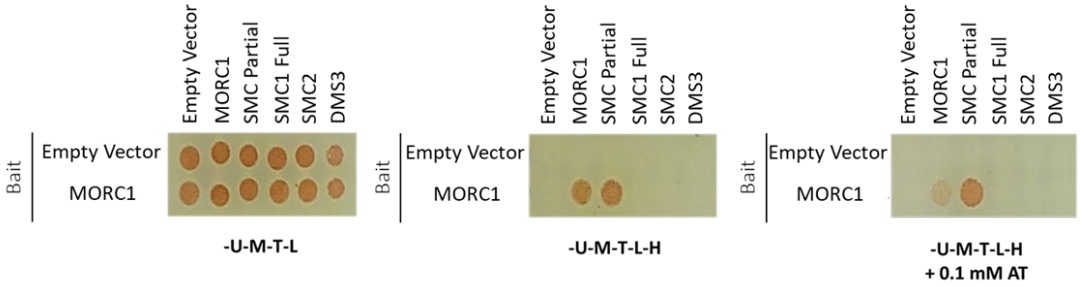

Figure 9. Yeast 2-hybrids interaction analysis between MORC1 and SMC/DMSs. MORC1 in pB27 was a bait; SMC1, SMC2 and DMS3 in pP6 were used as a prey. The plasmids were transformed into *S. cerevisiae* carrying *HIS3* reporter genes under the control of a LexA DNA binding domain. Transformants were plated onto minimal media, -Ura/-Met/-Trp/-Leu (-UMTL), -Ura/-Met/-Trp/-Leu/-His (-UMTLH) +/– 0.1 mM 3-AT.

To further narrow down the MORC1-interacting region/domain in SMC1, I generated constructs for SMC1-truncated mutants tagged HA (Figure 10a) under an estradiol-inducible promoter: SMC1-1 (1-344aa), SMC1-2 (345-958aa), and SMC1-3 (959-1218aa). From the Simple Modular Architecture Research Tool (SMART) (Schultz et al., 1998), SMC1-2 is predicted to have a hinge domain that divides the C-terminal and the N-terminal of the globular domain (Hirano & Hirano, 2002). These constructs were then used in a co-IP experiment with *N. benthamiana* transiently expressing SMC1 truncated proteins; note that the full-length SMC1 was failed to be detected for an unknown reason (Figure 6). Interestingly, only SMC1-2 that contains a hinge domain displayed interactions with MORC1; GFP was used as a negative control (Figure 10b). DMS3, a MORC6-interacting protein, is an unusual SMC protein that lacks the hallmark ATPase domain but has a hinge domain (Lorkovic et al., 2012, Schultz et al., 1998). These observations suggest that MORC1 and MORC6 interact with SMC family proteins via the hinge domain, although its functional relevance remains to be characterized.

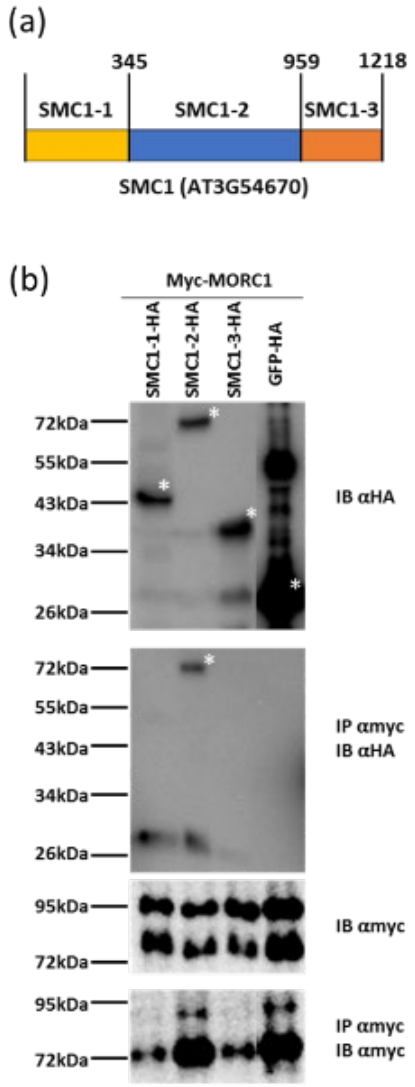

Figure 10. SMC1 interacts with MORC1 *in planta*. (a) Schematic representation of the deletion variants of SMC1. (b) Transient expression of *35S-Myc-MORC1*, *35S-SMC1-HA* and the SMC1 variants via agroinfiltration in *N. benthamiana*. Soluble extracts from the plants were subject to immunoblotting (IB) with αHA and αMyc or immunoprecipitation (IP) with αMyc, followed by IB with αHA and αMyc.

2.5 *Interaction of MIPs with tomato and potato MORC1*

Tomato (*Solanum lycopersicum*) and potato (*Solanum tuberosum*) MORC1 possesses about 70% a.a. homology to AtMORC1, and their C-terminal domains, which is required for homodimerization and phosphorylation, are considerably divergent from each other (Manosalva et al., 2015). StMORC1 shares 96% a.a. identity and 98.5% similarity with SlMORC1. Interestingly, the domain-swapping and mutational analyses of these solanaceous MORC1s demonstrated that the C-terminal region is important in species-specific effects on immunity.

I examined if the solanaceous MORC1s also interact with the MIPs. To further analyze the role of the divergent C-terminal domain in addition to the full-length construct, I generated two truncated mutants, as shown in Figure 11a. In this Y2H assay, both SlMORC1 and StMORC1 interacted with MIP3, even under more stringent conditions (-UMTLH + 0.1mM AT, Figure 11b). When the assay was performed in less stringent conditions without AT, MIP12 was able to interact with SlMORC1. Nonetheless, poor interaction of SlMORC1 and StMORC1 with the 14 MIPs suggests that AtMORC1-MIPs interaction seems to be limited in Arabidopsis. It remains to be seen, however, if potato and tomato counterparts would still interact with SlMORC1 and StMORC1.

The truncated mutants showed interaction with two more MIPs: MIP10 and MIP12 (Figure 11a). Interestingly, ΔN(474-644) mutants showed somewhat differential interactions between SlMORC1 and StMORC1 with the MIPs; the potato one interacted more strongly under the less stringent condition (-UMTLH) while the tomato one only interacted with MIP6 under the more stringent condition (-UMTLH + 0.1mM AT).

Although it is currently unclear how this difference was caused, it is possible that these two truncated MORC1s may have different structures when expressed in yeast.

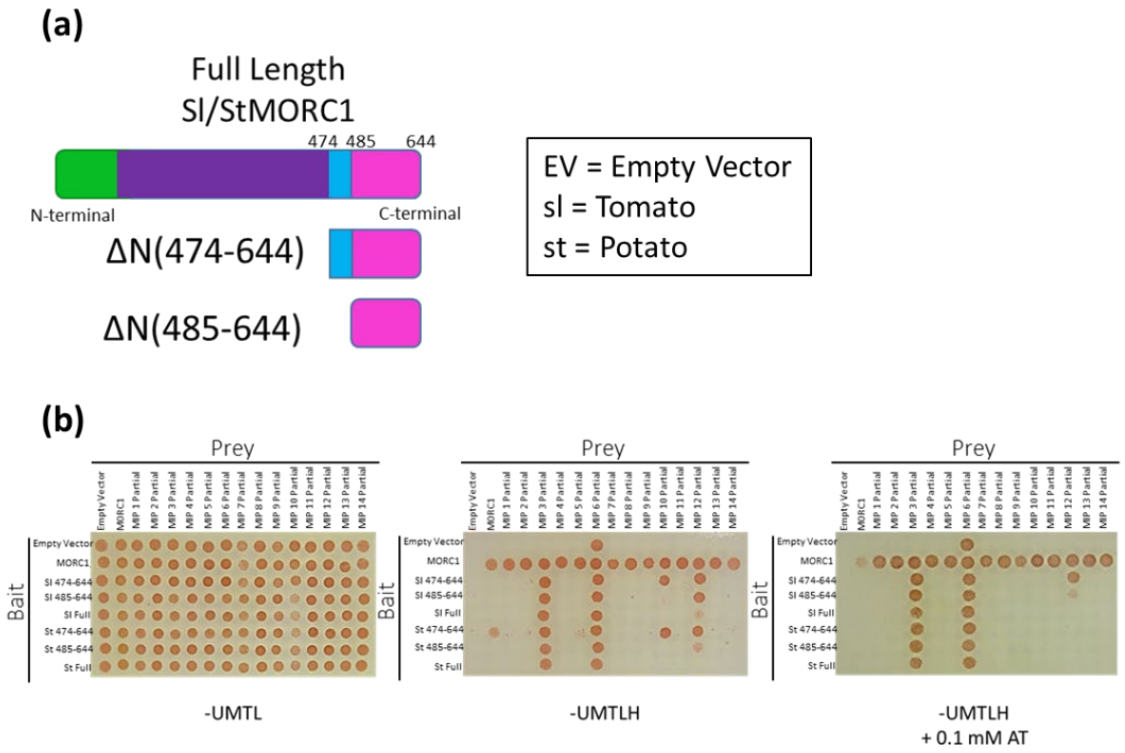

Figure 11. Interaction of tomato and potato MORC1 with MIPs. (a) Schematic diagram of truncated variants of tomato and potato MORC1 (Sl and StMORC1). (b) SlMORC1 and StMORC1 in pB27 were baits, and MIPs in pP6 (Figure 4) were used as preys. The plasmids were transformed into *S. cerevisiae* carrying *HIS3* reporter genes under the control of a LexA DNA binding domain. Transformants were plated onto minimal media, -Ura/-Met/-Trp/-Leu (-UMTL), -Ura/-Met/-Trp/-Leu/-His (-UMTLH) +/– 0.1 mM 3-AT.

3. MEDIATOR 9 IS A POSITIVE REGULATOR IN DEFENSE SIGNALING

3.1 *Domain analysis of MED9 in the MORC1 interaction*

The secondary structure model using PSIPRED revealed considerable similarity between the Arabidopsis MIP13 and its yeast (*Saccharomyces cerevisiae*) counterpart, MED9 (Figure 12; MIP13 is termed as MED9 hereafter). The domain analysis of yeast MED9 found two distinct domains. The N-terminal half plays a regulatory role in transcriptional induction, whereas the C-terminal half has a binding domain to MED4 and MED7 (Takahashi et al., 2009). The N-terminal domain has repeating glutamine residues which been found in the human and Drosophila TFIID TATA-box factors (Aeschbacher, 1991). The C-terminal domain is highly conserved across human, yeast, and Arabidopsis. Given the similarity to the yeast counterparts, the C-terminal domain of Arabidopsis MED9 likely mediates a protein-protein interaction.

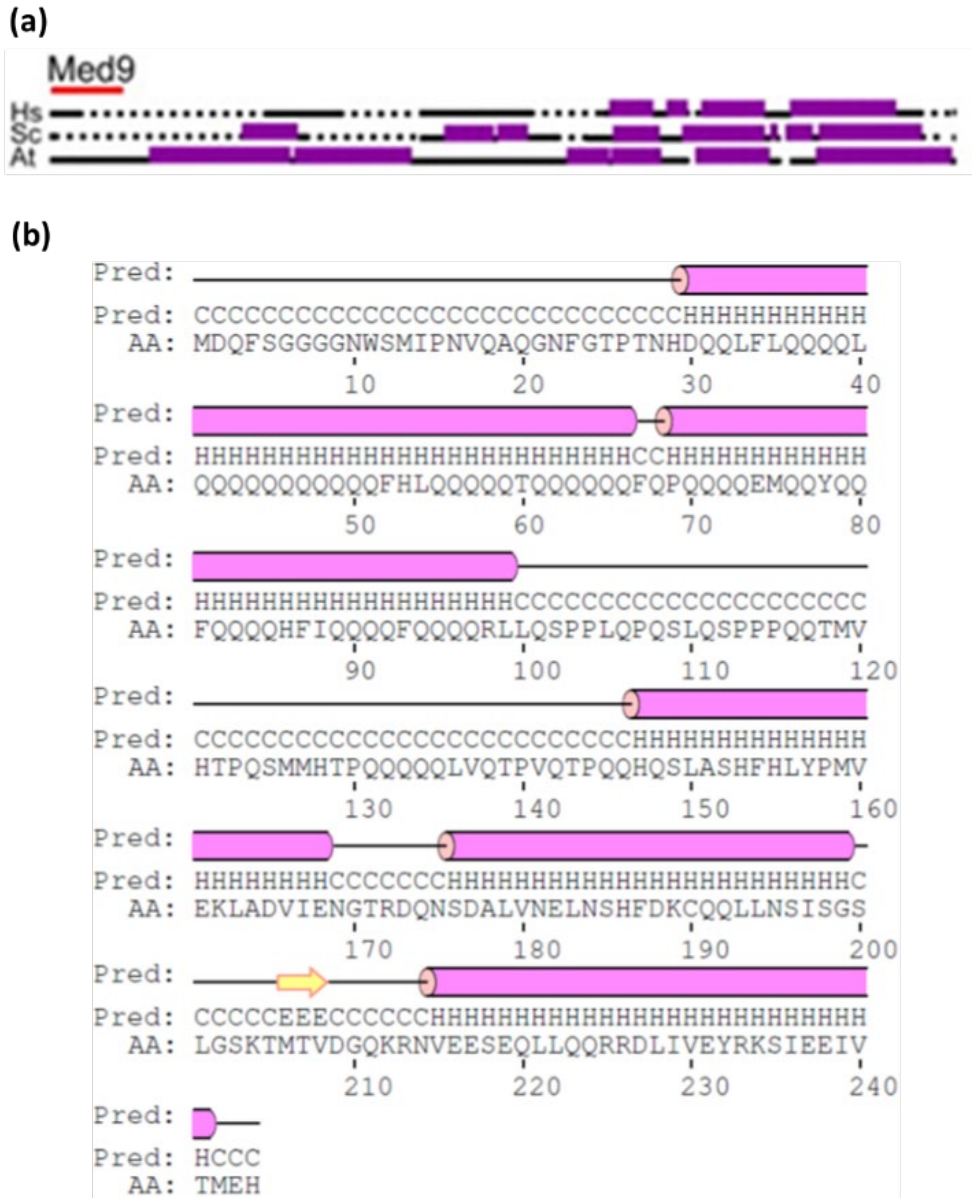

Figure 12. Secondary structure analysis of MED9. (a) Secondary structures among human, yeast, and Arabidopsis MED9 homologs were compared by PSIPRED and aligned by MAFFT. Purple denotes predicted protein helices. A black line indicates no secondary structure predicted, and a dotted line denotes a gap in the alignment. A red bar represents a length of 20 amino acids. Hs, *Homo sapiens*; Sc, *Saccharomyces cerevisiae*; At, *Arabidopsis thaliana*. (b) Secondary structure of AtMED9 predicted by PSIPRED. A pink bar, a black line, and an arrow denote a helice, a coil, and a strand. H: helix, E: strand, and C: coil.

I performed a Y2H assay by using two truncated MED9 mutants (Figure 13) to identify the MORC1-interacting domain in MED9: C-terminal deletion mutant (MED9ΔC) and N-terminal deletion mutant (MED9ΔN). As noted earlier, the original MED9 clone from the screening is generated from a cDNA library, which contains a part of MED9 (40 aa - 205 aa). In addition to MED9 and its partial protein (Figures 4 and 5), the C-terminal domain of MED9 (MED9ΔN; aa 118-244) interacted with MORC1 (Figure 13b), revealing that the region spanning between 118aa and 205aa is involved with the physical interaction with MORC1.

MED9 is rich in glutamine (~50% in the N-terminal domain). The glutamine-richness has been linked to a transcriptional (co)activator domain (Hsieh et al., 1994). MED9 truncated mutants above (Figure 11a) were fused with the LexA DNA-binding domain as a bait construct to assess transcriptional activity (Figure 13c). As anticipated, MED9ΔC activated the reporter autonomously, showing that the glutamine-rich area is a transcription-activating domain. MED9ΔN displayed the auto-activation as well. While MED9ΔN does not have a putative transactivation domain, it can interact with other mediator subunits or RNAP II, suggesting the autoactivation may be indirect by bringing in a transcriptional activator and machinery. In sum, Arabidopsis MED9 interacted via the C-terminal domain with MORC1 and displayed transcriptional activation capacity, suggesting a regulatory role in defense genes.

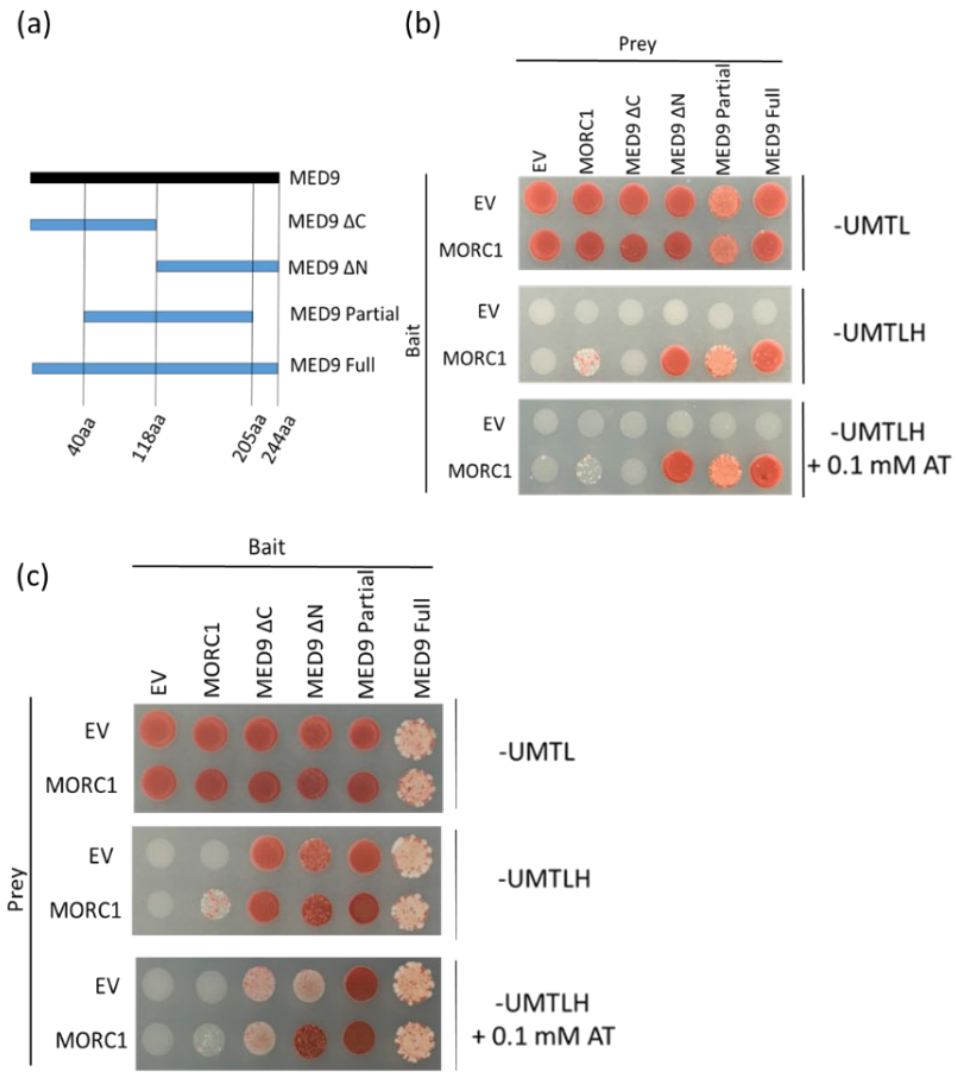

Figure 13. C-terminal half of MED9 interacts with MORC1. (a) Schematic diagram of MED9 deletion variants. (b) pB27 and pP6 constructs provided baits and preys, respectively. The plasmids were transformed into *S. cerevisiae* carrying *HIS3* reporter genes under the control of a LexA DNA binding domain (Y187 and L40). Transformants were plated onto minimal media, -Ura/-Met/-Trp/-Leu (-UMTL) and -Ura/-Met/-Trp/-Leu/-His (-UMTLH) with/without 0.1 mM 3-AT. (c) A reciprocal experiment of (b) in which MORC1, MED9 and its variants were switched from bait to prey and vice versa.

3.2 *MED9 appears to be a specific, among other mediator proteins, interactor with MORC1*

Interactions of MED9 raise the question of whether MORC1 interacts with other mediator subunits. To address this question, I performed a Y2H assay to test 14 additional mediator subunits. MORC1 and its truncated mutant carrying the C-terminal region (aa 400 - aa 635) and MED9 were used as bait containing the Gal4 DNA binding domain and as prey with the GAL4 activating domain. The Arabidopsis mediator complex carries 27 subunits, of which six seem to be Arabidopsis-specific (Kidd et al., 2011). The mediator complex comprises four main modules: head, middle, tail, cyclin-dependent kinase. The head domain is generally conserved and interacts with RNAP II. The middle-tail domain tends to be divergent among species and has been speculated to confer specific biological functions (Dotson et al., 2000).

To test diverse subunits in the Arabidopsis mediator complex, I generated prey constructs for the following subunits: MED6, MED11, MED19, MED20, and MED22 in the head module; MED2, MED9, MED10, and MED31 in the middle module; MED3 in the tail module, and CycC as the cyclin-dependent kinase module. MED26, MED36, and MED37 were also included, but their module affiliation is yet to be decided. Despite 14 mediator subunits tested out of the total 27, MED9 was the only one that displayed interaction with MORC1 (Figure 14). In addition to its canonical function in interfacing with transcription factors and RNAP II, the mediator complex has an emerging role in regulating chromatin topology (Meyer et al., 2008, Black et al., 2006, Kagey et al., 2010). Thus, MED9 may interact with MORC1 to coordinate chromatin architecture to accommodate transcriptional demands, and perhaps the MORC1-MED9 interaction

occurs under specific conditions such as biotic stress. Therefore, given MORC1 did not interact with other mediator subunits, MED9 is a specialized subunit that coordinates chromatin topology under a stress condition. Note that no genetic screening has identified MED9 in Arabidopsis to date.

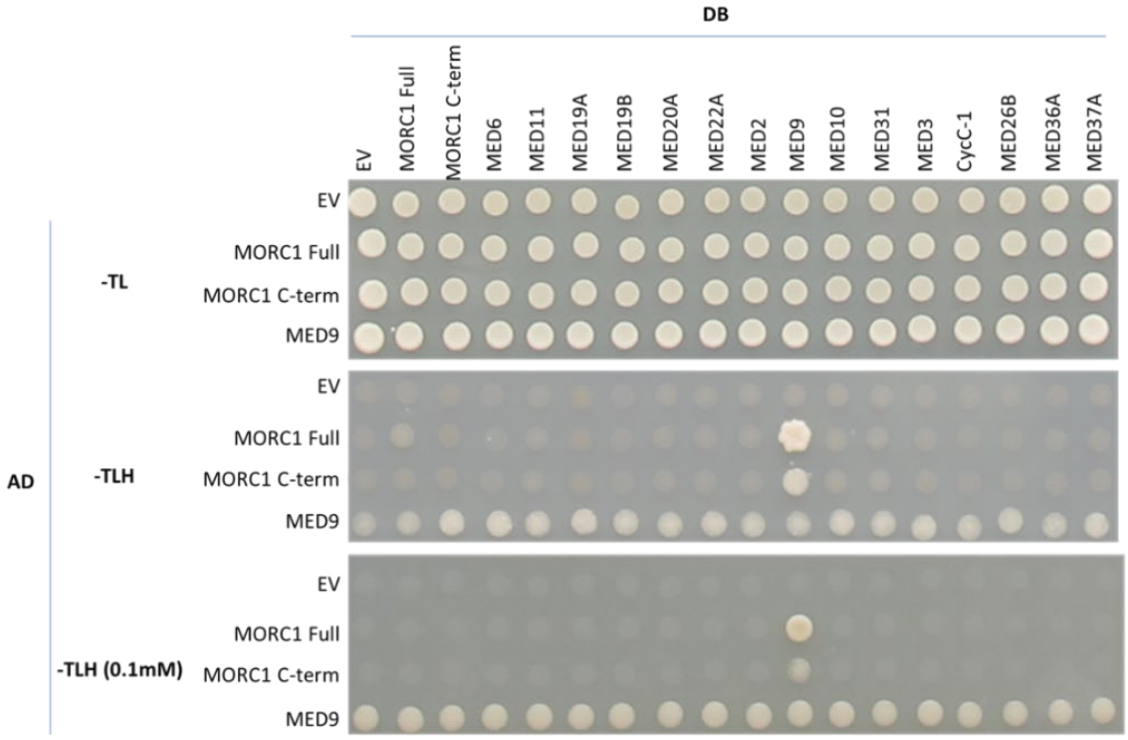

Figure 14. MED9, among many other mediator subunits examined, is the only one that interacts with MORC1. MED9 and full-length and a c-terminal variant of MORC1 in pPC97 were used as bait. 15 mediator subunits in pPC96 were used as prey. These bait and prey plasmids were transformed into *S. cerevisiae* carrying *HIS3* reporter genes under the control of a LexA DNA binding domain. Transformants were plated onto minimal media, -Ura/-Met/-Trp/-Leu (-UMTL), and -Ura/-Met/-Trp/-Leu/-His (-UMTLH) with/without 0.1 mM 3-AT.

3.3 *Bacterial resistance is modulated by MED9*

In Chapter 2, I showed that a knock-out mutant of MED9 displayed compromised resistance to *Pst*. As I have used a high-throughput imaging-based assay, I suspected the magnitude of altered resistance could have been underestimated. Thus, I performed a conventional leaf-disc method to assess bacterial resistance in *med9*, *morc1/2,* and their higher-ordered mutant (*med9 morc1/2*). For ease of reference, *med9 morc1/2* is termed as *tKO* (triple knock-out) hereafter.

Consistent with earlier outcomes (Figure 7), the single mutants, *morc1/2* and *med9*, were susceptible to both *VirPst* and *AvrPst*, suggesting that these components are involved in basal resistance and ETI. Unusually, *tKO* regained WT-level resistance through an unknown mechanism (Figure 15) as seen earlier (Figure 7). Restoring resistance by combining two susceptible mutants is counterintuitive, which indicates that the MORC1 and MED9 interaction is likely multifaceted, perhaps involving various differential gene regulation over time. For instance, these factors are essential in inducing defense genes early, while more engaged in curbing the induced genes later to minimize unnecessary fitness cost.

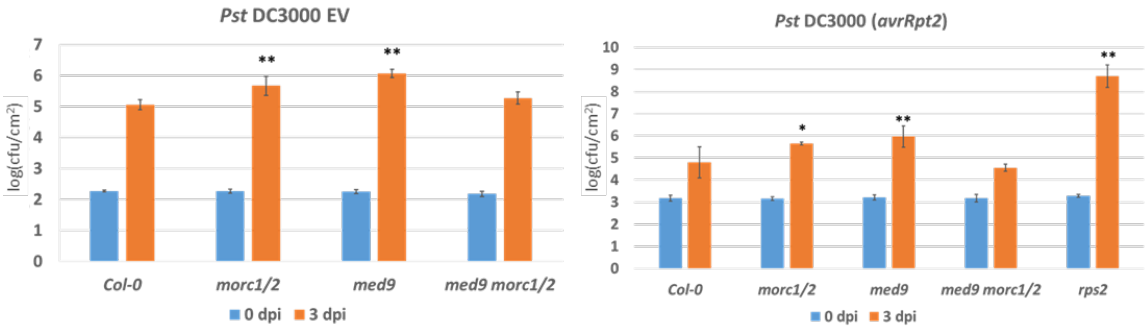

Figure 15. Resistance phenotypes of *med9*, *morc1/2,* and their combined mutant. Bacterial growth in the indicated plants were measured at 0 and 3 dpi with *VirPst* and *AvrPst.* Initial inoculum of *VirPst* and *AvrPst* was at 10^5 and $5x10^5$ cfu/ml, respectively; the mean ± SD (n = 3) is presented. Statistical difference from WT is indicated; *P < 0.05, **P<0.01 (*t*-test).

MED9 overexpression lines were generated to test a gain-of-function resistance phenotype. MED9 tagged with HA was expressed under an estradiol-inducible promoter (*MED9-OX*) (Figure 16). Expression of *MED9* was examined by using an HA immunoblotting analysis, showing that three independent lines had a comparable expression of MED9. All three *MED9-OX* lines were resistant to *Pst*, which carried the *luxCDABE* reporter. Note again, I suspected that this particular imaging analysis underestimates the difference in resistance; currently, the conventional assay is underway to verify this idea. In sum, the expression level of *MED9* was correlative to bacterial resistance to *Pst*, suggesting that MED9 is a positive regulator of plant antibacterial defense.

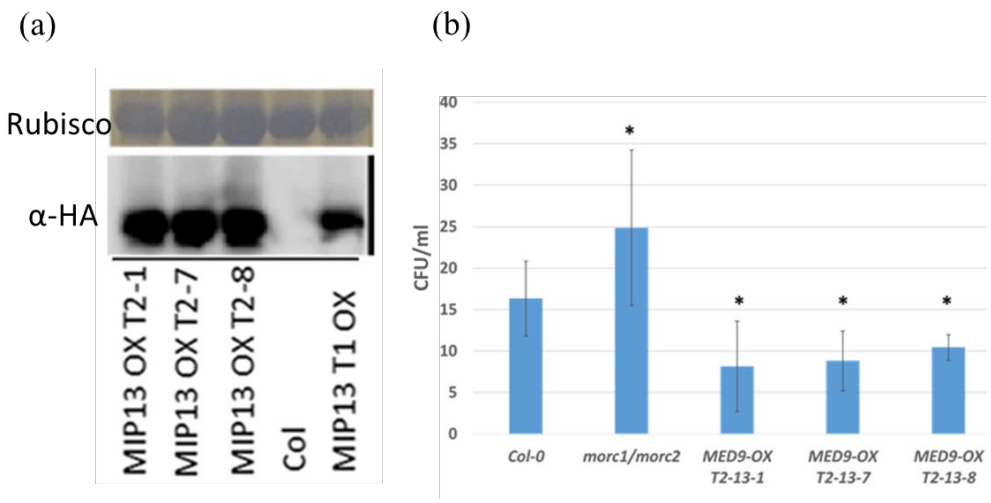

Figure 16. Overexpression of *MED9* enhances bacterial resistance in Arabidopsis. (a) *MED9* was overexpressed in Arabidopsis using an estradiol-inducible vector, pER8. The transgenic lines were treated with 10 μM estradiol for 48 hours, and proteins were extracted for immunoblotting with αHA. Rubisco proteins stained with Coomassie blue were used as a loading control. (b) 10^5 cfu/ml of *Pst* carrying a luminescent *luxCDABE* reporter gene was inoculated and analyzed at 2 dpi. Luminescence of *Pst* was monitored by an EMCCD is presented. Estradiol was sprayed 24 hours prior to *Pst* infection. Statistical difference from WT is indicated; *P < 0.05, (*t*-test).

3.4 *Transcriptional analysis of select defense genes to track defense signaling in* MED9*-associated genetic lines.*

I further characterized MED9 by tracking the expression of defense genes in *med9* and tKO together with *morc1/2* in reponse to *avrPst* and *virPst* infection. I chose three well-characterized defense genes for my targeted transcriptional analysis: *PR1*, *PR2,* and *PR5* (Shah et al., 1997). Transcription dynamics of defense genes are also known to be an important predictor for successful resistance. For instance, *PR1* induction was delayed in *morc1/2* when examined at multiple time points (Bordiya et al., 2016b) which explains the susceptible resistance phenotype against *AvrPst* and *VirPst*. Thus, I decided to use the same multiple time points for my transcriptional analysis: 0, 1, 6, 24, 48 hpi (hours post infection).

qRT-PCR analysis was carried out for qunatitaive transcriptional analysis in response to infection with *AvrPst* and *VirPst*; mock infection was used as a negative control. *PR1* was induced similarly in response to *AvrPst* among WT, *med9,* and *morc1/2* (Figure 17a). However, the induction of *PR1* was slow (see 24 hpi with *AvrPst* in Figure 17a) and trended upward even at 48 hpi. This upward trend, while to a lesser degree, was seen with *PR2* and *PR5* in *tKO* at 48 hpi. While it was less obvious than those responding to *AvrPst*, the induction of all the defense genes from 24 hpi to 48 hpi was most steep in *tKO*. *PR2* and *PR5* in *med9* and *morc1/2* s were induced less robustly and rapidly relative to WT (Figure 17b and c), consistent with their susceptible phenotypes to *AvrPst* and *VirPst*.

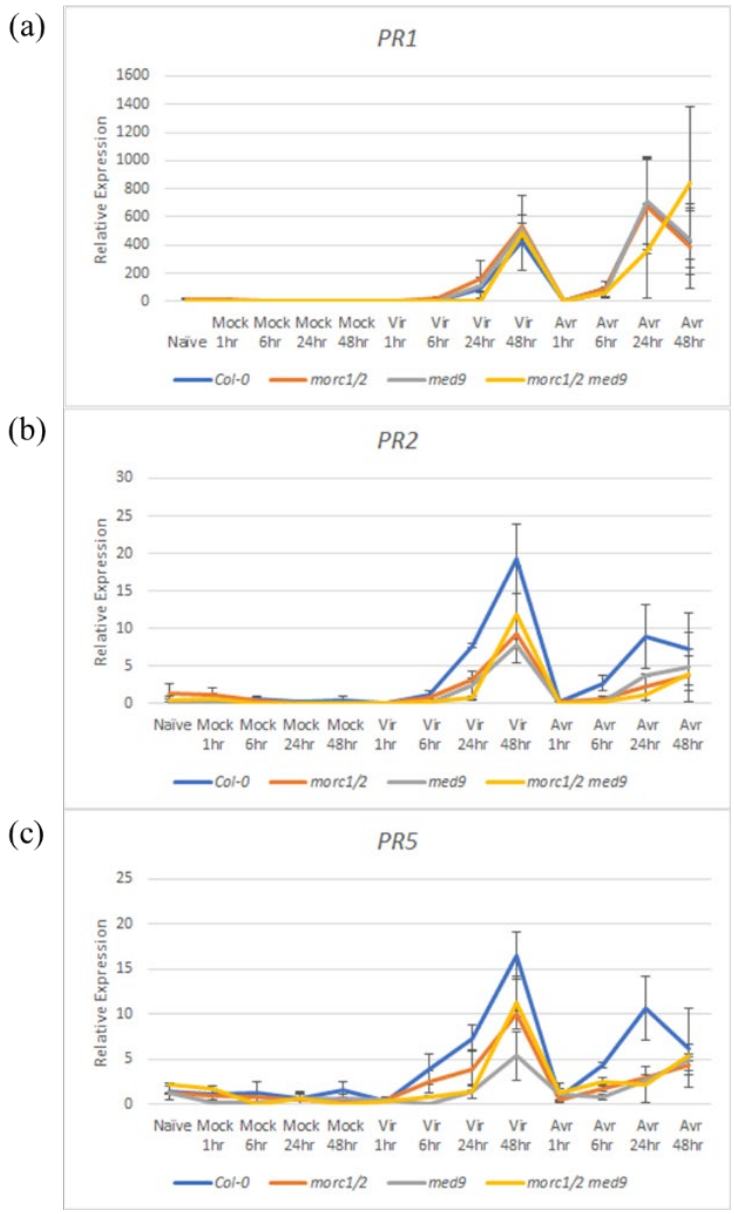

Figure 17. MED9 regulates the expression of select defense genes in response to *VirPst* and *AvrPst.* Total RNA was isolated from 3.5 week-old indicated lines that were infected with *VirPst*, *AvrPst,* and mock at 10^6 cfu/ml for the indicated time. Transcript levels were examined using real-time qRT-PCR with primers specific for the specific genes. *Tip41-like* gene was used as a control. The mean of three biological replicates ± SD is presented. Two technical replicates were performed. 10 mM of $MgCl_2$ was used as mock treatment. (a) *PR1* (b) *PR2* (c) *PR5*

3.5 *Kinetics of the MORC1-MED9 interaction in Arabidopsis*

Physical MORC1-MED9 interaction was established in the Y2H assay (Figure 4, 5, 13, and 14) and confirmed in an *N. benthamiana* co-IP experiment (Figure 6). As MORC1 displays nucleus-translocation in response to biotic stress (Kang et al., 2012), it is feasible that the MORC1-MED9 interaction depends on stress.

A transgenic line carrying *Myc-MORC1* and *MED9-Flag* under their cognate promoters was subject to a co-IP experiment. The MORC1-MED9 interaction was monitored at 6 and 24 hpi with *AvrPst* (Figure 18). The co-IP, in which MORC1 was precipitated and MED9 was examined for coimmunoprecipitation, showed that *AvrPst* significantly increased the MORC1-MED9 interaction at 24 hpi. In response to *AvrPst,* over 99% of the inducible defense genes in Arabidopsis peaks at around six hpi and begins curbing this induced expression at 24 hpi (Mine et al., 2018) (Bordiya and Kang, unpublished). Note that three *PR* genes that display a 24hr-peak are rather the exceptions than the rule in an overall group of genes showing a dynamic induction pattern. Given the kinetics of the defense gene induction, it is unlikely that MED9 interacts with MORC1 to enhance transcription. Instead, it is conceivable that MED9 interacts with MORC1 to restrain the full-blown expression of defense genes. Since MED14 interacts with a co-repressor LUG to facilitate target gene repression in Arabidopsis, MED9 could also function as a repressor in conjunction with MORC1, later time points.

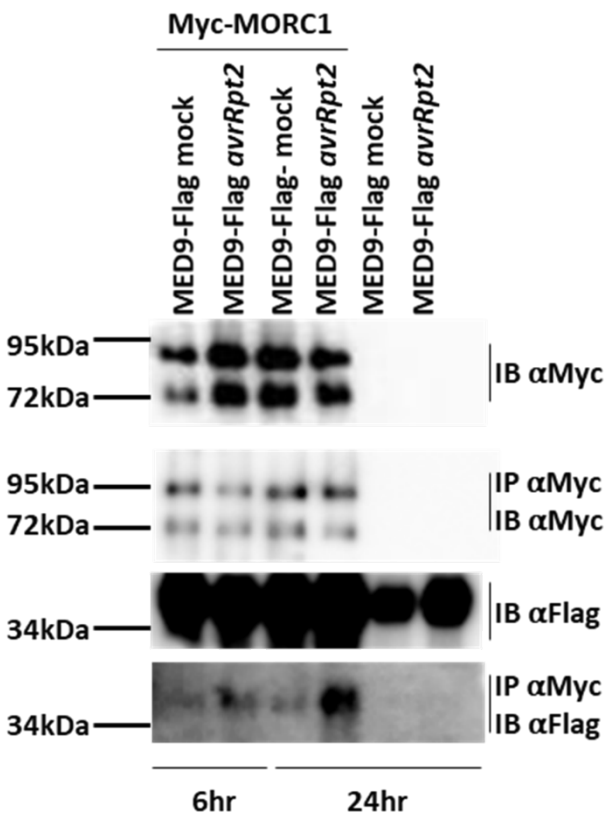

Figure 18. Interaction of MED9 with MORC1 is enhanced by ETI after the first wave of defense gene induction. 3.5 week-old transgenic Arabidopsis line (first four lanes) carrying *Myc-MORC1* and *MED9-Flag* were used; both transgenes were under their native promoters. Plants were infected with *AvrPst* at 10^6cfu/ml for the indicated times; a *MED9-Flag* transgeneic line was used as a negative control (the last two lanes). Proteins extracted were immunoprecipitated with αMyc. Expression of *Myc-MORC1* and *MED9-Flag* were examined by immunoblot (IB) analysis with αMyc and αFlag, respectively. Proteins co-immunoprecipitated by αMyc were detected by IB with αMyc and αFlag.

4. INTERACTION BETWEEN MED9 AND MORC1 IS IMPORTANT IN BALANCING GROWTH-DEFENSE

4.1 *Fitness cost assessed by repeated pathogen challenges*

morc1/2 and *med9* displayed compromised resistance to *AvrPst* and *VirPst*, while their higher-order mutant, tKO (*morc1/2 med9*), regained WT-level resistance (Figure 15). I further investigated this seemingly counterintuitive observation by tracking three commonly used defense genes (*PR1*, *PR2*, and *PR5*) to obtain a snapshot of defense signaling; this investigation revealed the slow but sustained expression of defense genes in *tKO*. While regaining bacterial resistance to the level of WT through extended-expression is likely beneficial to the host, it is frequently observed that excessive resistance incurs fitness-cost (Huot et al., 2014). Therefore, I hypothesized that regaining resistance in *tKO* likely incurs fitness-penalty.

I measured the size and weight of *morc1/2*, *med9,* and *tKO* (Figure 20a) three weeks after germination and did not find any significant difference relative to WT; note that their representative pictures were presented earlier (Figure 19). These plants were then repeatedly infected with *AvrPst* at a clinical dose of 1 x 10^5 cfu/ml for three weeks and evaluated for their growth characteristics (Figure 20): the total weight, the weight and number of leaves, the weight and number of inflorescence, the number of siliques. The same growth characteristics of those which received mock infection were compared to deduce fitness cost.

Remarkably, only *tKO* plants showed a significant reduction in all six measurements in response to *AvrPst* infection relative to the mock control (Figure 20), indicating severe fitness cost due to recurrent infection. For instance, the total leaf weight

of *tKO* was reduced by over 25% in response to *AvrPst* infection, while those of WT and the single mutants showed negligible changes. In particular, siliques, the long and narrow seedpods in Arabidopsis, in *tKO* were significantly reduced in number, suggesting that sexual reproduction was also affected as a part of fitness penalty.

Figure 19. Phenotypes of 3.5 week-old WT(Col-0), *morc1/2*, *med9*, and *morc1/2 med9*.

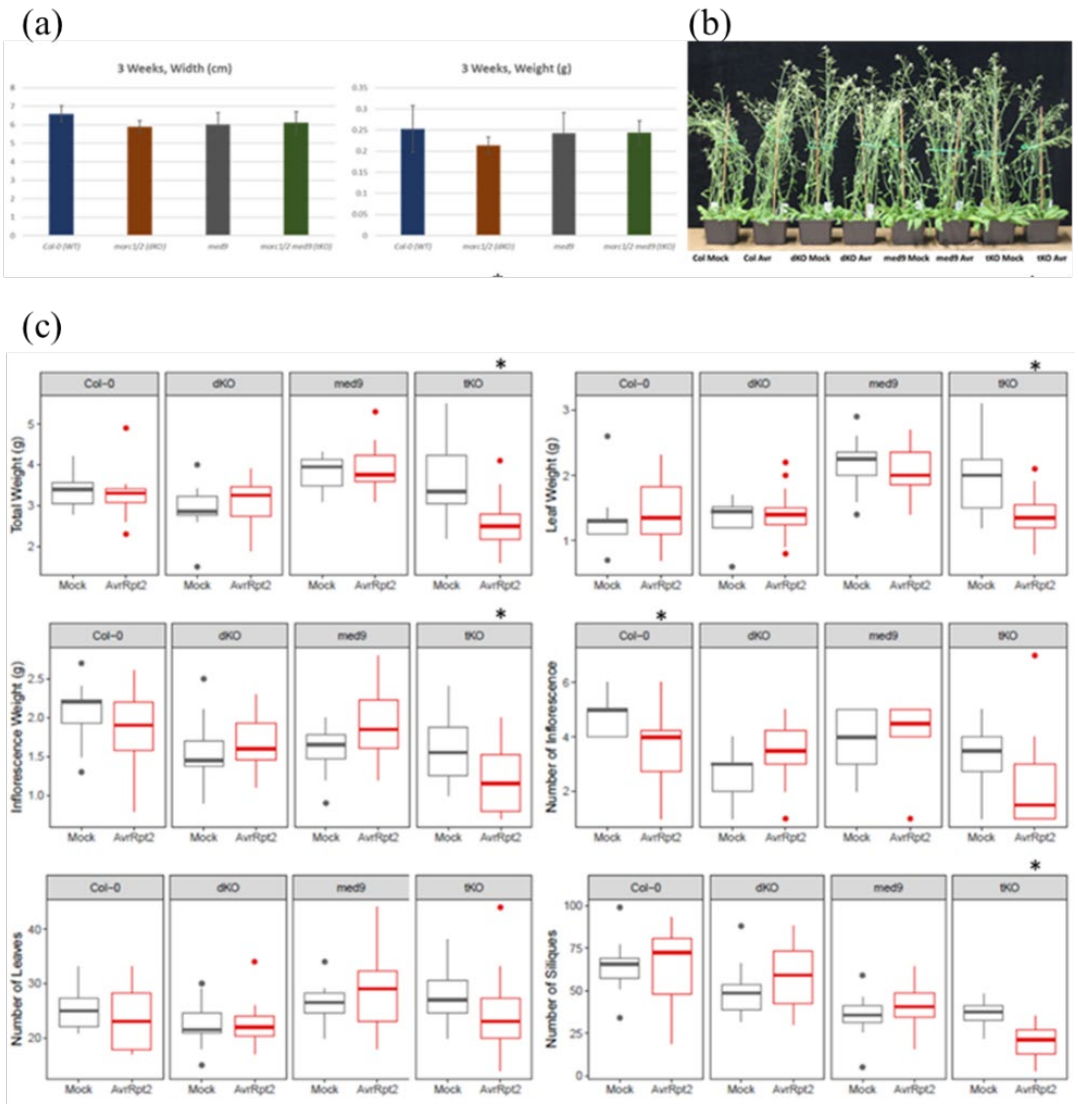

Figure 20. Fitness cost assessment by serial pathogen challenges. 3.5 weeks-old WT (Col-0), *morc1/2* (*dKO*), *med9*, and *med9 morc1/2* (*tKO*) were infected with *AvrPst* at 10^5 cfu/ml every two days for three weeks. (a) Width and weight of 3.5 weeks-old plants were measured. (b) A photo of plants after the serial infection. (c) Several growth and development characteristics were measured after the serial infection. To this end, weight of total plants, leaf, inflorescence were measured and number of inflorescences, leaves, and siliques were counted. A minimum of ten plants in each line were examined. Statistical difference between mock and *AvrPst* treatment is indicated; *P < 0.05, (*t*-test).

4.2 *Transcription dynamics of defense genes, upregulated and downregulated, in Arabidopsis*

I used selected-defense marker genes (*PR1, PR2,* and *PR5*) at multiple time points to track defense signaling in *med9*-associated lines (Figure 17), which revealed that *tKO* supports slow but prolonged induction. I here extended the transcriptional analysis to the defense genes that we identified via an RNA-seq approach (Bordiya and Kang, unpublished). For a transcriptome dynamic analysis under biotic stress, Dr. Bordiya, a former graduate student in the lab, performed an RNA-seq analysis of WT at 0, 1, 6, 24, and 48 hpi with mock, *AvrPst* and *VirPst*.

Clustering analysis of the transcriptome dataset above was performed to identify distinct expression patterns of expression kinetics (Oluwadamilare and Kang, unpublished). Among a few clustering algorithms tested, SOM (self-organizing map) provided the most consistent and reliable clusters, resulting in five upregulated (U1 - U5) and four downregulated (D1 - D4) groups (Figure 21) (Oluwadamilare and Kang, unpublished).

U1 and U3 represent a group of defense genes that peak at 6 and 24 hpi in response to *AvrPst* and *VirPst*, respectively. U5 resembles U1/U3 except for its additional induction at 1 hpi with all treatments, suggesting that these genes also respond to the physical disruption involved with syringe infiltration. Note that I used a syringe-infiltration method to deliver pathogens uniformly. U2 contains genes that react to *VirPst* faster than *AvrPst.* U4 responds slower than U1/U3/U5 with an induction peak to *AvrPst* at generally 24 hpi, which includes the *PR* genes.

All the down-regulated groups have an expression valley at 6 hpi in response to *AvrPst*. While D1/D2 resemble D4 to some degree, their suppression at 1 hpi to all the treatments was especially notable. D3, in contrast, showed a marginal induction at 1 hpi to all the treatments. It was noteworthy that all the downregulated genes showed the most suppression at 6 hpi to *AvrPst*, faster than those to *VirPst*, raising the possibility that this down-regulation is part of the defense response.

The GO (gene ontology) analysis was performed as shown in Figure 22 to gain insight into the function of these dynamically expressed genes. A significant number of upregulated genes belong to the GO 'defense response', while the downregulated genes have a substantial presence of GO related to 'photosynthesis', including photosynthesis, plastid translation, and chloroplast organization. Photosynthesis-related genes as a defense-downregulated group in Arabidopsis were reported in two transcriptome studies (Lewis et al., 2015, Mine et al., 2018), although their exact roles in defense signaling are currently unclear.

The significant presence of down-regulated genes, like up-regulated counterparts, suggest that a master transcriptional regulator likely coordinates suppression of the photosynthetic process in response to biotic stress. Thus, the binding motif in the promoter (1kb in length) of the downregulated genes was analyzed (Figure 23). This motif analysis identified a G-box (CACGTG) in 31 down-regulated genes in the D4 cluster. The presence of a G-box was noteworthy since PIFs (Phytochrome Interacting Factors), which are G-Box binding proteins, are well-known transcription factors in photosynthesis (Leivar & Quail, 2011a). Furthermore, PIFs have been proposed as a signal integrating hub in which multiple cellular processes, including photosynthesis,

would be coordinated (Paik et al., 2017). My observations, together with these research developments, therefore raise the possibility that PIFs may suppress the D4 cluster and modulate the fitness balance between growth and immunity.

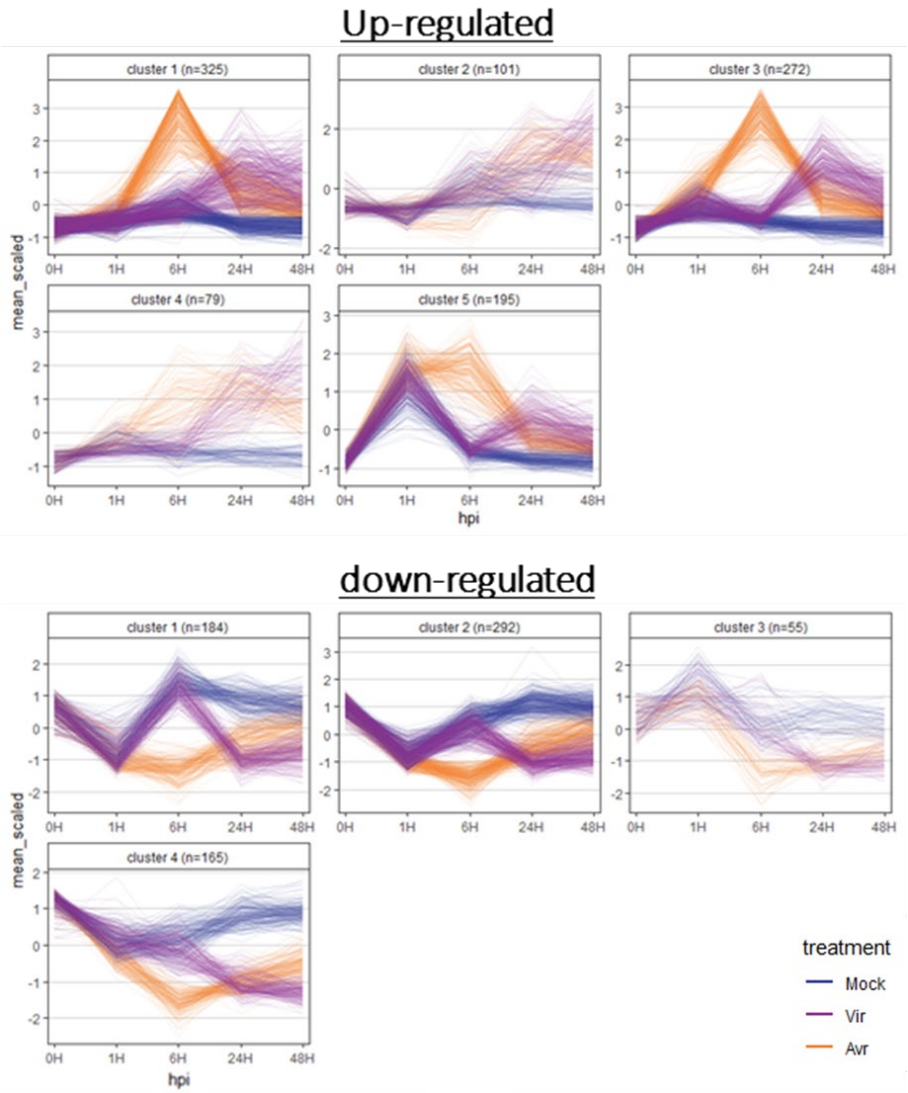

Figure 21. Kinetics and clustering analysis of defense transcriptome in response to *VirPst* and *AvrPst* infection (Oluwadamilare and Kang, unpublished). RNA extracted from 3.5-weeks old Arabidopsis infected with *VirPst* and *AvrPst* for the indicated times was subject to conventional RNA-seq analysis. Transcripts with a dynamic change were clustered via SOM algorithm.

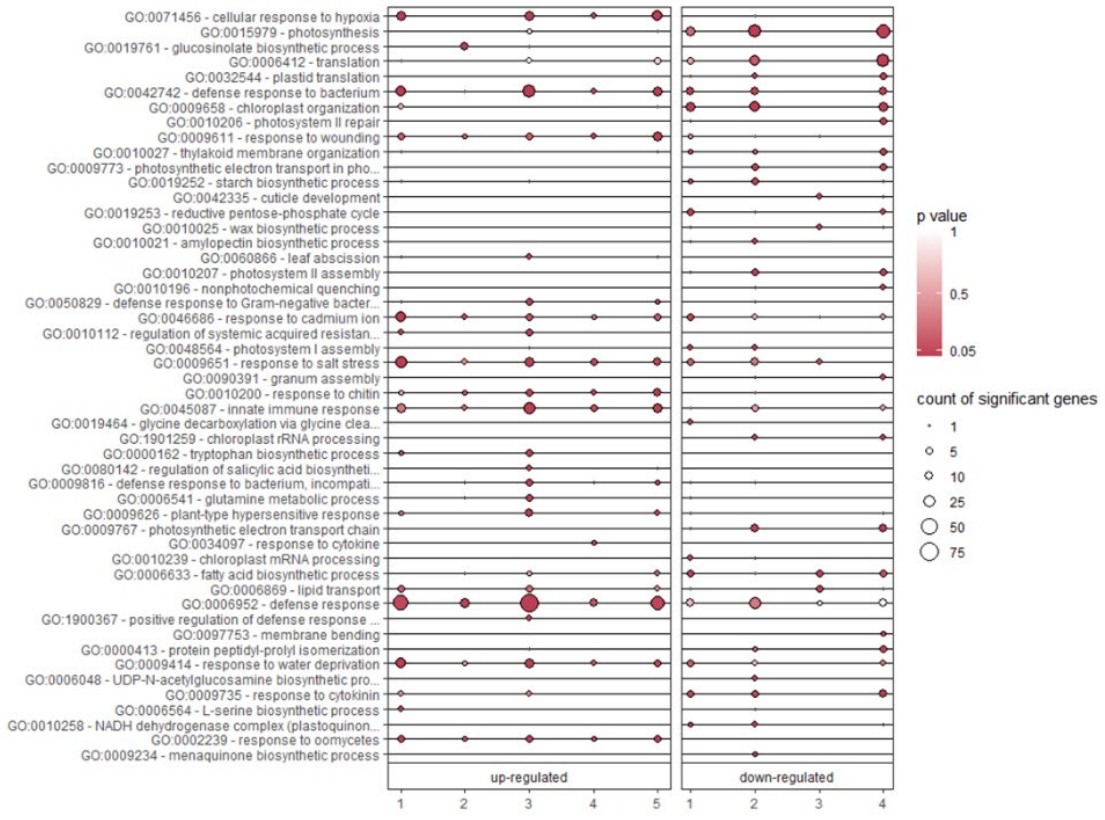

Figure 22. Gene ontology analysis for upregulated and downregulated defense genes (Oluwadamilare and Kang, unpublished).

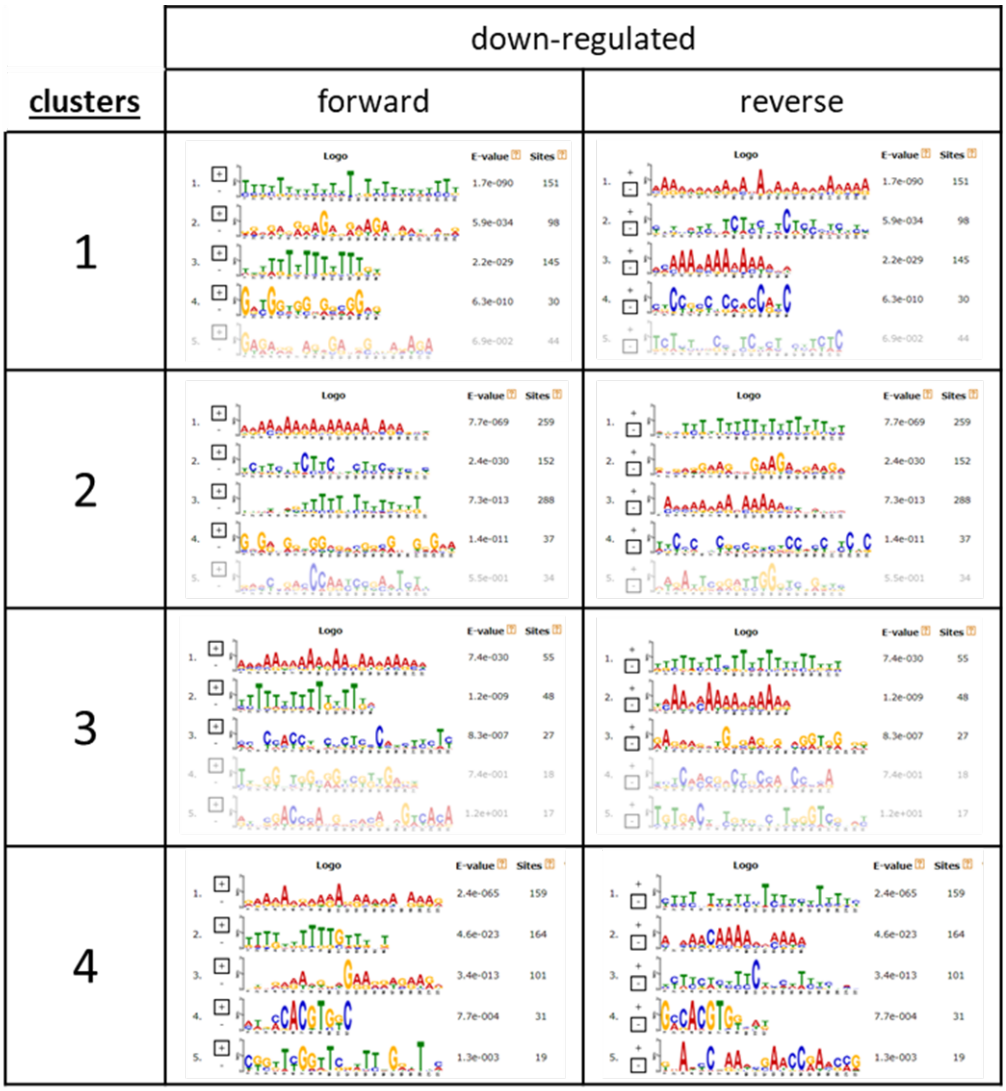

Figure 23. Motif analysis of the down-regulated gene clusters (Oluwadamilare and Kang, unpublished).

4.3 *Targeted transcriptome analysis found that MORC1 and MED9 together wind down defense responses*

I performed the transcriptional analysis of select defense genes using RNA-mediated oligonucleotide annealing, selection, and ligation with next-generation sequencing (RASL-seq) [36, 37]. We used RASL-seq to analyze the induction dynamics of defense genes in Arabidopsis challenged with *AvrPst* and *VirPst*. We used hundreds of probes targeting defense genes, transposable elements, hormone response genes, growth/photosynthesis genes, and housekeeping genes. This targeted approach monitored over a hundred genes that belong to the clusters of defense genes at 0, 1, 6, 24 and 48 hpi with mock, *AvrPst*, and *VirPst*. This approach included 74 upregulated and 28 downregulated genes. U1, U3, and D4 represented more in the analysis, as they included more upregulated and downregulated defense genes. In addition, U4, with late induction kinetics, had multiple genes included.

In U1/U3, *morc1/2* displayed notably enhanced induction at 6 hpi with *AvrPst* relative to the other three lines (Figure 24a), while *tKO* showed less robust expression at 6 and 24 hpi with *VirPst*. However, U1/U3 with faster induction kinetics was not significantly changed in *tKO* (Figure 17). *PR1* and *PR5* were included in the U4 cluster. Consistent with Figure 17, the U4 cluster displayed slower induction kinetics reacting to *AvrPst*. Specifically, the other three lines curbed expression by 48 hpi with *AvrPst*, while *tKO* appeared to still maintain induction at the same time. These observations together suggest that sluggish induction kinetics in *tKO* is limited to U4.

Among the down-regulated clusters, I analyzed most genes from D4, as this cluster mirrored U1/U3, a group of defense genes with faster kinetics. WT showed a

suppression valley at 6 hpi with *AvrPst* (Figure 24b). *med9* and *tKO,* on the other hand, had a valley at 24 instead, although these two lines showed comparable recovery to each other. In D4, I chose 12 genes with G boxes in their promoters (1kb in length). Thus, I separately presented the D4 genes with and without the G boxes (Figure 25). The presence of the G box provided more dynamic transcription changes in all the lines, highlighting the importance of the G-box in this downregulation. Again, *med9* and *tKO* showed slow recovery, as seen in Figure 24b. These G-box-containing genes were individually presented in Figure 26.

Unlike the up-regulated defense genes, *tKO* was not significantly separated from *med9* in transcription dynamics reacting to *AvrPst*. This data suggests that the fitness cost observed with *tKO* may involve additional factor in addition to photosynthesis-related processes. Alternatively, my targeted transcriptome analysis might have missed a group of under-regulated genes that are significantly affected more in *tKO* than its single mutants.

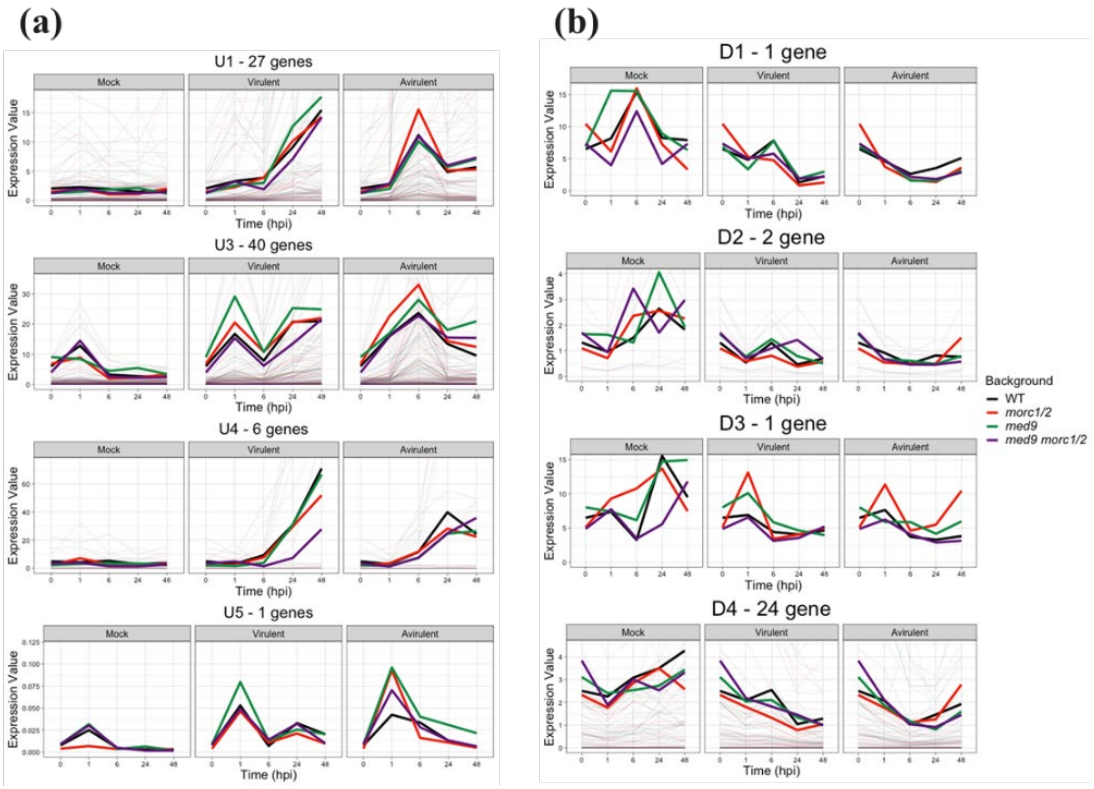

Figure 24. MED9 and MORC1/2 are involved in regulating transcription kinetics of defense genes. A time-course and targeted transcription analysis were performed on WT (Col-0), *morc1/2*, *med9* and *med9 morc1/2* infected with Mock, *VirPst* or *AvrPst* for the indicated times by using RASL-seq. The y-axis represents the mean expression value of defense genes in each cluster into four clusters is presented. The x-axis denotes the corresponding timepoint (hpi). The treatment method is denoted above each facet of line graph. (a) Four clusters of upregulated genes (b) four clusters of downregulated genes.

(a) With G-Box

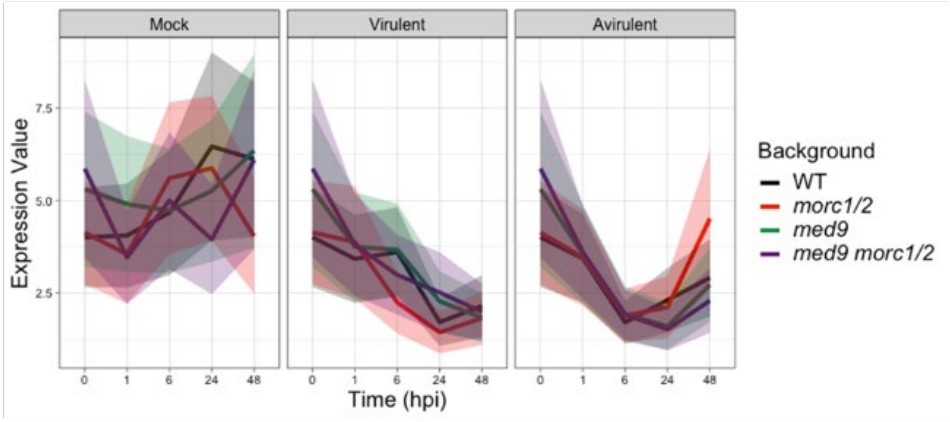

(b)

Without G-Box

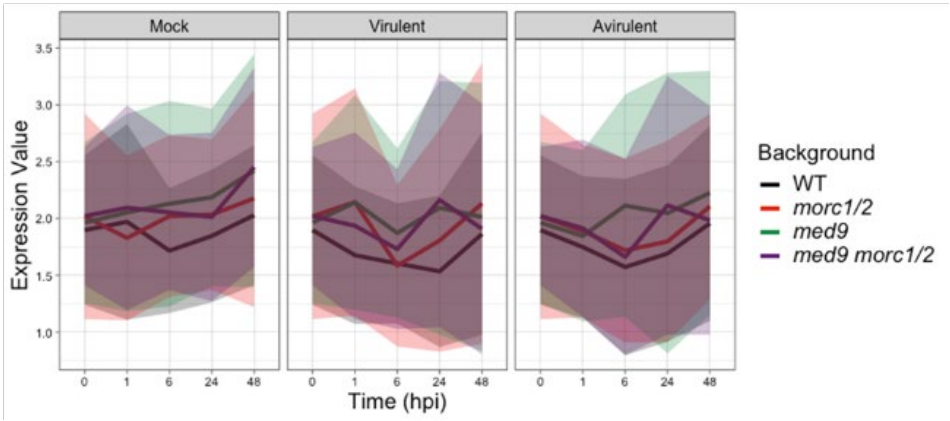

Figure 25. Down-regulated defense genes with and without the G-box. The downregulated defense genes were grouped to two, depending on the presence of the G-box: (a) 'with G-box' , (b) 'without G-box'. The y-axis represents the mean expression value of defense genes in each group is presented. The x-axis denotes the corresponding timepoint (hpi). Standard error (SE) among the grouped genes is represented by the shaded regions.

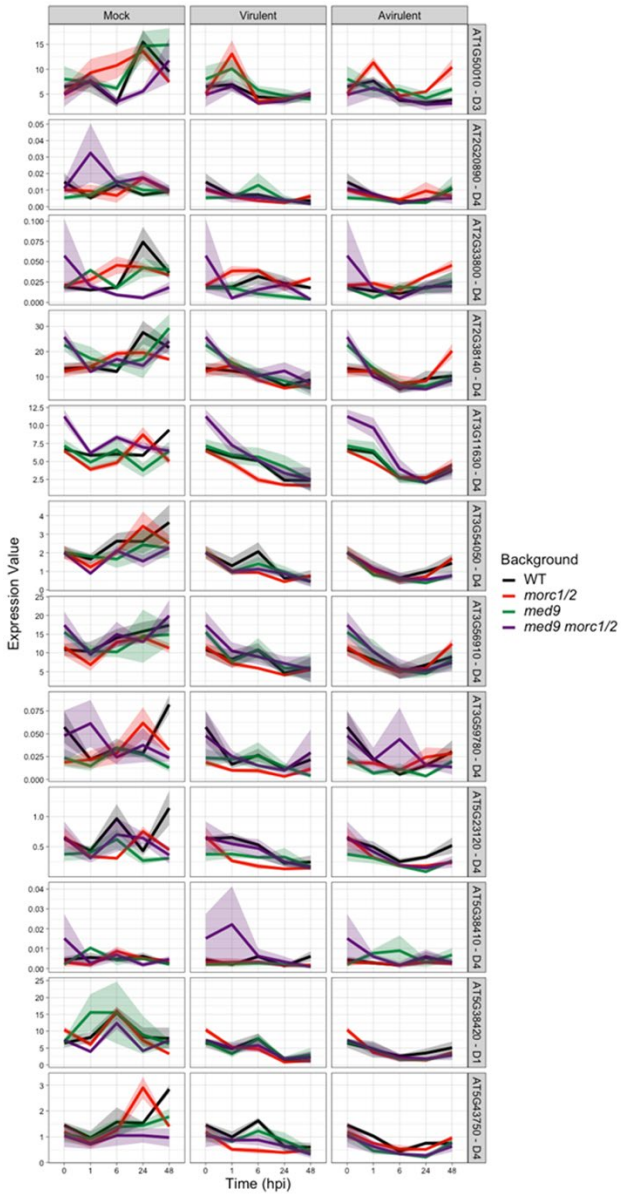

Figure 26. Twelve genes containing the G-box in the down-regulated clusters. The time course RASL-seq data representing the mean expression value in the y-axis calculated among three biological replicates for genes containing the G-box motif are presented. WT (Col-0), *morc1/2*, *med9,* or *med9 morc1/2* were challenged with Mock, *VirPst*, and *AvrPst*. The x-axis denotes the corresponding timepoint (hpi). SE among biological replicates is represented by the shaded regions, colored with the corresponding color. Gene names along with the associated downregulated gene cluster are denoted on the right hand side of each facet.

4.4 *Characterization of PIFs in plant defense signaling*

Down-regulated genes identified from the RNA-seq approach revealed the presence of the G-box in the promoter region when motif identification software, such as Homer and Tomtom [38, 39], were used. PIF is a well-characterized G-box binding protein and, in some cases, negatively regulates photosynthesis genes [40]. From these observations, I hypothesized that PIFs negatively regulate photosynthesis to support defense responses.

To address my hypothesis, I obtained transgenic lines constitutively expressing *PIF3* and *PIF4* (*35S::PIF-Myc* and *35S::PIF4-Myc*) and challenged them with *AvrPst* and *VirPst* (Figure 27). These *PIF* overexpression lines displayed enhanced resistance to *AvrPst* relative to WT while showing little to no difference to *VirPst* (Figure 27), suggesting that PIFs are involved in ETI. However, when their transcription was analyzed in our RNA-seq data, neither *PIF3* nor *PIF4* show any up-regulated induction pattern (data not shown).

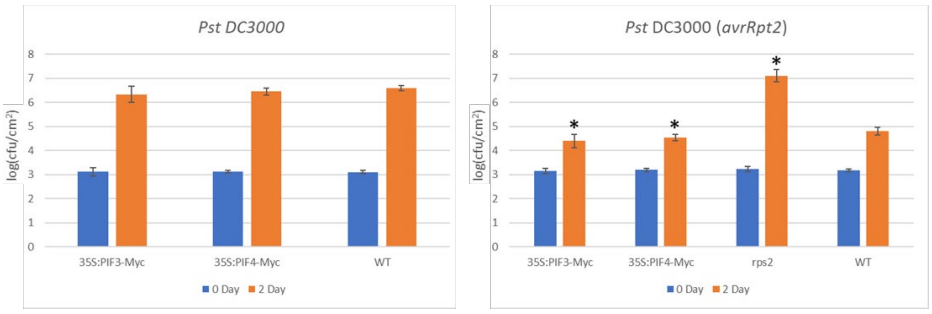

Figure 27. Resistance phenotypes of PIF3 and PIF4 overexpressing Arabidopsis. *PIF3-myc* and *PIF4-myc* under 35S promoter were overexpressed in Arabidopsis. Bacterial growth in these transgenic lines were measured at 0 and 2 dpi with *VirPst* and *AvrPst* at 10^5 cfu/ml. The mean ± SD (n = 2) is presented. Two independent biological replicates were performed. Statistical difference from WT is indicated; *P < 0.05 (*t*-test).

However, transcription factors often fine-tune the expression of the target genes via its nuclear localization [41]. To characterize the nucleus-cytoplasm shuttling of PIF3 and PIF4 under biotic stress, I performed a subcellular fractionation experiment using *35s::PIF3-myc* and *35::PIF4-myc* at 6 hpi with Mock, *VirPst*, and *AvrPst* (Figure 28). PIF4 was stable and readily detected in both the cytosol and nucleus under all treatments (Figure 28b). However, PIF3, by contrast, showed a significant increase in the nucleus in response to *AvrPst* (Figure 28a). Since *PIF3* is under the 35S promoter, which supports constant expression, this increase likely reflects that PIF3 levels become stabilized reacting *AvrPst*. PIF proteins are known to subject to ubiquitin-mediated degradation [42]. Thus, the stabilization under biotic stress may play an important role in modulating photosynthesis suppression.

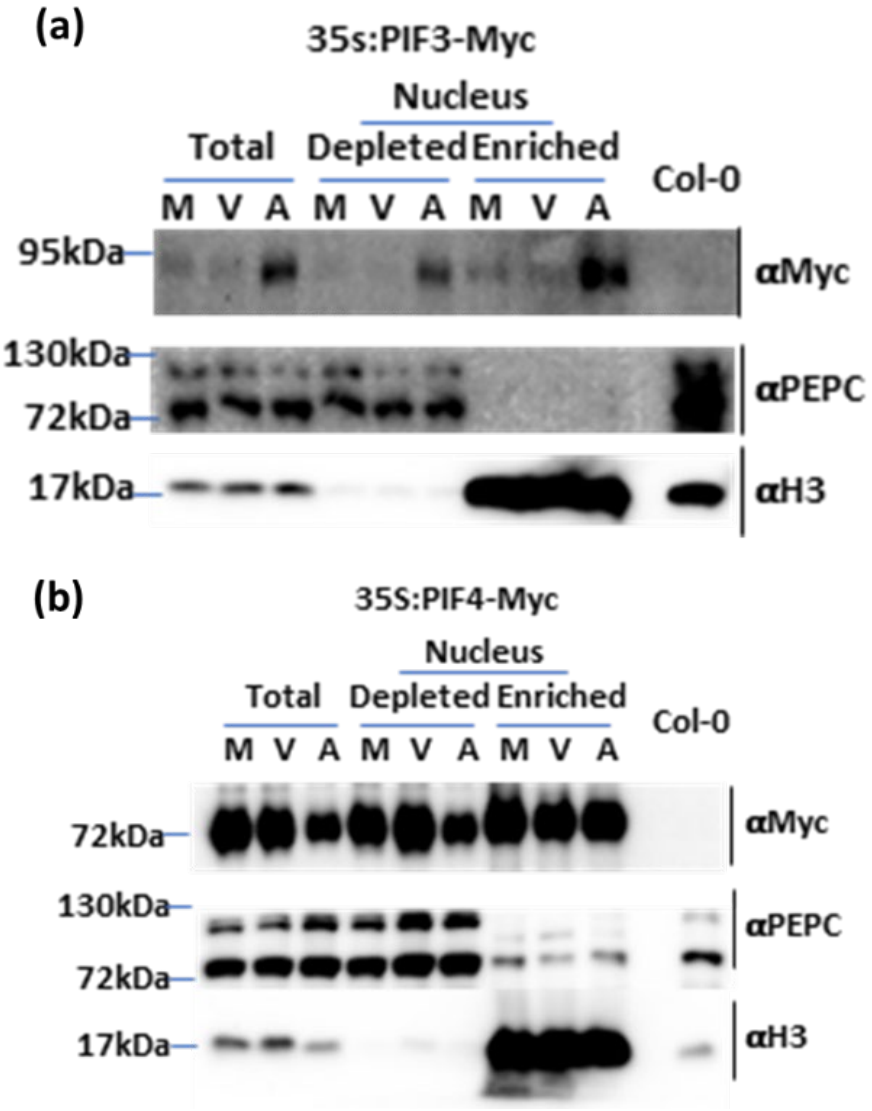

Figure 28. Subcellular localization of PIF3/4 in response to *Pst.* Transgenic Arabidopsis plants overexpressing (a) *PIF3-Myc* and (b) *PIF4-Myc* were infected with mock (M), *AvrPst* (A), and *VirPst* at 10^6 cfu/ml for 6 hr. Homogenized tissue was separated into nucleus-depleted or -enriched fractions. These fractionated extracts were examined by immunoblotting with αMyc. Antibodies against histone H3 and PEPC (phosphoenolpyruvate carboxylase), a nuclear and a cytosolic protein, respectively, were used to ensure appropriate enrichment or depletion of nuclei. Protein extracts from WT (Col-0) was used as a negative control.

5. SUMMARY

This project began with a Y2H screening for proteins interacting with MORC1, which functions in both immunity and epigenetics in plants. 14 proteins, termed as MORC1-interacting proteins (MIPs), were identified, and eight of them were predicted to be nuclear-localized and putative chromatin remodeling components. MED9, a member of the mediator complex which interfaces between transcription factors and RNAP II, was identified as one of the MIPs. My genetics analysis found that MED9 is a positive regulator for plant defense signaling, just like MORC1, since each mutant displayed compromised resistance to *Pst.* Remarkably, a combined mutant, in which MED9 and MORC1/2 (note that MORC2 needs to be also removed as it is the closest homolog to MORC1) are largely absent, regained WT-level bacterial resistance, suggesting that an unrecognized complex interaction leads to the unexpected outcome. Moreover, the physical interaction between MORC1 and MED9 was further enhanced at 24 hpi with *AvrPst*, not at 6 hpi, suggesting that a combinatorial function from these factors operates well after the initial wave of defense gene induction.

To characterize this enigmatic resistance trait in *tKO*, I tracked the transcription dynamics of the defense genes that were up- and down-regulated at multiple-time points, reacting to *AvrPst*. Interestingly, *tKO* displayed sluggish but sustained expression of late defense genes that mainly peak at 24 hpi with *AvrPst*. However, this sustained expression pattern, which may explain how WT-level resistance was restored in *tKO*, came with a measurable fitness cost. The fitness cost became evident when *tKO* was infected repeatedly with *AvrPst*. This extended biotic stress triggered a significant reduction in growth and reproduction of *tKO*, while there was little to no effect on those of WT, *med9,*

and *morc1/2*. Down-regulated defense genes had a significant number of photosynthesis-related genes, many of which had the G-box in their promoter. While marginal, the recovery from rapid suppression for the down-regulated genes with the G-box was slow in *tKO* relative to WT, raising the possibility that prolonged downregulation of the photosynthesis-related process may be the cause of growth retardation. PIF3 is a G-box-binding factor that often negatively regulates photosynthetic processes. Thus, to assess if this transcription factor is involved in immunity, I tested a *PIF3* overexpression line for the resistance phenotype and found enhanced resistance to *AvrPst*. Remarkably, PIF3 became stabilized in the nucleus, and its level significantly increased in response to *AvrPst*.

In sum, I found that sustained expression of the up-regulated defense genes in *tKO* restored resistance but incurred fitness penalty. PIF3 appears to be a candidate master regulator that swiftly suppresses the photosynthetic process to promote defense responses. This dynamic transcriptional reprogramming seems to require coordinated action between MORC1 and MED9. These research findings will, therefore, provide a molecular guideline for plant breeders on how growth and defense should be optimized by modulating key coordinators such as MORC1, MED9, and PIF3.

6. MATERIALS AND METHODS

6.1 *Generating DNA constructs*

The coding sequences (CDS) for *MIPs* and *MORC1* were amplified *via* PCR and cloned into pJET (Thermo Fisher) blunt end vector.

The following yeast two-hybrid constructs were constructed to confirm the MORC1-MIP interaction: CDS was inserted to the pB27 bait plasmid carrying a 5' LexA DNA binding domain by using SfiI sites and the pP6 prey plasmid with a 5' GAL4 activating domain by using *SfiI* sites.

The following yeast two-hybrid plasmids were constructed to test the interaction of MORC1 with mediator subunits (Figure 14). The CDSs were cloned into pDONR with Gateway LR Clonase II (Invitrogen). pDONR mediators and *MORC1* full/C-terminal vectors were recombined to pDEST-AD or -DB vectors by transforming 1µl of LR reaction into DB3.1 competent cells. The CDS was cloned into either pPC86 (Gal4 transcriptional activation domain) or pPC97 (Gal4 binding domain).

The following plasmids for SMC expressions were constructed to perform a co-IP experiment. The CDS of the SMC genes were cloned into pER8 tagged at the 3' end with triple HA (pET-HA) by using *AscI* sites. Truncated SMC mutants were generated by using the primers listed in Table 4.

The BAC T7N22 was purified via $CsCl_2$ to amplify genomic MED9. This amplicon was digested with *XhoI* site to make and inserted to the pBKS to make pBKS-gMED9. It is ready to be targeted by Cas9 Nuclease (Cas Nuclease NLS, NEB) which is a double-stranded DNA endonuclease that is guided to its target. The CAS reaction at room temperature was performed in the following mix:1x Cas Nuclease reaction buffer,

300 nM sgRNA, 1 μM Cas9 Nuclease in 27 ul total volume without the DNA substrate. This mix was incubated for 10 minutes. 30 nM substrate DNA was added to the mix and incubated at 37°C for 15 minutes. 1ul of Proteinase K was added and incubated for 10 minutes. A flag-tag amplified from Flag-pBA by using gMED9-F/R in Table 4 was ligated together with pBSK-MED9 T4 DNA ligase (Fisher), which makes pBSK-gMED9-Flag. The gMED9-Flag fragment mobilized by *XhoI* and was ligated to pPZP.h using *SalI*.

6.2 *Yeast-2-hybrids*

We performed Mediators and MORC1 yeast two hybrid with AT3G21350 MED6, AT5G42020 AtMED37, AT5G48630 AtCycC, AT5G52470 AtMED36B, AT1G11760 MED2, AT1G16430 AtMED22, AT1G44910 AtMED35, AT55080 AtMED9, AT2G28230 AtMED20, AT3G01435 AtMED11, AT3G09180 AtMED3, AT4G25630 AtMED36A, AT5G05140 AtMED26, AT5G12230 AtMED19A, AT5G19480 AtMED19B, AT5G19910 AtMED31 and AT5G41910 AtMED10.

pB27 bait and pP6 prey plasmid were transformed into Y187 and L40 yeast strains, respectively. pPC86 or pPC97 (Gal4 transcriptional activation or binding domain) were introduced to the yeast strain Y8800 (AD) or Y8930 (DB), respectively.

These two yeast-2-hybrid systems use HIS3 reporter genes. The HIS3 encodes the gene for imidazoleglycerol-phosphate dehydratase, the product of which forms an enzyme required for synthesis of the amino acid, histidine (His). Minimum media containing histidine was used to show the growth, while those without were used to test the interaction between prey and bait. Amino-1,2,4-triazole (AT) is a competitive histidine synthesis inhibitor that was used to test the interaction strength. Stronger

interaction leads to higher HIS3 expression, which can outcompete AT. 0.1mM was used for a stringent condition.

6.3 *Transient expression in Nicotiana benthamiana*

The CDSs were cloned into the pER8 vector, which was transformed into Agrobacterium strain GV2260. The HcPro silencing suppressor from Tobacco etch virus was used to enhance transient expression. pBIN-GFP was grown on plates containing kanamycin and used as a negative control. Agrobacteria were cultured in LB liquid media for one day at 28°C. Growing the culture and its infiltration process were performed as described (Menke et al., 2005). The infiltration mix was adjusted to 0.5 and were incubated at room temperature for additional 2 hours. The infiltration solutions were mixed with an equal ratio for components for the expression, including pBA-HcPro (also labeled as pBA-TEV) and infiltrated by a needless syringe into leaves of *N. benthamiana*. 30 μM estradiol in 0.1% Tween-20 was sprayed on the leaves to induce the expression of pER8-driven constructs. These plants were further grown for additional two days at room temperature.

6.4 *Immunoblotting analysis*

Immunoblotting analysis was performed as described using an enhanced chemiluminescence method (Kang & Klessig, 2005). Frozen tissue samples, mostly stored at -75°C deep freezer, were ground with a ceramic bead with 4x SDS sample buffer containing DTT at 60 mg/ml, by using a paint shaker (used as a homogenizer). Once homogenized, these samples were boiled for 5 minutes and centrifuged at 21,100 xg for 1 minute. The supernatant was loaded (5 μl per sample in general) into SDS-PAGE along with a protein ladder (Fisher Ez-Run, 5 μl in general) and transferred onto a PVDF

membrane (Immobilon) using 10x transfer buffer with methanol. Membranes were treated with methanol and allowed dried completely. After again soaked in methanol and washed with PBS three times for 5 minutes, the membrane was placed in 3B1M Buffer (3% BSA, 1% milk in 1x PBS) for 30 minutes at room temperature and incubated at 4°C in 3B1M Buffer with an antibody and shaking at 200rpm. The membranes were washed with PBS, PBS-T, and PBS buffer twice each for 5 minutes for a total washing of 30 minutes, treated with ECL2 solution (Fisher) and imaged using an EM-CCD camera (Azure Biosystems, C600). Antibodies used include HRP-conjugated anti-Myc (Santa Cruz Biotechnology; 1:5,000), HRP-conjugated anti-FLAG (Sigma; 1:5,000), HRP-conjugated anti-HA (Sigma; 1:10,000), anti-PEPC [Rockland; 1:10,000, secondary antibody: HRP-conjugated anti-Rabbit (Abcam; 1:10,000)], and anti-Histone H3 [(Abcam; 1:10,000, secondary antibody: HRP-conjugated anti-Rabbit (Abcam; 1:10,000)].

6.5 *Co-immunoprecipitation*

Leaves of Arabidopsis or *N. benthamiana* were homogenized with mortar and pestle in liquid nitrogen. Samples were grounded again in 750 ul extraction buffer (GTEN buffer (150 mM NaCl, 1 mM EDTA, 25 mM Tris 7.5, and 10% glycerol) with 2% polyvinylpolypyrrolidone, 1x protease inhibitor cocktail (PIC), and 0.1% Triton X-100. These protein extracts were collected and spun at 5,000 x g at 4°C for 5 minutes, 0.5 ml of which was then subject to size exclusion chromatography by using Illustra NAP-5 Sephadex G-25 DNA grade columns (GE Healthcare). Eluates were collected in 1.5ml Eppendorf tubes, added to 20 µl of anti-mouse IgG agarose beads (Sigma), and incubated at 4°C for 2 hours with a mild rotation. After removing the anti-mouse IgG agarose

beads, the remaining solutions were added with 20 µl of agarose beads conjugated with a target antibody and incubated at 4°C overnight. These solutions were washed a minimum of six times with 1 ml IP buffer (GTEN buffer with 0.15% NP-40 and 5 mM DTT) and added with 30 µl of 4x SDS sample buffer before proceeding to immunoblotting analysis.

6.6 *Imaging-based and conventional leaf-disc-based resistance assay*

Arabidopsis plants were grown in soil at 22°C, 60% relative humidity, and a 16-hour light period. 3.5-week-old plants were infiltrated using a needleless syringe with an indicated inoculum of *Pseudomonas syringae* pv. *Tomato* (*Pst*) *DC3000* carrying a luminescent *luxCDABE* reporter gene grown for two days at 28°C in King's B medium with appropriate antibiotics. Each pot image was captured luminescence after 2 days post infiltration using a high throughput EM (Electron Multiplying)-CCD camera (Hamamatsu). The camera was cooled to -80°C, and the image-acquisition was made by using HCImage Live software (Hamamatsu) at the following parameters: binning at 4, photon imaging mode at 1, and exposure time at 2 min. Lighted images of plants were captured without EM under a minimum light. Plants were dark-acclimated for 20 minutes to reduce background luminescence. Luminescence from images was quantitated by using ImageJ (Schneider et al., 2012). The mean grey value of luminescence was measured by selecting the infected area, which was used to calculate actual luminescence by subtracting background luminescence. To analyze anti-bacterial conventional leaf-disc-based resistance assay in Arabidopsis, leaves were needleless syringe infiltrated with 10^5 cfu/ml of *Pst DC3000* in 10mM MgCl2. In 3 DPI, three leaf disks were obtained of the plant and homogenized in a shaker for 1 minute in 500 µl of 0.01% Triton X-100. Waiting for 10 minute in mild rotating shaker, and homogenized samples in a shaker for

1 minute. Samples were vortexed briefly and serially diluted. 20 µl of all dilutions were then plated on LB kanamycin plates and colonies were counted after 36 hours.

6.7 *Fitness cost test*

3.5 weeks after germination, two leave from each plant were infected with *Pst* carrying *AvrRpt2* at 1 x 10^5 CFU/ml in every two days for three weeks. If all the leaves bigger than 0.75 cm in length were infected, these plants skipped the infection till the next round. Upon completion of the treatment, plants were imaged to check the growth and development characteristics presented in Figure 20.

6.8 *RNA preparation, cDNA synthesis and qPCR analysis*

Two leaves were generally collected in a single tube and homogenized in a shaker for 1 minutes using a bead. Their RNAs were extracted using the Purelink RNA Mini kit 250 (Fisher). For their quantitation, RNAs were converted to cDNAs by using by SuperScript RT (Invitrogen) . Maxima SYBR Green qPCR Master Mix (Fisher) was used for quantitative PCR (qPCR). PCR was performed with the following temperature/time profile: 50 °C for 2 min and 95 °C for 10 min, followed by 40 cycles of 95 °C for 25 sec and 60 °C for 1 min.

6.9 *Preparation of equilibrated biotinylated oligo-dT streptavidin-coated beads*

Transferred 3 ul of MagnaBind streptavidin bead slurry (Thermo Scientific; 21344) into a PCR tube on a magnet stand and waited until all beads were bound to the magnetic side. The supernatant was removed and the beads were washed twice gently with 6 ul of Sol A (DEPC-treated 0.1 M NaOH, DEPC-treated 0.05 M NaCl). The beads were washed again using 6 ul of Sol B (DEPC-treated 0.1 M NaCl). The beads were then resuspend in 9 ul of 1x B&W buffer (5 mM Tris-HCl (pH 7.5), 0.5 mM EDTA, 1 M

NaCl) and mixed with 2 ul of biotinylated oligo dT probes (Promega; PR-Z5261, 50pmol/μL, to get final concentration of 5uM). This mix was incubated in a shaking incubator for 60 minutes at room temperature to allow for the binding of the biotinylated oligo dT probes with the streptavidin beads. The tube was placed on a magnetic stand for 2 min and the beads were washed twice with 1x B&W and once with 4x SSC (0.6M NaCl, 60mM Sodium Citrate pH7.0).

6.10 ***RASL-seq library preparation***

10ul of oligo-dT coated streptavidin beads was added to 1ug of total RNA extract and incubated with slow rotation at 4 ℃ for 1 hour and then placed on a magnetic stand for 2 minutes. The supernatant was discarded and washed using 20 ul of 1x SSC twice by pipetting. 20 ul of 10 nM probe mix and 10 ul of 2x SSC was added and the mixture was incubated at 70°C for 10 minutes followed by incubation at 45°C for 60 minutes. The samples were then placed on a magnetic stand for 2 min until the beads bound to the magnetic side. The beads were washed twice with 50 ul washing buffer (20 mM Tris-HCl pH 7.5, 0.1 M NaCl) and once with 20ul 1x Rnl2 buffer (T4 dsRNA Ligase2, NEB; M0239L), ensuring the beads were resuspending completely. The beads were then resuspended in 1 ul of 10x ligase buffer, 0.5 ul of Rnl2 and 8.5 ul of dH2O. After mixing well by pipetting, the solution was incubated at 37°C for 1 hour. After ligation, the samples were placed on a magnetic stand for 2 minutes and the supernatant was discarded. A PCR mixture was prepared by combining 5 ul of the ligated probes, 0.9 ul of 3 uM P5_barcode primer, 0.9 ul of 3 uM P7_barcode primer, 1 ul of 2.5 mM dNTP, 2 ul of 5x Herculase II buffer and 0.2 ul of Herculase II DNA polymerase. After addition of the PCR mixture the samples were incubated at 95 ℃ for 2 min followed by 16 PCR

cycles at 95 ℃ for 15 sec, 54 ℃ for 20 sec, and 72 ℃ for 25 sec. After PCR, the samples was briefly centrifuge and placed on a magnetic stand for 2 min. The supernatant was mixed into a single tube and run on a 2% agarose gel. A band was cut out at the expected size (176 bp) from the gel and DNA was extracted using a standard band isolation kit. Concentration was measured using the Qubit dsDNA HS Assay Kit for library quantification. Additionally, the library quality was evaluated using a Bioanalyzer.

6.11 *RASL-seq Analysis*

Raw count tables were normalized in a per sample fashion using three housekeeping genes, AT1G13320, AT2G28390, and AT5G60390, respectively. The mean gene expression value, along with the standard error, was calculated for a minimum of three replicates.

6.12 *Genetic resources*

The mutant lines were obtained from the Arabidopsis Information Resource (TAIR). *cpl3* (c-terminal phosphatase-like3), SALK 051322; *napp* (WAVE protein), SALK 014298; *smc1*, CS87452; *sant domain protein*, SALK 024424; *bzip29* (basic leucine zipper29), SALK 018426; *mobile domain protein* (aminotransferase-like), SALK 066042; *med9*, SALK 029118.

6.13 *Plants growth*

Plants were grown in soil in a growth chamber under long-day photoperiod (16 hours light, 12k lux of cool white fluorescence bulbs) at 23°C, 60% relative humidity.

6.14 *Cytoplasmic-nuclear fraction*

Plant tissues in 1g were homogenized using mortar and pestle in liquid nitrogen and subsequently with 5 ml Nuclear Isolation (NI) buffer (250mM Sucrose, 15mM NaCl,

15mM PIPES/pH 6.8, 0.8% Triton X-100, 1x PIC). This homogenization lasted about 5 minutes inside a cold room at 4°C. Protein extracts were centrifuged at 300 x g for 5min at 4°C, filtered by Miracloth (Calbiochem), and centrifuged again at 1500 x g for 10 minutes at 4 °C. Supernatant in 1 ml was saved as 'cytoplasm fraction', and the rest was discarded. Another round of centrifugation at 2,000 x g for 5 min at 4°C was performed to further remove the remaining supernatant, and the pellet was resuspended in 1 ml of the NI buffer. The nucleus was centrifuged at 1,500 x g for 2 min at 4°C, and the supernatant was discarded. This wash step was repeated two more times. The final resuspended nucleus pellet was resuspended with 20 µl of 4x SDS sample buffer.

6.15 *RNA-Seq data processing (Oluwadamilare and Kang, unpublished)*

First, raw single-end sequence reads (100 bp) were de-multiplexed and sequencing quality was examined using FastQC v0.11.7 (Andrews, 2010). Raw reads were found and removed adapters using the Cutadapt software v.2.4 (Martin, 2011). Trimmed sequences of at least 40 bp for each sample were aligned to the Arabidopsis Araport11 (Cheng et al., 2017) reference genome and transcriptome annotation using Hisat2 v2.1.0 (Kim et al., 2019a) with the --dta option and all other parameters set to default. We used Samtools v1.9 to compress to BAM format and sort with SAM output files (Li et al., 2009). All mapping statistics were obtained using Samtools. Aligned reads for each sample were assembled and merged based on the loci to which they mapped using Stingtie v2.1.3b (Pertea et al., 2015) using default parameters with the option to natively estimate transcript abundance in FPKM.

6.16 *GO enrichment analysis of DEGs in up- and down-regulated clusters (Oluwadamilare and Kang, unpublished)*

We used the elim algorithm with fisher test statistic, topGO package in R (Alexa & Rahnenführer, 2009) was used to functionally annotate each cluster against the BioMart database (www.plants.ensembl.org). The top 25 functional GO terms sorted by p-values for up- and down-regulated clusters were visualized using ggplot2.

6.17 *Promoter motif analysis of genes in up- and down-regulated clusters (Oluwadamilare and Kang, unpublished)*

An upstream sequence in 1kb from the transcriptional start site of all DEGs were collected. The collected sequences were sorted into their gene clusters and analyzed using MEME suite v5.1.1 tools (Bailey et al., 2009). Using MEME, the motifs appearing in most, but not all, sequences (ZOOPS) were collected. Motifs 5 to 25 bp in length, with an E-value less than 0.05, were selected. To remove false positives, all sequences collected were reshuffled and run through MEME using identical parameters.

Table 2. List of RASL probes used in this study

Housekeeping	Acceptor probe sequence	Donor probe sequence
AT4G34270	GGAGCTGTCGTTCACTCCCAAATCAATCTGATCTTrCrA	/5Phos/CAGTTCTCCCACTGAAGAGTAGATCGGAAGAGCACAC
AT3G18780	GGAGCTGTCGTTCACTCAAACCCCAGCTTTTTAAGrCrC	/5Phos/TTTGATCTTGAGAGCTTAGAAGATCGGAAGAGCACAC
AT4G27960	GGAGCTGTCGTTCACTCAAAGGATCATCTGGGTTTrGrG	/5Phos/ATCCGTTAACAAAGAACAGAAGATCGGAAGAGCACAC
AT5G46630	GGAGCTGTCGTTCACTCTAAAATTTCAGGTGAGAGrArT	/5Phos/TTTGTGGATAGCCAAAGTCCAGATCGGAAGAGCACAC
AT1G13440	GGAGCTGTCGTTCACTCCCTCAGTGTATCCCAAAArTrT	/5Phos/CCCTTCATTTTGCCTTCAGAAGATCGGAAGAGCACAC
AT4G05320	GGAGCTGTCGTTCACTCACTTATTCATCAGGGATTrArT	/5Phos/ACAAGGCCCCAAAACACAAAAGATCGGAAGAGCACAC
AT1G58050	GGAGCTGTCGTTCACTCAATCAACAGGAAGTTTTGrCrT	/5Phos/AAATGATGTCCTAGTGGTGTAGATCGGAAGAGCACAC
AT1G13320	GGAGCTGTCGTTCACTCACATTGTCAATAGATTGGrArG	/5Phos/AGCTTGATTTGCGAAATACCAGATCGGAAGAGCACAC
AT2G28390	GGAGCTGTCGTTCACTCTGCAAGTGGATCAAATGCrTrG	/5Phos/CATAGAGTTCAAAATCTGGTAGATCGGAAGAGCACAC
AT5G60390	GGAGCTGTCGTTCACTCTAAGAGAGTCGATCATAArCrG	/5Phos/AAAGTCTCATCATTTGGCACAGATCGGAAGAGCACAC
Defense	Acceptor probe sequence	Donor probe sequence
AT3G48090	GGAGCTGTCGTTCACTCTCATATAGTCTCGCAGAGrGrA	/5Phos/GAATGCGATTTGTGATTTTTAGATCGGAAGAGCACAC
AT4G39030	GGAGCTGTCGTTCACTCGGATCGCAAAAGAGTAAGrCrA	/5Phos/TTGTAGCCTTCTTTGTTCAGAGATCGGAAGAGCACAC
AT1G19250	GGAGCTGTCGTTCACTCGATGCTGAACGTGGAAATrGrC	/5Phos/AATGACGTTTGTAGAATCTGAGATCGGAAGAGCACAC
AT2G19190	GGAGCTGTCGTTCACTCGTCATATCTCTCTCTTAGrArC	/5Phos/GCTGATCCACGATTCCTCTAAGATCGGAAGAGCACAC
AT1G02450	GGAGCTGTCGTTCACTCCTTGTCTTCGTTTCGCTCrTrT	/5Phos/CTGTTTGATCTTCTTCTTGTAGATCGGAAGAGCACAC
AT1G64280	GGAGCTGTCGTTCACTCAGAAGTCGAATCTGTCAGrGrG	/5Phos/ACGAATTTCCTAATTCCAAAAGATCGGAAGAGCACAC
AT2G04450	GGAGCTGTCGTTCACTCTCCACACTCCTGTACCTTrTrG	/5Phos/AAATGACCATCAATCTCCTGAGATCGGAAGAGCACAC
AT3G52430	GGAGCTGTCGTTCACTCAAACCTCCTTCTTCGTCArCrC	/5Phos/AATGTATTCGCATAACTCTCAGATCGGAAGAGCACAC
AT5G13320	GGAGCTGTCGTTCACTCTTTGCACAGAGGATCTAGrArT	/5Phos/TGATCCCAAAGGTAGTCTCCAGATCGGAAGAGCACAC
AT2G14610	GGAGCTGTCGTTCACTCGATCACATCATTACTTCArTrT	/5Phos/AGTATGGCTTCTCGTTCACAAGATCGGAAGAGCACAC

AT3G57260	GGAGCTGTCGTTCACTCCCGAGTCGAGATTTGCGTrCrG	/5Phos/AATAGGTTTTGGTATGAGTAAGATCGGAAGAGCACAC
AT1G75040	GGAGCTGTCGTTCACTCAGGGCAGAAAGTGATTTCrGrT	/5Phos/AGTTAGCTCCGGTACAAGTGAGATCGGAAGAGCACAC
AT1G74710	GGAGCTGTCGTTCACTCTGTCACTAAACATTTTCTrGrG	/5Phos/ACAAAAGCTCGTACCTGAGAAGATCGGAAGAGCACAC
AT1G62300	GGAGCTGTCGTTCACTCTTCCCTCGTAGGTTGTAArTrC	/5Phos/AGAATTGATCTGTCTTCCGCAGATCGGAAGAGCACAC
AT5G46350	GGAGCTGTCGTTCACTCCCTTGAGGACTCAAGTTCrTrT	/5Phos/CGAGGGTAGATCAAAACCTAAGATCGGAAGAGCACAC
AT4G31800	GGAGCTGTCGTTCACTCTTGTAACCTTTTGTCCGTrArT	/5Phos/TTCCTCCATTGAAATCCATCAGATCGGAAGAGCACAC
AT5G07100	GGAGCTGTCGTTCACTCCACTGACTTGGGATCTTGrArA	/5Phos/ATGCTCTTTCAACGTGTTTCAGATCGGAAGAGCACAC
AT5G24110	GGAGCTGTCGTTCACTCCCATATGGATGATTTGGArTrC	/5Phos/ATAGCTTTCAAACGGGGATTAGATCGGAAGAGCACAC
AT2G38470	GGAGCTGTCGTTCACTCAAGTAGTAAAATCCTTTGrGrT	/5Phos/GGCAGAAATGTACAAAAGGAAGATCGGAAGAGCACAC
AT5G22570	GGAGCTGTCGTTCACTCCATTACTGGTTATCTCACrGrG	/5Phos/TACTGATCTATAGCTTGCTCAGATCGGAAGAGCACAC
AT1G80840	GGAGCTGTCGTTCACTCTGACGTTGGGCTCGTCACrTrT	/5Phos/TCTTCGATTCAATCATATCTAGATCGGAAGAGCACAC
AT2G40750	GGAGCTGTCGTTCACTCTGATGATCATCAAACATCrArT	/5Phos/CGTCTCTTGCCAAACCAATGAGATCGGAAGAGCACAC
AT3G01080	GGAGCTGTCGTTCACTCAACCTCAAAAGAACCGGArGrA	/5Phos/TTGGCCTGTGTTATTATTGTAGATCGGAAGAGCACAC
AT2G21900	GGAGCTGTCGTTCACTCATATGGAGCAGAATGAGArGrA	/5Phos/AACTATACGTATTTGCCGTCAGATCGGAAGAGCACAC
AT5G01900	GGAGCTGTCGTTCACTCATAGTGTCATGATGATAArGrT	/5Phos/CGTGAGATGTCCAGAAAGGAAGATCGGAAGAGCACAC
AT1G80590	GGAGCTGTCGTTCACTCTATTAATGTTCAATCCTGrGrA	/5Phos/AAGGGTTCTAATCCAAAGCAAGATCGGAAGAGCACAC
AT3G56400	GGAGCTGTCGTTCACTCTGAGTTGTTAAGTCATGGrCrC	/5Phos/TTCAACGAGTTGGTTCATAAAGATCGGAAGAGCACAC
AT3G63380	GGAGCTGTCGTTCACTCTCAAGGTTTCTTGAGAGArTrG	/5Phos/GGCTTCTTGAACCCTTAAATAGATCGGAAGAGCACAC
AT2G06050	GGAGCTGTCGTTCACTCGCATCACCTTGTTGAACArGrC	/5Phos/TTGCATACCTAGTTCCTTATAGATCGGAAGAGCACAC
AT1G44350	GGAGCTGTCGTTCACTCGTCTTCGATCATATTCTTrTrG	/5Phos/CACCATTTCCAGCTTCTTCAAGATCGGAAGAGCACAC
AT2G30770	GGAGCTGTCGTTCACTCTGTCCCTGCGGCTATGTTrArT	/5Phos/ATCCCTTTACTTTGACATCTAGATCGGAAGAGCACAC
AT3G22600	GGAGCTGTCGTTCACTCTAAATAGGGACAAATAAArGrA	/5Phos/ATGCAATCTGAGTGGCACAAAGATCGGAAGAGCACAC
AT3G26830	GGAGCTGTCGTTCACTCACCAAACCATATATTCAGrTrG	/5Phos/GTGAAGAACTTGAAAGAAGGAGATCGGAAGAGCACAC

AT2G24850	GGAGCTGTCGTTCACTCAAGATTCGGGTTTCTTGGrGrA	/5Phos/CAAAAGAGACAAGGAATATCAGATCGGAAGAGCACAC
AT1G28480	GGAGCTGTCGTTCACTCCCGGAGATATGAGTAGCCrArT	/5Phos/AACCCTATCTAACCCTCCAAAGATCGGAAGAGCACAC
AT2G04400	GGAGCTGTCGTTCACTCTAAGTATGAGAAATGTTCrCrT	/5Phos/GCCAAAAAGTCCAGCTATTCAGATCGGAAGAGCACAC
AT2G26400	GGAGCTGTCGTTCACTCATGCCAAAAGACACATGArArC	/5Phos/CAAAATGTCTTCGGTTTCCAAGATCGGAAGAGCACAC
AT2G29460	GGAGCTGTCGTTCACTCTCTACTGATCGAAGAGTArTrC	/5Phos/ATTGTTGTCTCTTAGGCTGAAGATCGGAAGAGCACAC
AT2G45760	GGAGCTGTCGTTCACTCATTTGTCACCATACTCATrCrT	/5Phos/CTCAACCTGTAACTCAAGAAAGATCGGAAGAGCACAC
AT3G28510	GGAGCTGTCGTTCACTCTGTGTTTCAATCTCCAAGrTrA	/5Phos/GTTCTTAGCCAAAACCTTGAAGATCGGAAGAGCACAC
AT4G21840	GGAGCTGTCGTTCACTCGTCCATCACACACTGCACrArT	/5Phos/GTTATCTCCATTCTTCTTCCAGATCGGAAGAGCACAC
AT1G13340	GGAGCTGTCGTTCACTCTCTCCAATAGCTTCACAGrGrG	/5Phos/TCTTCTCTGAATGACATCACAGATCGGAAGAGCACAC
AT2G35980	GGAGCTGTCGTTCACTCTGAGGTACTTAAAGGAAGrCrC	/5Phos/TTAGATCATCGCAATCAACCAGATCGGAAGAGCACAC
AT3G13610	GGAGCTGTCGTTCACTCCAATAACTGACTCTGGTTrTrT	/5Phos/GGGTTCACAAAGATAGGAACAGATCGGAAGAGCACAC
AT3G46080	GGAGCTGTCGTTCACTCCGTTCTTCCCAACTCCAArCrT	/5Phos/TCCAATTGACTAAACTCTCCAGATCGGAAGAGCACAC
AT4G23150	GGAGCTGTCGTTCACTCAAAATCCGAGAATCCTAArCrA	/5Phos/AGATTTTTGTGCCGAAGATTAGATCGGAAGAGCACAC
AT5G03610	GGAGCTGTCGTTCACTCATCGTTTCTTTCCCGCGTrArA	/5Phos/TCTTTCCAAAAGTATGGGATAGATCGGAAGAGCACAC
AT5G24200	GGAGCTGTCGTTCACTCATGATCTGTCTGAAAATCrCrG	/5Phos/GTGATATGATTGTGTTCACCAGATCGGAAGAGCACAC
AT3G18250	GGAGCTGTCGTTCACTCTCGGCACAAGAGAATAACrArG	/5Phos/AGCGGAGAGGATACAACAACAGATCGGAAGAGCACAC
AT3G28930	GGAGCTGTCGTTCACTCGGAAACCATGACCGGAGCrArC	/5Phos/ATTCGAGAATTAAATTAACAAGATCGGAAGAGCACAC
AT1G51760	GGAGCTGTCGTTCACTCTTGCATCTCGACGTAATTrCrT	/5Phos/CAATCCCTAACATATCGCCTAGATCGGAAGAGCACAC
AT1G21240	GGAGCTGTCGTTCACTCAAGAGAAGAATCAAAAATrGrG	/5Phos/AACCGTGCAAGTGATCGAAAAGATCGGAAGAGCACAC
AT2G13810	GGAGCTGTCGTTCACTCAACCCGCAAACTTAGAGArArT	/5Phos/GATGAAACTTCAATCGCGACAGATCGGAAGAGCACAC
AT2G30750	GGAGCTGTCGTTCACTCGGCAAACATCGAGACCAArArA	/5Phos/GCTTCAGTTAGATCAGGTTGAGATCGGAAGAGCACAC
AT4G35180	GGAGCTGTCGTTCACTCATGGATGCAGGCTTTTTCrTrT	/5Phos/CTTGGTTATGTACACCATCTAGATCGGAAGAGCACAC
AT5G05730	GGAGCTGTCGTTCACTCAATGCATCCTCTAGCCTGrArA	/5Phos/TAACAGAACGAAAACAGCATAGATCGGAAGAGCACAC

AT3G17810	GGAGCTGTCGTTCACTCCTCAGCTTTTCTCTGCTCrArA	/5Phos/CTGCTTCTTTCTGTCTCTTAAGATCGGAAGAGCACAC
AT4G21830	GGAGCTGTCGTTCACTCTCGCCTTTGAAAACATGGrCrC	/5Phos/TAAATGTCCATCACACACTGAGATCGGAAGAGCACAC
AT4G23140	GGAGCTGTCGTTCACTCCTTTGCAGGATCTTCTTGrArA	/5Phos/CACATAAAAGACCGATATGGAGATCGGAAGAGCACAC
AT4G37150	GGAGCTGTCGTTCACTCTTGATCTCCATCACTTCTrTrT	/5Phos/AACCGGAGAGTTCTCAATCAAGATCGGAAGAGCACAC
AT5G26340	GGAGCTGTCGTTCACTCCGACGTATGTGCAGATCArTrT	/5Phos/ACCACGACTAGAATTGCGAAAGATCGGAAGAGCACAC
AT1G45145	GGAGCTGTCGTTCACTCAGACCACCATGCTTCATCrArG	/5Phos/CTTCTCATTGATCTCATCTTAGATCGGAAGAGCACAC
AT3G28540	GGAGCTGTCGTTCACTCTCAATATGGTTGTCCATTrCrT	/5Phos/TCCTCTACGTATCAAAGCTGAGATCGGAAGAGCACAC
AT5G17990	GGAGCTGTCGTTCACTCATGTCTCTCCTTTAGCTCrTrC	/5Phos/AGAAGAACTAGAAAGGCACTAGATCGGAAGAGCACAC
AT1G21310	GGAGCTGTCGTTCACTCCCGGTGGTGGAGGAGAAGrArA	/5Phos/TAGAAATAGTTAGCGGTTGAAGATCGGAAGAGCACAC
AT2G45220	GGAGCTGTCGTTCACTCACTTTTGCTTCCGGTAATrArA	/5Phos/TCGTCTTCCCTATACCATCAAGATCGGAAGAGCACAC
AT1G33960	GGAGCTGTCGTTCACTCTGCTCTTCTGAATGCCCTrTrT	/5Phos/TGATTCTAGCTCCTCTTGTTAGATCGGAAGAGCACAC
AT2G30550	GGAGCTGTCGTTCACTCTGACGCCAAAACGGTGGArArT	/5Phos/TTGTAAATGCTCTTTCAAAAAGATCGGAAGAGCACAC
AT2G39530	GGAGCTGTCGTTCACTCTGCGAAGAGAAGAAGACTrGrG	/5Phos/CCGATGCATATCCTTTACTAAGATCGGAAGAGCACAC
AT3G46090	GGAGCTGTCGTTCACTCCTCCATCGAATCTAAGTCrCrA	/5Phos/AATCCAAACAAGCCACTCTCAGATCGGAAGAGCACAC
AT1G26390	GGAGCTGTCGTTCACTCAGCTTTAACATCCATCAArTrC	/5Phos/TCTTCAAATTCCCCAAGAAAAGATCGGAAGAGCACAC
AT2G44240	GGAGCTGTCGTTCACTCTGAAACATAGATGCGTAArTrA	/5Phos/TCAAAAGCTTGAACACACAGAGATCGGAAGAGCACAC
AT1G72520	GGAGCTGTCGTTCACTCTCGTTGGCGTATGGGTAGrTrC	/5Phos/TTCAACAAGTAATTTAAGCCAGATCGGAAGAGCACAC
AT5G39670	GGAGCTGTCGTTCACTCCATTCTCCTGCAGTTCTCrArA	/5Phos/GGTTAGATCCTTGCTTTAAGAGATCGGAAGAGCACAC
AT3G60450	GGAGCTGTCGTTCACTCACTAAACAGGTGAATGGCrTrT	/5Phos/ATGACAGGTTCATAACTGACAGATCGGAAGAGCACAC
AT3G25882	GGAGCTGTCGTTCACTCCCGTTACAATCCAACGAGrTrT	/5Phos/TCTCAACCCAAGATTCTGACAGATCGGAAGAGCACAC
AT2G37040	GGAGCTGTCGTTCACTCCGGATCAATGATTTTACCrTrT	/5Phos/CACAAATCGCCGTGAAAACCAGATCGGAAGAGCACAC
AT1G01470	GGAGCTGTCGTTCACTCAAACTGATCTCACAGATCrGrG	/5Phos/AATCGAATGACTGTAAGGATAGATCGGAAGAGCACAC
AT3G44300	GGAGCTGTCGTTCACTCGGAGTGACATGAACTGACrGrA	/5Phos/ATCACAACCGATTACTTGTTAGATCGGAAGAGCACAC

AT1G35710	GGAGCTGTCGTTCACTCGCGGACCAGTTTGATGAArTrC	/5Phos/CGTCTTTAGAAGTTTTGCTGAGATCGGAAGAGCACAC
AT3G47540	GGAGCTGTCGTTCACTCCTACAATAGTCTCTATAGrTrA	/5Phos/CCCAATCCTTGCCTTGACCGAGATCGGAAGAGCACAC
AT2G27690	GGAGCTGTCGTTCACTCGGATTTCATCTCCATGATrArG	/5Phos/CCATCTCTTTCCCGATACAAAGATCGGAAGAGCACAC
AT3G44720	GGAGCTGTCGTTCACTCTCGATGCCTCAAAATCCArCrG	/5Phos/TAAAACATGTACTCGAAGTTAGATCGGAAGAGCACAC
AT4G39950	GGAGCTGTCGTTCACTCTTGACGTAGTTTAGTTTTrGrG	/5Phos/GATGTCGGATTCTTGAACGAAGATCGGAAGAGCACAC
AT4G37370	GGAGCTGTCGTTCACTCCGCCAACTTCTTAACCCGrTrG	/5Phos/TCTCGTAATCTGAAACCAACAGATCGGAAGAGCACAC
AT1G21250	GGAGCTGTCGTTCACTCGCTACTGTCTCCAAGTCGrGrG	/5Phos/CTTTCTTTATAGCAACTATGAGATCGGAAGAGCACAC
AT5G44568	GGAGCTGTCGTTCACTCTCCTGCACTATGATGACTrTrA	/5Phos/TGGCTTATGGGCCTTTATCTAGATCGGAAGAGCACAC
AT2G39518	GGAGCTGTCGTTCACTCATAAAACAGCAAGACAGArTrG	/5Phos/AAAGCAAAGAGAAGAAGACTAGATCGGAAGAGCACAC
AT1G73805	GGAGCTGTCGTTCACTCAATTCCGCTGGAGTCGTTrArT	/5Phos/ATACCCTTCGTTTACTATCTAGATCGGAAGAGCACAC
AT5G39510	GGAGCTGTCGTTCACTCCTTCTTGCTCTTTCCAATrGrT	/5Phos/TATCGTCTACTCCATGAAGCAGATCGGAAGAGCACAC
AT1G76490	GGAGCTGTCGTTCACTCTTCTGCACACCTTTAGAArArC	/5Phos/CATATTCATCCCCATAGCATAGATCGGAAGAGCACAC
AT1G32640	GGAGCTGTCGTTCACTCAGCTGTTCTTGCGTATAGrArT	/5Phos/CCTAAAACCCATCTTCACCGAGATCGGAAGAGCACAC
AT4G04490	GGAGCTGTCGTTCACTCCCGAGGATACAAGACTGTrArA	/5Phos/TCGAGACCTCATCCACTGAAAGATCGGAAGAGCACAC
AT5G24530	GGAGCTGTCGTTCACTCTGGAGACCGCAAACAGTArGrT	/5Phos/GTCTTGAAGAAGAATGGTTAAGATCGGAAGAGCACAC
AT5G52750	GGAGCTGTCGTTCACTCATAGCTTCCTTAGCTTCArTrC	/5Phos/ACGATAACCGGTACATCAACAGATCGGAAGAGCACAC
AT3G53180	GGAGCTGTCGTTCACTCATTAGTATCGGTGAATGArGrT	/5Phos/TGCTTATATGCATCCGGATTAGATCGGAAGAGCACAC
AT1G21270	GGAGCTGTCGTTCACTCAATGTCCAATGTTGTTACrArT	/5Phos/TTCTGATGCTGTCATAGCCAAGATCGGAAGAGCACAC
AT5G55450	GGAGCTGTCGTTCACTCTTTTCTAATCCCTTATTCrTrT	/5Phos/TCTCACTCAACTCTGTTGTGAGATCGGAAGAGCACAC
AT1G51820	GGAGCTGTCGTTCACTCCCCTTAGAGCCTGAATCTrCrT	/5Phos/GCAATGTGTACGTAAGAGTAAGATCGGAAGAGCACAC
AT1G55210	GGAGCTGTCGTTCACTCTCCGTTATATTTCCCTGTrCrT	/5Phos/TGAAAGCAAAGTTCATCGCCAGATCGGAAGAGCACAC
AT1G10585	GGAGCTGTCGTTCACTCGAAAAAACACACTAGCGTrTrA	/5Phos/GCGTAGACTTATCATTTGGGAGATCGGAAGAGCACAC
AT2G18660	GGAGCTGTCGTTCACTCGTGTGTATACGACACGAArTrG	/5Phos/TTACCGGCATCAGTATTAGCAGATCGGAAGAGCACAC

AT3G03470	GGAGCTGTCGTTCACTCTGAACTGTTGCTTCTCGGrArT	/5Phos/AGATCAACTTCTTCACCTTCAGATCGGAAGAGCACAC
AT2G04430	GGAGCTGTCGTTCACTCACTTCTCCCGCGACCTTTrTrT	/5Phos/AAGCAGATGTTAGCTATTAAAGATCGGAAGAGCACAC
AT5G19590	GGAGCTGTCGTTCACTCGAAGGGTATTTAGCAGTTrArT	/5Phos/CCCAGCAACCTCAAAGACAAAGATCGGAAGAGCACAC
AT1TE12295	GGAGCTGTCGTTCACTCCCAATCGCTATCGCTATArTrC	/5Phos/CAACAAGCTTGTAATCACTAAGATCGGAAGAGCACAC
AT2TE06405	GGAGCTGTCGTTCACTCTATGAGTATATTCGTCGArGrA	/5Phos/TCTTTGAGACGGCGTAATCCAGATCGGAAGAGCACAC
AT3TE61000	GGAGCTGTCGTTCACTCCAAATTTCTGGATAAAGTrArC	/5Phos/AACGCCATTCTTCTGCTCATAGATCGGAAGAGCACAC
AT3TE76010	GGAGCTGTCGTTCACTCTTTGAAATGCTGCCTCATrTrA	/5Phos/AAAACCTTACCAAGAAAACCAGATCGGAAGAGCACAC
AT3TE92525	GGAGCTGTCGTTCACTCTACTCTTTCGGTCATCTArCrG	/5Phos/TCTCCACCCCAATCGCTATCAGATCGGAAGAGCACAC
AT4TE32060	GGAGCTGTCGTTCACTCTCTTTGAGACGGCGTAATrCrC	/5Phos/GATACGATAGACTAACTTCTAGATCGGAAGAGCACAC
AT5TE44570	GGAGCTGTCGTTCACTCGAAATGCTGCCTCATTAArArA	/5Phos/ACCTTACCAGGAAAACTCAAAGATCGGAAGAGCACAC
AT5G24770	GGAGCTGTCGTTCACTCTGATCTCCGATATTGCCArArC	/5Phos/GATGTTGTATCCTTTCTTCAAGATCGGAAGAGCACAC
AT1G06160	GGAGCTGTCGTTCACTCAATCCTCAAGAACCACAArGrT	/5Phos/GTTGTATTACTTTCTTGCGTAGATCGGAAGAGCACAC
AT5G44420	GGAGCTGTCGTTCACTCAAGGTTAATGCACTGATTrCrT	/5Phos/TGCATGCATTACTGTTTCCGAGATCGGAAGAGCACAC
AT2G39940	GGAGCTGTCGTTCACTCTTTCTAGCTATGGTTTCCrArA	/5Phos/GTCTTTGGGACTGATTTTGGAGATCGGAAGAGCACAC
AT4G23810	GGAGCTGTCGTTCACTCTTGAATTGAAAATGTAATrCrT	/5Phos/TGGCGATGATGACTCTCGCTAGATCGGAAGAGCACAC
AT3G45140	GGAGCTGTCGTTCACTCTTTTCTGGCGACTCATAGrArA	/5Phos/CTCTTTTAAGGCTTCATCTGAGATCGGAAGAGCACAC
AT1G19220	GGAGCTGTCGTTCACTCCTGCATGAAAGTTGAAGCrTrG	/5Phos/GGAAGCTGTTATTACCATGTAGATCGGAAGAGCACAC
AT4G14560	GGAGCTGTCGTTCACTCTTTGTAGCCTTCTCTCTCrGrG	/5Phos/AATATTCACCTACTGTGAACAGATCGGAAGAGCACAC
AT2G23170	GGAGCTGTCGTTCACTCTCTTGACCACATACCGAArGrT	/5Phos/TATGAAATCAGCCAGTTCTTAGATCGGAAGAGCACAC
AT5G44420	GGAGCTGTCGTTCACTCGGACGTAACAGATACACTrTrG	/5Phos/TGTGCTGGGAAGACATAGTTAGATCGGAAGAGCACAC
AT3G12500	GGAGCTGTCGTTCACTCCACTCCAATCCACCGTTArArT	/5Phos/GATGTTCGTAATCACTCCATAGATCGGAAGAGCACAC
AT3G04720	GGAGCTGTCGTTCACTCCAAAATCATTACATAATArTrC	/5Phos/AAACGCGATCAATGGCCGAAAGATCGGAAGAGCACAC
AT3G23240	GGAGCTGTCGTTCACTCTTAAGGTCCCTAATACAArArT	/5Phos/CCTAATCTTTCACCAAGTCCAGATCGGAAGAGCACAC

AT5G24780	GGAGCTGTCGTTCACTCTGGTGCCAAAACGGCTACrArA	/5Phos/AGATAAACGAAACGACATAGAGATCGGAAGAGCACAC
AT3G45140	GGAGCTGTCGTTCACTCATGTGTTGATAAAAGATCrCrA	/5Phos/ACGTGACCATCACTAGGGTCAGATCGGAAGAGCACAC
AT1G54040	GGAGCTGTCGTTCACTCTAATAAAACAGCCAGCCArTrA	/5Phos/AATAAATTGGCTCCTTATTGAGATCGGAAGAGCACAC
AT1G17990	GGAGCTGTCGTTCACTCTGATACATACAGATTTGGrTrG	/5Phos/TATTGACTGGTCAAAGCGGTAGATCGGAAGAGCACAC
AT4G23810	GGAGCTGTCGTTCACTCTACGTCTTTGCAGGAATTrGrA	/5Phos/GTGAAGAAGAGAAGCAAGTTAGATCGGAAGAGCACAC
AT4G01370	GGAGCTGTCGTTCACTCTTTCACCGAGTATACAACrCrG	/5Phos/ACAGACCAAATATCAATTGCAGATCGGAAGAGCACAC
AT2G39940	GGAGCTGTCGTTCACTCACCCAACTAGTTCCAAAArTrC	/5Phos/TCAAAGTCACCGACCTTCACAGATCGGAAGAGCACAC
AT2G43710	GGAGCTGTCGTTCACTCTTGTTTTTGTCTTTGTCCrTrT	/5Phos/TTAGAGCTGCACTTCTCTGTAGATCGGAAGAGCACAC
AT2G46370	GGAGCTGTCGTTCACTCACTCTTCTCCAATCTTGArCrT	/5Phos/TGAGTTAAACCAACCGGTTTAGATCGGAAGAGCACAC
AT5G03280	GGAGCTGTCGTTCACTCCCATGCTAACAATCTTCTrCrC	/5Phos/ACAGGACTCATTGGTTCAATAGATCGGAAGAGCACAC
AT1G72260	GGAGCTGTCGTTCACTCAGACCATTCCGTTCAAAGrCrA	/5Phos/AATGAAAATGGTCGAGAGAAAGATCGGAAGAGCACAC
AT5G24770	GGAGCTGTCGTTCACTCCGGTGCCAAAACGGCTACrArA	/5Phos/AGATAAACGAAACGACATAGAGATCGGAAGAGCACAC
AT1G66340	GGAGCTGTCGTTCACTCCAAAGCTCATGCATTTCTrCrT	/5Phos/TTTGTGGATTTGTCAGTGTTAGATCGGAAGAGCACAC
AT3G23150	GGAGCTGTCGTTCACTCGCCACTTCATAACCGTCCrArT	/5Phos/CTCTGCCATTTGAAGATCAAAGATCGGAAGAGCACAC
AT4G31550	GGAGCTGTCGTTCACTCGCCTGAAGAAGAAATATTrCrT	/5Phos/CCTGCATCGCGGATTGGTTAAGATCGGAAGAGCACAC
AT2G24570	GGAGCTGTCGTTCACTCTCACCGGTGATCGCAGAArGrA	/5Phos/CATGAAAGAAGAGTTAGAAGAGATCGGAAGAGCACAC
AT1G50640	GGAGCTGTCGTTCACTCACAACAGATCATCGTGTTrCrG	/5Phos/GTCTTCTTCTTCTTGGTTTTAGATCGGAAGAGCACAC
AT1G19180	GGAGCTGTCGTTCACTCGCCCGGCGTAGAATATAGrTrC	/5Phos/AATGGTGCAGTTTGAGACTCAGATCGGAAGAGCACAC
AT1G74950	GGAGCTGTCGTTCACTCAAGCTCAGATCTCCAAAArCrT	/5Phos/ACCCTTCTCCTTCAGGTAACAGATCGGAAGAGCACAC
AT3G17860	GGAGCTGTCGTTCACTCGGTTGCAGAGCTGAGAGArArG	/5Phos/AACTAATGCATTCAGACATTAGATCGGAAGAGCACAC
AT1G17380	GGAGCTGTCGTTCACTCTACTTCCATAATCTCTTTrArG	/5Phos/CTTTGTCTACGGGGAACTCAAGATCGGAAGAGCACAC
AT2G34600	GGAGCTGTCGTTCACTCGTTCCAAGTCGCATTTTGrTrT	/5Phos/TGCATCTCCATCTCTTTGAAAGATCGGAAGAGCACAC
AT1G30135	GGAGCTGTCGTTCACTCAGTGGGAAAAAGACGAAGrTrT	/5Phos/CCAAGTCACAATTTTGCTGTAGATCGGAAGAGCACAC

AT1G70700	GGAGCTGTCGTTCACTCCCAAAGCATTACAAACAArTrG	/5Phos/ATCAAATACAGAGACGCCCTAGATCGGAAGAGCACAC
AT5G20900	GGAGCTGTCGTTCACTCCACTATCATACAACACATrTrA	/5Phos/CACACAGCAGCGTACATGATAGATCGGAAGAGCACAC
AT1G06160	GGAGCTGTCGTTCACTCAATCCTCAAGAACCACAArGrT	/5Phos/GTTGTATTACTTTCTTGCGTAGATCGGAAGAGCACAC
AT4G14560	GGAGCTGTCGTTCACTCTCAAAACACCTTTTGGTCrGrA	/5Phos/GGCAAAAACAAATTCTACTTAGATCGGAAGAGCACAC
AT4G14561	GGAGCTGTCGTTCACTCAAGATAAAGATGGTGACTrGrG	/5Phos/ATGTTGGTTGGTGATGTTCCAGATCGGAAGAGCACAC
AT4G14562	GGAGCTGTCGTTCACTCCTAACCTCTGATTGGAAArCrT	/5Phos/CGTCTACACCGATCACGAAAAGATCGGAAGAGCACAC
AT4G14563	GGAGCTGTCGTTCACTCTTTCTTGGGTGCTAAGCArArA	/5Phos/TTATTCGAAGGGAATCATCGAGATCGGAAGAGCACAC
AT4G14564	GGAGCTGTCGTTCACTCAATAAGTTCGGTGTACGGrArT	/5Phos/GTTTACCCCATCAATGTTTTAGATCGGAAGAGCACAC
photoreceptor	Acceptor probe sequence	Donor probe sequence
AT1G09530	GGAGCTGTCGTTCACTCCTGAGAAGCCCATCACGCrTrT	/5Phos/GTTTAACCAGGTCCATCTATAGATCGGAAGAGCACAC
AT1G09570	GGAGCTGTCGTTCACTCTTTCCCAGCTTGTCTCAArGrT	/5Phos/ACTGAACATCTCCATTCATCAGATCGGAAGAGCACAC
AT2G18790	GGAGCTGTCGTTCACTCAATTCCATGTTTAACTGTrArA	/5Phos/ACCGAAAGCCTGCATCAAAAAGATCGGAAGAGCACAC
AT2G20180	GGAGCTGTCGTTCACTCGGCCCGAGGTTGGATCATrArC	/5Phos/TGCTGGTTCGGTACAAAGACAGATCGGAAGAGCACAC
AT2G25760	GGAGCTGTCGTTCACTCGACTACATGTTGAATATGrArC	/5Phos/CAGCGTCCTGATGTTTTTAGAGATCGGAAGAGCACAC
AT2G43010	GGAGCTGTCGTTCACTCTTCTGAATTGCAGACTGArTrC	/5Phos/CATAACCGGAAATCGAGGTAAGATCGGAAGAGCACAC
AT2G46970	GGAGCTGTCGTTCACTCCCCAAAAGCCCATAGACTrArA	/5Phos/CAACACAGAGTAGACGATCAAGATCGGAAGAGCACAC
AT3G03940	GGAGCTGTCGTTCACTCTAATTTTCTTCCTTGGCTrGrT	/5Phos/TCATCCTCTTCCAAATTGATAGATCGGAAGAGCACAC
AT3G13670	GGAGCTGTCGTTCACTCAGCATCCATTATCAATGCrCrC	/5Phos/AGAGATTCGAACATGATGATAGATCGGAAGAGCACAC
AT3G59060	GGAGCTGTCGTTCACTCCGGTTCATAACCGGGAATrTrG	/5Phos/AGACAATTGCATCTGACTTTAGATCGGAAGAGCACAC
AT4G00050	GGAGCTGTCGTTCACTCATCTAGAAAATTTGGAGTrTrC	/5Phos/ATTTGTGGATGTGGTGGAGAAGATCGGAAGAGCACAC
AT4G16250	GGAGCTGTCGTTCACTCAACCGGGAGTTCGATAACrGrA	/5Phos/TTAGGAAATAAGAGCGTTCGAGATCGGAAGAGCACAC
AT5G18190	GGAGCTGTCGTTCACTCGTCTCTTGAGTTTCATCCrArT	/5Phos/CATTTTACGTTTTGGTACGCAGATCGGAAGAGCACAC
AT5G35840	GGAGCTGTCGTTCACTCTGCTGCTTAATAGTGTCTrCrT	/5Phos/GAAAGGATTTGCTGAAGCCTAGATCGGAAGAGCACAC

AT5G61270	GGAGCTGTCGTTCACTCCAACCGTTGAGACTTTGArGrT	/5Phos/CCAAATAGGGTTATTCGAGGAGATCGGAAGAGCACAC
AT1G15980	GGAGCTGTCGTTCACTCCATCGGAAGATCTCGACGrTrA	/5Phos/AGACGAGTTTGAAAGTTGAGAGATCGGAAGAGCACAC
AT1G32080	GGAGCTGTCGTTCACTCCAACTTGTACAAAGTTAGrCrT	/5Phos/CCAATCAGACCAGTCACAACAGATCGGAAGAGCACAC
AT1G70760	GGAGCTGTCGTTCACTCTTTGAGGTAAACGTTCTTrTrA	/5Phos/TAGAGTCTGGGTCTGTTGGTAGATCGGAAGAGCACAC
AT1G73060	GGAGCTGTCGTTCACTCCTTATGGACCTAAAGAAArTrT	/5Phos/GGTGACAGAAGTACCAGGTAAGATCGGAAGAGCACAC
AT1G73655	GGAGCTGTCGTTCACTCCAAATCCTAAGGACGGTGrGrA	/5Phos/ATTATCACTCTACGTTTACCAGATCGGAAGAGCACAC
AT1G74880	GGAGCTGTCGTTCACTCTTCTTGACTCTACATTCGrCrT	/5Phos/CGTAAACAAGTTTCTCACACAGATCGGAAGAGCACAC
AT1G76450	GGAGCTGTCGTTCACTCATTCGAAAAGCTCTGAGGrArG	/5Phos/AAGATAACCATGGAGAAATCAGATCGGAAGAGCACAC
AT2G20890	GGAGCTGTCGTTCACTCGGCTTCAATGTAAGCCTTrArA	/5Phos/AAATGGCATCTCGGTCTTGAAGATCGGAAGAGCACAC
AT2G24090	GGAGCTGTCGTTCACTCCCTGCTCTGCTTAAGTCGrCrC	/5Phos/TTTCGATTGACTTTCAAGTAAGATCGGAAGAGCACAC
AT2G33800	GGAGCTGTCGTTCACTCTGTATGTGTTCTTCCTTGrTrA	/5Phos/CATTTTCACCTGCAACCTTAAGATCGGAAGAGCACAC
AT2G38140	GGAGCTGTCGTTCACTCTCGCATTCCCAAAAGAGTrGrA	/5Phos/TTGAAACGCTTTCCTTTAGCAGATCGGAAGAGCACAC
AT3G11630	GGAGCTGTCGTTCACTCTGGATCACTCCTTCCTTGrTrC	/5Phos/GATTATGAAAAGTCCTCTCAAGATCGGAAGAGCACAC
AT3G12780	GGAGCTGTCGTTCACTCGTGTTGTGTCCAGAGCTTrCrG	/5Phos/TTGAAAGTTTTGATAGAGTCAGATCGGAAGAGCACAC
AT3G18890	GGAGCTGTCGTTCACTCTAGCACCAATACAGCATArTrA	/5Phos/ATCACCGATGCATTTCCCAAAGATCGGAAGAGCACAC
AT3G27830	GGAGCTGTCGTTCACTCGGGAAGTGATTGATGGAArGrC	/5Phos/GAGAGTAGGATAAGATGAGGAGATCGGAAGAGCACAC
AT3G47650	GGAGCTGTCGTTCACTCTGGGATCTTGAAGTCTGArArG	/5Phos/CAGTTCTCTCTTCTGTACCAAGATCGGAAGAGCACAC
AT3G54050	GGAGCTGTCGTTCACTCTCCTGTGAAAATCTCCAArCrC	/5Phos/AAACTTCCAATGTACCTTGCAGATCGGAAGAGCACAC
AT3G55330	GGAGCTGTCGTTCACTCATAGAGAAACGCATAAGCrArT	/5Phos/CTTTATTGTCAGAGACAGCAAGATCGGAAGAGCACAC
AT3G56910	GGAGCTGTCGTTCACTCCGAATACGAAAAGCAGCArArA	/5Phos/CAGTTGAGTCACTTAGACATAGATCGGAAGAGCACAC
AT3G59780	GGAGCTGTCGTTCACTCACAAAAAAGACTCCAGCArGrC	/5Phos/AGATTTACAATAATGGGTGTAGATCGGAAGAGCACAC
AT3G63190	GGAGCTGTCGTTCACTCTGCTTGTACCCCAAGGAArArC	/5Phos/ATCAGGGCAAATAGTAAAAGAGATCGGAAGAGCACAC
AT3G63490	GGAGCTGTCGTTCACTCGCTTGTCAAACTCCATGArArG	/5Phos/CCTCCTTTAATCTGTTCGATAGATCGGAAGAGCACAC

AT4G17560	GGAGCTGTCGTTCACTCAAGCCTTGCTCTTCTTACrTrT	/5Phos/TCCTGTGACTCACCACTTTTAGATCGGAAGAGCACAC
AT4G24770	GGAGCTGTCGTTCACTCGTAAACCTCGTAGTTGCTrArA	/5Phos/TATCTAAAGGTCACCGACAAAGATCGGAAGAGCACAC
AT4G30950	GGAGCTGTCGTTCACTCCCAATTTGTCTGAATCCArTrA	/5Phos/GCTTTCTGCTAACTGTTCCCAGATCGGAAGAGCACAC
AT5G03940	GGAGCTGTCGTTCACTCTTAACCAAATTGGGCTGArArA	/5Phos/TAGTTTTAGTTACCAGAGCCAGATCGGAAGAGCACAC
AT5G17870	GGAGCTGTCGTTCACTCTCACCATCCCTAATCCTCrCrT	/5Phos/CCATTACCCAATTTTGGAACAGATCGGAAGAGCACAC
AT5G30510	GGAGCTGTCGTTCACTCAGGTATTTCTTTTTCAAGrArA	/5Phos/GCTCTTCAGCTGCTGCTTTCAGATCGGAAGAGCACAC
AT5G43750	GGAGCTGTCGTTCACTCCGAGCTCCTCTCTCCAATrTrT	/5Phos/GTATATCTGAGGCTCGAAGTAGATCGGAAGAGCACAC
AT5G45680	GGAGCTGTCGTTCACTCAAGCTCTCTCAAGCTTTArCrC	/5Phos/TATGTACTCAATGTCAAAGAAGATCGGAAGAGCACAC
AT5G47190	GGAGCTGTCGTTCACTCGCTAGCTACCTTTGGAGArTrT	/5Phos/GAAGACAACACAAGACAAGAAGATCGGAAGAGCACAC
AT5G52970	GGAGCTGTCGTTCACTCGTCGACTCCAGAAACTACrGrA	/5Phos/GGTATGTCTAAATCAACCGTAGATCGGAAGAGCACAC
AT5G54600	GGAGCTGTCGTTCACTCACTTTGACTGTATCTCCArArA	/5Phos/CTTGACATGCATTTTGTGGAAGATCGGAAGAGCACAC
AT5G55220	GGAGCTGTCGTTCACTCTATATTCTGCTTGATTATrGrT	/5Phos/TGGTGATGCTCTCTCTTTGAAGATCGGAAGAGCACAC
AT5G63310	GGAGCTGTCGTTCACTCCCAAAATCAGGAACAAAArCrA	/5Phos/CCAAAGCTCATCATCGGTAAAGATCGGAAGAGCACAC
AT1G04820	GGAGCTGTCGTTCACTCATATTACCAGAAAGGCAGrArA	/5Phos/ACGATTTAACACACAAAGGAAGATCGGAAGAGCACAC
AT1G50010	GGAGCTGTCGTTCACTCACATAAAACCGACAACCTrTrC	/5Phos/TTAGTACTCCTCTCCTTCATAGATCGGAAGAGCACAC
AT1G77490	GGAGCTGTCGTTCACTCATTTGGAAACAAGTACGArTrG	/5Phos/GTCGATGGTTAACCTAATCCAGATCGGAAGAGCACAC
AT3G05730	GGAGCTGTCGTTCACTCTCTACTGTTTTCAGAAACrTrT	/5Phos/GGGTGATACTACTCCATGGGAGATCGGAAGAGCACAC
AT3G23810	GGAGCTGTCGTTCACTCCAATTGCCAATAAACGGCrTrT	/5Phos/AATCAGAAAACCAAACGAAGAGATCGGAAGAGCACAC
AT3G25770	GGAGCTGTCGTTCACTCTTCGTGTACCAACGTCCArArA	/5Phos/CGACTTAAAACATACTCGAGAGATCGGAAGAGCACAC
AT5G15960	GGAGCTGTCGTTCACTCGTGTGTTTTGGTTAGTGArTrG	/5Phos/ATGAGAAGAGATGTGGGCTTAGATCGGAAGAGCACAC

Table 3. List of barcode primers

Name	Sequence
Dual_P5_BC_1	AATGATACGGCGACCACCGAGATCTACACGACTGACTACACT CTTTCCGATCTGGAGCTGTCGTTCACTC
Dual_P5_BC_2	AATGATACGGCGACCACCGAGATCTACACGCATGCATACACT CTTTCCGATCTGGAGCTGTCGTTCACTC
Dual_P5_BC_3	AATGATACGGCGACCACCGAGATCTACACATCGATCGACACT CTTTCCGATCTGGAGCTGTCGTTCACTC
Dual_P5_BC_4	AATGATACGGCGACCACCGAGATCTACACCTAGCTAGACACT CTTTCCGATCTGGAGCTGTCGTTCACTC
Dual_P5_BC_5	AATGATACGGCGACCACCGAGATCTACACGTACGTACACACT CTTTCCGATCTGGAGCTGTCGTTCACTC
Dual_P5_BC_6	AATGATACGGCGACCACCGAGATCTACACGTCAGTCAACACT CTTTCCGATCTGGAGCTGTCGTTCACTC
Dual_P5_BC_7	AATGATACGGCGACCACCGAGATCTACACACGTACGTACACT CTTTCCGATCTGGAGCTGTCGTTCACTC
Dual_P5_BC_8	AATGATACGGCGACCACCGAGATCTACACATGCATGCACACT CTTTCCGATCTGGAGCTGTCGTTCACTC
Dual_P5_BC_9	AATGATACGGCGACCACCGAGATCTACACCTGACTGAACACT CTTTCCGATCTGGAGCTGTCGTTCACTC
Dual_P5_BC_10	AATGATACGGCGACCACCGAGATCTACACAGTCAGCTACACT CTTTCCGATCTGGAGCTGTCGTTCACTC
Dual_P5_BC_11	AATGATACGGCGACCACCGAGATCTACACCAGTCGACACACT CTTTCCGATCTGGAGCTGTCGTTCACTC
Dual_P5_BC_12	AATGATACGGCGACCACCGAGATCTACACACGTAGCAACACT CTTTCCGATCTGGAGCTGTCGTTCACTC
Dual_P5_BC_13	AATGATACGGCGACCACCGAGATCTACACGATCGATAACACT CTTTCCGATCTGGAGCTGTCGTTCACTC
Dual_P5_BC_14	AATGATACGGCGACCACCGAGATCTACACCGTATCGAACACT CTTTCCGATCTGGAGCTGTCGTTCACTC
Dual_P5_BC_15	AATGATACGGCGACCACCGAGATCTACACCATGTCAGACACT CTTTCCGATCTGGAGCTGTCGTTCACTC
Dual_P5_BC_16	AATGATACGGCGACCACCGAGATCTACACCGTACATGACACT CTTTCCGATCTGGAGCTGTCGTTCACTC
Dual_P5_BC_17	AATGATACGGCGACCACCGAGATCTACACACTGAGTCACACT CTTTCCGATCTGGAGCTGTCGTTCACTC
Dual_P5_BC_18	AATGATACGGCGACCACCGAGATCTACACCGATCGTGACACT CTTTCCGATCTGGAGCTGTCGTTCACTC
Dual_P5_BC_19	AATGATACGGCGACCACCGAGATCTACACTGACTGCGACACT CTTTCCGATCTGGAGCTGTCGTTCACTC
Dual_P5_BC_20	AATGATACGGCGACCACCGAGATCTACACTGCATGAGACACT CTTTCCGATCTGGAGCTGTCGTTCACTC
Name	Sequence
Full_RP_BC_1	CAAGCAGAAGACGGCATACGAGATGTACGAGTGTGACTGGAG TTCAGACGTGTGCTCTTCCGATCT

Full_RP_BC_2	CAAGCAGAAGACGGCATACGAGATTAGCTCATGTGACTGGAGTTCAGACGTGTGCTCTTCCGATCT
Full_RP_BC_3	CAAGCAGAAGACGGCATACGAGATGCTAGTATGTGACTGGAGTTCAGACGTGTGCTCTTCCGATCT
Full_RP_BC_4	CAAGCAGAAGACGGCATACGAGATCATGCTGTGTGACTGGAGTTCAGACGTGTGCTCTTCCGATCT
Full_RP_BC_5	CAAGCAGAAGACGGCATACGAGATACGTGATGGTGACTGGAGTTCAGACGTGTGCTCTTCCGATCT
Full_RP_BC_6	CAAGCAGAAGACGGCATACGAGATCGATACTAGTGACTGGAGTTCAGACGTGTGCTCTTCCGATCT
Full_RP_BC_7	CAAGCAGAAGACGGCATACGAGATAGCTCAGAGTGACTGGAGTTCAGACGTGTGCTCTTCCGATCT
Full_RP_BC_8	CAAGCAGAAGACGGCATACGAGATGACTGTGCGTGACTGGAGTTCAGACGTGTGCTCTTCCGATCT
Full_RP_BC_9	CAAGCAGAAGACGGCATACGAGATTCAGTCTCGTGACTGGAGTTCAGACGTGTGCTCTTCCGATCT
Full_RP_BC_10	CAAGCAGAAGACGGCATACGAGATCATGCACAGTGACTGGAGTTCAGACGTGTGCTCTTCCGATCT
Full_RP_BC_11	CAAGCAGAAGACGGCATACGAGATCTAGCGCTGTGACTGGAGTTCAGACGTGTGCTCTTCCGATCT
Full_RP_BC_12	CAAGCAGAAGACGGCATACGAGATTACGTGTAGTGACTGGAGTTCAGACGTGTGCTCTTCCGATCT
Full_RP_BC_13	CAAGCAGAAGACGGCATACGAGATTGCATATCGTGACTGGAGTTCAGACGTGTGCTCTTCCGATCT
Full_RP_BC_14	CAAGCAGAAGACGGCATACGAGATCTGACACTGTGACTGGAGTTCAGACGTGTGCTCTTCCGATCT
Full_RP_BC_15	CAAGCAGAAGACGGCATACGAGATAGCTACACGTGACTGGAGTTCAGACGTGTGCTCTTCCGATCT
Full_RP_BC_16	CAAGCAGAAGACGGCATACGAGATTACGTAGGGTGACTGGAGTTCAGACGTGTGCTCTTCCGATCT
Full_RP_BC_17	CAAGCAGAAGACGGCATACGAGATGTCAACTGGTGACTGGAGTTCAGACGTGTGCTCTTCCGATCT
Full_RP_BC_18	CAAGCAGAAGACGGCATACGAGATGCATTAGCGTGACTGGAGTTCAGACGTGTGCTCTTCCGATCT
Full_RP_BC_19	CAAGCAGAAGACGGCATACGAGATGCTAGCCGGTGACTGGAGTTCAGACGTGTGCTCTTCCGATCT
Full_RP_BC_20	CAAGCAGAAGACGGCATACGAGATATGCCGTAGTGACTGGAGTTCAGACGTGTGCTCTTCCGATCT
Name	Sequence
i7_SP	GATCGGAAGAGCACACGTCTGAACTCCAGTCAC
i5_SP	GAGTGAACGACAGCTCCAGATCGGAAAGAGTGT
Custom_Read1_SP	ACACTCTTTCCGATCTGGAGCTGTCGTTCACTC

Table 4. List of oligonucleotides used in cloning, genotype and RT-PCR

Name	Sequence
SALK-051322_LP	CAGAAAAGCTGATGCTTCCAC
SALK-051322_RP	CAGGCTAGCAAGCTGTACGAG
SALK 110826 LP	GCATTTGTTTGTTTCCCTCTG
SALK 110826 RP	GATTGGGACTAGCAGGAATCC
SALK 066042 LP	ACCGTTCTGCTCCTTCTCTTC
SALK 066042 RP	TTGTAATCATTCCAAGCTGCC
SALK_024424_LP	CTTCTTCATTCTTGTGCTCCG
SALK_024424_RP	TGAAGAGAACAGCATTCCAGG
SALK 0142980 LP	TAATTGCAATGCTTGCTCATG
SALK 0142980 RP	TTTGAATTTTGTCAGCCCAAG
SALK 029120 LP	TAAACGGGTTTTGTTTCATGC
SALK 029120 RP	TCGAAAATGGAACACGAGATC
SALK 058074 LP	TGCTAAAATCTCAATAGTTGGAGC
SALK 058074 RP	TGTTCAAAGCCTTTGTGGAAC
SALK 029120 LP	CAAACGGGTTTTGTTTCATGC
SALK 029120 RP	TCGAAAATGGAACACGAGATC
Tip41-Like-R-q	GGATACCCTTTCGCAGATAGAGAC
Tip41-Like-F-q	GCGATTTTGGCTGAGAGTTGAT
LBb-1 SALK	GCGTGGACCGCTTGCTGCAACT
PR1-R_QRT	CCACCATTGTTACACCTCACTTT
PR1-F_QRT	AAAACTTAGCCTGGGGTAGCGG
PR2-R_QRT	TGTAAAGAGCCACAACGTCC
PR2-F_QRT	ATCAAGGAGCTTAGCCTCAC
PR2_SMQ_QT_R	AAAATCACAAGCTTAGGGTAGAAA
PR2_QT_F	AACACAAATCATGCATCTAACCAG
PR5-R_QRT	GAAGCACCTGGAGTCAATTC
PR5-F_QRT	CTCTTCCTCGTGTTCATCAC
PR5-F_q New	CGGCATTGCTGTTATGGC
PR5-R_q New	CTGTCGGGAAGCACCTGGAG
pER-HA-For	GTTACGTACATGTACCTTATGA
pER-HA-Rev	TTAATTAAGACGTCTGTACACC
CRT1-1680-RC	CTGCAGGTGGTTGTGGGTTGA
CRT1-940	TTGCACGCTAAAACATTGGAA
SAIL_893_B06-LP	TTGCAGTTTGGAACCAAAATC
SAIL_893_B06-RP	AGGATATACGGCTCCGAGATG
pP6 2nd new Forward	GATCCGGCCCGTCCGGC
pP6 2nd new Reverse	CATGGCCGGACGGGCCG
pER8 F_NEW	AATATGCTCGACTCTAGGATCTTC
pET28a R	GCTAGTTATTGCTCAGCGGT
pET28a F	TTAATACGACTCACTATA
pET28-seq-R	GATATAGTTCCTCCTTTCAGCAA

pET28-seq-F	GGCAGCCATATGGCTAGCATGACT
MED9-F-internal-seq	TGTGATCGTGCTCTTACTCTTTTG
MED9-R-internal-seq	AACCACATTCTCTTTATTAT
MED9 Nterm F	GGCCGGACGGGCCATGGATCAATTCTCAGGAGGAGG A
MED9 Nterm R	GGCCCCAGTGGCCTTACGTCTGTTGCGGCGGAGGTG ATTG
MED9 Cterm F	GGCCGGACGGGCCATGGTTCACACGCCTCAATCTAT G
MED9 Cterm R	GGCCCCAGTGGCCCTAATGCTCCATTGTCACAATCTC
SMC1 coIP 1-345 For	GGCGCGCCATGCCTGCGATACAATCCCC
SMC1 coIP 1-345 Rev	GGCGCGCCTTCAATTTCTTTGGAATGCT
SMC1 coIP 346-959 For	GGCGCGCCATGCAGATGCAGAAAAGCATTAA
SMC1 coIP 346-959 Rev	GGCGCGCCTTCGAGCTCACACTTCTCAG
SMC1 coIP 960-1218 For	GGCGCGCCATGCATATTACCCTTCCTGTCTT
SMC1 coIP 960-1218 Rev	GGCGCGCCCGATTCTTGGTAGTTCCTAA
At3G47460_SMC2_F	GGCCGCAGGGGCCATGCATATAAAGGAGATATG
At5G48600_SMC3_F	GGCCGCAGGGGCCATGGAGGAAGATGAGCCAATGG G
At2G27170_SMC3_F	GGCCGCAGGGGCCATGAATTTATTGGAGAGTGCTGG
At5G62410_SMC4_F	GGCCGCAGGGGCCATGCTGCGAGTGTGAGTGGA
At5G15920_SMC5_F	GGCCGCAGGGGCCATGTCTGAACGTCGTGCTAAGC
At5G07660_SMC6A _F	GGCCGCAGGGGCCATGGATGAACATGGCGACCAT
At5G61460_SMC6B _F	GGCCGCAGGGGCCATGGTAAAATCTGGTGCTCGAGC CA
At3G49250_DMS3_F	GGCCGCAGGGGCCATGTATCCGACTGGTCAACAGAT
At3G47460_SMC2_ R	GGCCCCAGTGGCCTTAGCTCTGTTTTGTTACTGTCC
At5G48600_SMC3_ R	GGCCCCAGTGGCCCTAAGCAGGAGTTTTCTGACAAA
At2G27170_SMC3_ R	GGCCCCAGTGGCCTCAGGTATCGTGGGACTGATCTTT C
At5G62410_SMC4_ R	GGCCCCAGTGGCCTCACTTGGTCTGCTTTGTTACTG
At5G15920_SMC5_ R	GGCCCCAGTGGCCTTAGGAACATTGACTAGCTTCGG
At5G07660_SMC6A _R	GGCCCCAGTGGCCTCAAGAACGTGGAGCAGCCAT

At5G61460_SMC6B_R	GGCCCCAGTGGCCTCAAGAACGAGGAGCAGCCAT
At3G49250_DMS3_R	GGCCCCAGTGGCCTCATCTGGGTGTGTTCATTGGC
MED9_pET28a_F	GGATCCATGGATCAATTCTCAGGAG
MED9_pET28a_R	GTCGACCTAATGCTCCATTGTCACA
HA for MED9-F	TCCGTTACGTACATGTATCCTT
HA for MED9-R	ATAGGCCCGGGAAGACTAGCA
Flag for MED9-F	TCTACGTACGAGATGGACTACA
Flag for MED9-R	ACTAGGCCCGGGCTCGACTTT
SMC2_701~1300 (For)	GTGTCGCTTTTGAGTATGTGC
SMC2_1201~1800	CGTGATGCAAAGATTTCTGTT
SMC2_1701~2300	GTATCAGCACAACTTTTGTAAAG
SMC2_2201~2800	TATGCTTCTCAACAAGTTTG
pDEST DB F	GCCGTCACAGATAGATTGGCTTCAGTGG
pDEST DB R	GAGTAACTCTTTCCTGTAGGTCAGG
MORC1_pENTR_For	CACCCCAATTTGTGGTTTCAATGTC
MORC1_pENTR_Rev	AACTTGTTGCATCTCCTTCTT
pPZP.h-MED9-Rev	AGCGCGAAACTAGGATAAA
pDEST-AD-F	CACAACCAATTGCCTCCTCTAACG
pDEST-AD-R	CTTACTTAGAGCTCGACGTCTTAC

LITERATURE CITED

Aeschbacher R, Schrott, M., Potrykus, I. And Saul, M. , 1991. Isolation and molecular characterization of PosF21, an Arabidopsis thaliana gene which shows characteristics of a b-Zip class transcription factor. *The Plant Journal* **1**, 303-16.

Al-Sady B, Ni W, Kircher S, Schäfer E, Quail PH, 2006. Photoactivated phytochrome induces rapid PIF3 phosphorylation prior to proteasome-mediated degradation. *Mol Cell* **23**, 439-46.

Aldea M, Hamilton JG, Resti JP, Zangerl AR, Berenbaum MR, Delucia EH, 2005. Indirect effects of insect herbivory on leaf gas exchange in soybean. *Plant Cell and Environment* **28**, 402-11.

Alexa A, Rahnenführer J, 2009. Gene set enrichment analysis with topGO. *Bioconductor Improv* **27**.

Allen BL, Taatjes DJ, 2015b. The Mediator complex: a central integrator of transcription. *Nature reviews. Molecular cell biology* **16**, 155-66.

An C, Mou Z, 2013b. The function of the Mediator complex in plant immunity. *Plant Signal Behav* **8**, e23182.

Andrews S, 2010. FastQC: a quality control tool for high throughput sequence data. In.: Babraham Bioinformatics, Babraham Institute, Cambridge, United Kingdom.

Asai T, Tena G, Plotnikova J*, et al.*, 2002. MAP kinase signalling cascade in Arabidopsis innate immunity. *Nature* **415**, 977.

Ausubel FM, 2005. Are innate immune signaling pathways in plants and animals conserved? *Nature Immunology* **6**, 973.

Backstrom S, Elfving N, Nilsson R, Wingsle G, Bjorklund S, 2007. Purification of a plant mediator from Arabidopsis thaliana identifies PFT1 as the Med25 subunit. *Mol Cell* **26**, 717-29.

Bailey TL, Boden M, Buske FA*, et al.*, 2009. MEME Suite: tools for motif discovery and searching. *Nucleic Acids Res* **37**, W202-W8.

Bilgin DD, Zavala JA, Zhu J, Clough SJ, Ort DR, Delucia EH, 2010. Biotic stress globally downregulates photosynthesis genes. *Plant Cell Environ* **33**, 1597-613.

Black JC, Choi JE, Lombardo SR, Carey M, 2006. A mechanism for coordinating chromatin modification and preinitiation complex assembly. *Mol Cell* **23**, 809-18.

Bonawitz ND, Kim JI, Tobimatsu Y*, et al.*, 2014. Disruption of Mediator rescues the stunted growth of a lignin-deficient Arabidopsis mutant. *Nature* **509**, 376.

Bordiya Y, Zheng Y, Nam J-C*, et al.*, 2016a. Pathogen Infection and MORC Proteins Affect Chromatin Accessibility of Transposable Elements and Expression of Their Proximal Genes in Arabidopsis. *Molecular Plant-Microbe Interactions* **29**, 674-87.

Borges LL, Santana FA, Castro ISL*, et al.*, 2013. Differentially expressed proteins during an incompatible interaction between common bean and the fungus Pseudocercospora griseola. *Molecular Breeding* **32**, 933-42.

Borggrefe T, Yue X, 2011. Interactions between subunits of the Mediator complex with gene-specific transcription factors. *Semin Cell Dev Biol* **22**, 759-68.

Brabbs TR, He Z, Hogg K*, et al.*, 2013. The stochastic silencing phenotype of Arabidopsis morc6 mutants reveals a role in efficient RNA-directed DNA methylation. *Plant J* **75**, 836-46.

Buendía-Monreal M, Gillmor CS, 2016. Mediator: A key regulator of plant development. *Developmental Biology* **419**, 7-18.

Burdon JJ, Thrall PH, 2003. The fitness costs to plants of resistance to pathogens. *Genome biology* **4**, 227.

Caillaud M-C, Asai S, Rallapalli G, Piquerez S, Fabro G, Jones JD, 2013. A downy mildew effector attenuates salicylic acid–triggered immunity in Arabidopsis by interacting with the host mediator complex. *PLoS biology* **11**, e1001732.

Campos ML, Yoshida Y, Major IT*, et al.*, 2016. Rewiring of jasmonate and phytochrome B signalling uncouples plant growth-defense tradeoffs. *Nat Commun* **7**, 12570.

Canet JV, Dobon A, Tornero P, 2012. Non-recognition-of-BTH4, an Arabidopsis mediator subunit homolog, is necessary for development and response to salicylic acid. *Plant Cell* **24**, 4220-35.

Chen R, Jiang H, Li L*, et al.*, 2012. The Arabidopsis mediator subunit MED25 differentially regulates jasmonate and abscisic acid signaling through interacting with the MYC2 and ABI5 transcription factors. *The Plant Cell* **24**, 2898-916.

Chen Y, Pang Q, Dai S, Wang Y, Chen S, Yan X, 2011. Proteomic identification of differentially expressed proteins in Arabidopsis in response to methyl jasmonate. *J Plant Physiol* **168**, 995-1008.

Cheng CY, Krishnakumar V, Chan AP, Thibaud-Nissen F, Schobel S, Town CD, 2017. Araport11: a complete reannotation of the Arabidopsis thaliana reference genome. *The Plant Journal* **89**, 789-804.

Chisholm ST, Coaker G, Day B, Staskawicz BJ, 2006. Host-microbe interactions: shaping the evolution of the plant immune response. *Cell* **124**, 803-14.

Conaway RC, Conaway JW, 2011. Origins and activity of the Mediator complex. *Seminars in Cell & Developmental Biology* **22**, 729-34.

Da Cunha L, Mcfall AJ, Mackey D, 2006. Innate immunity in plants: a continuum of layered defenses. *Microbes Infect* **8**, 1372-81.

Daviere JM, Achard P, 2013. Gibberellin signaling in plants. *Development* **140**, 1147-51.

Dempsey DA, Pathirana MS, Wobbe KK, Klessig DF, 1997. Identification of an Arabidopsis locus required for resistance to turnip crinkle virus. *Plant Journal* **11**, 301-11.

Dhawan R, Luo H, Foerster AM*, et al.*, 2009. HISTONE MONOUBIQUITINATION1 interacts with a subunit of the mediator complex and regulates defense against necrotrophic fungal pathogens in Arabidopsis. *Plant Cell* **21**, 1000-19.

Dotson MR, Yuan CX, Roeder RG*, et al.*, 2000. Structural organization of yeast and mammalian mediator complexes. *Proc Natl Acad Sci U S A* **97**, 14307-10.

Fallath T, Kidd BN, Stiller J*, et al.*, 2017. MEDIATOR18 and MEDIATOR20 confer susceptibility to Fusarium oxysporum in Arabidopsis thaliana. *PLoS ONE* **12**, e0176022.

Fan J, Crooks C, Lamb C, 2008. High-throughput quantitative luminescence assay of the growth in planta of Pseudomonas syringae chromosomally tagged with Photorhabdus luminescens luxCDABE. *Plant J* **53**, 393-9.

Galvao VC, Fankhauser C, 2015. Sensing the light environment in plants: photoreceptors and early signaling steps. *Curr Opin Neurobiol* **34**, 46-53.

Gangappa SN, Berriri S, Kumar SV, 2017. PIF4 Coordinates Thermosensory Growth and Immunity in Arabidopsis. *Curr Biol* **27**, 243-9.

Gohre V, Jones AM, Sklenar J, Robatzek S, Weber AP, 2012. Molecular crosstalk between PAMP-triggered immunity and photosynthesis. *Mol Plant Microbe Interact* **25**, 1083-92.

Guo J, Pang Q, Wang L, Yu P, Li N, Yan X, 2012. Proteomic identification of MYC2-dependent jasmonate-regulated proteins in Arabidopsis thaliana. *Proteome Sci* **10**, 57.

Hammond-Kosack KE, Jones JD, 1996. Resistance gene-dependent plant defense responses. *The Plant Cell* **8**, 1773-91.

Hirano M, Hirano T, 2002. Hinge-mediated dimerization of SMC protein is essential for its dynamic interaction with DNA. *EMBO J* **21**, 5733-44.

Hoppmann V, Thorstensen T, Kristiansen PE*, et al.*, 2011. The CW domain, a new histone recognition module in chromatin proteins. *The EMBO Journal* **30**, 1939-52.

Horton JR, Elgar SJ, Khan SI, Zhang X, Wade PA, Cheng X, 2007. Structure of the SANT domain from the Xenopus chromatin remodeling factor ISWI. *Proteins* **67**, 1198-202.

Hsieh M, Tintut Y, Gralla JD, 1994. Functional roles for the glutamines within the glutamine-rich region of the transcription factor sigma 54. *J Biol Chem* **269**, 373-8.

Huot B, Yao J, Montgomery BL, He SY, 2014. Growth-defense tradeoffs in plants: a balancing act to optimize fitness. *Mol Plant* **7**, 1267-87.

Huq E, Quail PH, 2002. PIF4, a phytochrome-interacting bHLH factor, functions as a negative regulator of phytochrome B signaling in Arabidopsis. *EMBO J* **21**, 2441-50.

Imura Y, Kobayashi Y, Yamamoto S*, et al.*, 2012. CRYPTIC PRECOCIOUS/MED12 is a Novel Flowering Regulator with Multiple Target Steps in Arabidopsis. *Plant and Cell Physiology* **53**, 287-303.

Ishiga Y, Uppalapati SR, Ishiga T, Elavarthi S, Martin B, Bender CL, 2009. The phytotoxin coronatine induces light-dependent reactive oxygen species in tomato seedlings. *New Phytol* **181**, 147-60.

Iyer LM, Abhiman S, Aravind L, 2008. MutL homologs in restriction-modification systems and the origin of eukaryotic MORC ATPases. *Biology Direct* **3**, 8.

Jakoby M, Weisshaar B, Droge-Laser W*, et al.*, 2002. bZIP transcription factors in Arabidopsis. *Trends Plant Sci* **7**, 106-11.

Jones JD, Dangl JL, 2006. The plant immune system. *Nature* **444**, 323-9.

Jung C, Lyou SH, Yeu S*, et al.*, 2007. Microarray-based screening of jasmonate-responsive genes in Arabidopsis thaliana. *Plant Cell Rep* **26**, 1053-63.

Kagey MH, Newman JJ, Bilodeau S*, et al.*, 2010. Mediator and cohesin connect gene expression and chromatin architecture. *Nature* **467**, 430-5.

Kang HG, Klessig DF, 2005. Salicylic acid-inducible Arabidopsis CK2-like activity phosphorylates TGA2. *Plant Molecular Biology* **57**, 541-57.

Kang HG, Hyong WC, Von Einem S*, et al.*, 2012. CRT1 is a nuclear-translocated MORC endonuclease that participates in multiple levels of plant immunity. *Nat Commun* **3**, 1297.

Kang HG, Kuhl JC, Kachroo P, Klessig DF, 2008. CRT1, an Arabidopsis ATPase that interacts with diverse resistance proteins and modulates disease resistance to turnip crinkle virus. *Cell Host Microbe* **3**, 48-57.

Kang HG, Oh CS, Sato M*, et al.*, 2010. Endosome-associated CRT1 functions early in resistance gene-mediated defense signaling in Arabidopsis and tobacco. *Plant Cell* **22**, 918-36.

Karasov TL, Chae E, Herman JJ, Bergelson J, 2017. Mechanisms to Mitigate the Trade-Off between Growth and Defense. *Plant Cell* **29**, 666-80.

Karim S, Holmström K-O, Mandal A*, et al.*, 2007. AtPTR3, a wound-induced peptide transporter needed for defence against virulent bacterial pathogens in Arabidopsis. *Planta* **225**, 1431-45.

Kelleher RJ, Flanagan PM, Kornberg RD, 1990. A novel mediator between activator proteins and the RNA polymerase II transcription apparatus. *Cell* **61**, 1209-15.

Kerchev PI, Fenton B, Foyer CH, Hancock RD, 2012. Plant responses to insect herbivory: interactions between photosynthesis, reactive oxygen species and hormonal signalling pathways. *Plant Cell Environ* **35**, 441-53.

Kharshiing E, Sinha SP, 2016. Deficiency in phytochrome A alters photosynthetic activity, leaf starch metabolism and shoot biomass production in tomato. *J Photochem Photobiol B* **165**, 157-62.

Kidd BN, Cahill DM, Manners JM, Schenk PM, Kazan K, 2011. Diverse roles of the Mediator complex in plants. *Seminars in Cell & Developmental Biology* **22**, 741-8.

Kidd BN, Edgar CI, Kumar KK*, et al.*, 2009. The mediator complex subunit PFT1 is a key regulator of jasmonate-dependent defense in Arabidopsis. *Plant Cell* **21**, 2237-52.

Kim D, Paggi JM, Park C, Bennett C, Salzberg SL, 2019a. Graph-based genome alignment and genotyping with HISAT2 and HISAT-genotype. *Nature biotechnology* **37**, 907-15.

Kim H, Yen L, Wongpalee SP*, et al.*, 2019b. The Gene-Silencing Protein MORC-1 Topologically Entraps DNA and Forms Multimeric Assemblies to Cause DNA Compaction. *Mol Cell* **75**, 700-10 e6.

Koiwa H, Barb AW, Xiong L*, et al.*, 2002. C-terminal domain phosphatase-like family members (AtCPLs) differentially regulate Arabidopsis thaliana abiotic stress signaling, growth, and development. *Proceedings of the National Academy of Sciences of the United States of America* **99**, 10893-8.

Krahmer J, Ganpudi A, Abbas A, Romanowski A, Halliday KJ, 2018. Phytochrome, Carbon Sensing, Metabolism, and Plant Growth Plasticity. *Plant Physiol* **176**, 1039-48.

Larivière L, Geiger S, Hoeppner S, Röther S, Sträßer K, Cramer P, 2006. Structure and TBP binding of the Mediator head subcomplex Med8–Med18–Med20. *Nature Structural &Amp; Molecular Biology* **13**, 895.

Leivar P, Monte E, 2014. PIFs: systems integrators in plant development. *Plant Cell* **26**, 56-78.

Leivar P, Monte E, Al-Sady B*, et al.*, 2008. The Arabidopsis phytochrome-interacting factor PIF7, together with PIF3 and PIF4, regulates responses to prolonged red light by modulating phyB levels. *Plant Cell* **20**, 337-52.

Leivar P, Quail PH, 2011a. PIFs: pivotal components in a cellular signaling hub. *Trends Plant Sci* **16**, 19-28.

Leivar P, Quail PH, 2011b. PIFs: pivotal components in a cellular signaling hub. *Trends in Plant Science* **16**, 19-28.

Lewis LA, Polanski K, De Torres-Zabala M*, et al.*, 2015. Transcriptional Dynamics Driving MAMP-Triggered Immunity and Pathogen Effector-Mediated Immunosuppression in Arabidopsis Leaves Following Infection with Pseudomonas syringae pv tomato DC3000. *Plant Cell* **27**, 3038-64.

Li H, Handsaker B, Wysoker A*, et al.*, 2009. The sequence alignment/map format and SAMtools. *Bioinformatics* **25**, 2078-9.

Li Y, Yang Y, Hu Y*, et al.*, 2019. DELLA and EDS1 Form a Feedback Regulatory Module to Fine-Tune Plant Growth–Defense Tradeoff in Arabidopsis. *Molecular Plant* **12**, 1485-98.

Lindeberg M, Cunnac S, Collmer A, 2012. Pseudomonas syringae type III effector repertoires: last words in endless arguments. *Trends Microbiol* **20**, 199-208.

Liu ZW, Shao CR, Zhang CJ*, et al.*, 2014. The SET domain proteins SUVH2 and SUVH9 are required for Pol V occupancy at RNA-directed DNA methylation loci. *PLoS Genet* **10**, e1003948.

Liu ZW, Zhou JX, Huang HW*, et al.*, 2016. Two Components of the RNA-Directed DNA Methylation Pathway Associate with MORC6 and Silence Loci Targeted by MORC6 in Arabidopsis. *PLoS Genet* **12**, e1006026.

Lorkovic ZJ, Naumann U, Matzke AJ, Matzke M, 2012. Involvement of a GHKL ATPase in RNA-directed DNA methylation in Arabidopsis thaliana. *Curr Biol* **22**, 933-8.

Maleck K, Levine A, Eulgem T*, et al.*, 2000. The transcriptome of Arabidopsis thaliana during systemic acquired resistance. *Nature genetics* **26**, 403-10.

Manohar M, Choi HW, Manosalva P, Austin CA, Peters JE, Klessig DF, 2017. Plant and Human MORC Proteins Have DNA-Modifying Activities Similar to Type II Topoisomerases, but Require One or More Additional Factors for Full Activity. *Mol Plant Microbe Interact* **30**, 87-100.

Manosalva PM, Manohar M, Kogel KH, Kang HG, Klessig D, 2015. The GHKL ATPase MORC1 modulates species-specific plant immunity in Solanaceae. *Molecular plant-microbe interactions : MPMI*.

Martin M, 2011. Cutadapt removes adapter sequences from high-throughput sequencing reads. *EMBnet. journal* **17**, 10-2.

Menke FL, Kang HG, Chen Z, Park JM, Kumar D, Klessig DF, 2005. Tobacco transcription factor WRKY1 is phosphorylated by the MAP kinase SIPK and mediates HR-like cell death in tobacco. *Molecular Plant-Microbe Interactions* **18**, 1027-34.

Meyer KD, Donner AJ, Knuesel MT, York AG, Espinosa JM, Taatjes DJ, 2008. Cooperative activity of cdk8 and GCN5L within Mediator directs tandem phosphoacetylation of histone H3. *Embo J* **27**, 1447-57.

Mine A, Seyfferth C, Kracher B, Berens ML, Becker D, Tsuda K, 2018. The Defense Phytohormone Signaling Network Enables Rapid, High-Amplitude Transcriptional Reprogramming during Effector-Triggered Immunity. *Plant Cell* **30**, 1199-219.

Moissiard G, Cokus SJ, Cary J*, et al.*, 2012b. MORC Family ATPases Required for Heterochromatin Condensation and Gene Silencing. *Science* **336**, 1448-51.

Nabity PD, Zavala JA, Delucia EH, 2009. Indirect suppression of photosynthesis on individual leaves by arthropod herbivory. *Ann Bot* **103**, 655-63.

Navarro L, Bari R, Achard P*, et al.*, 2008. DELLAs control plant immune responses by modulating the balance of jasmonic acid and salicylic acid signaling. *Curr Biol* **18**, 650-5.

Nicolau M, Picault N, Descombin J*, et al.*, 2020. The plant mobile domain proteins MAIN and MAIL1 interact with the phosphatase PP7L to regulate gene expression and silence transposable elements in Arabidopsis thaliana. *PLoS Genet* **16**, e1008324.

Paik I, Kathare PK, Kim JI, Huq E, 2017. Expanding Roles of PIFs in Signal Integration from Multiple Processes. *Mol Plant* **10**, 1035-46.

Park E, Kim Y, Choi G, 2018. Phytochrome B Requires PIF Degradation and Sequestration to Induce Light Responses across a Wide Range of Light Conditions. *Plant Cell* **30**, 1277-92.

Park E, Park J, Kim J, Nagatani A, Lagarias JC, Choi G, 2012. Phytochrome B inhibits binding of phytochrome-interacting factors to their target promoters. *Plant J* **72**, 537-46.

Pertea M, Pertea GM, Antonescu CM, Chang T-C, Mendell JT, Salzberg SL, 2015. StringTie enables improved reconstruction of a transcriptome from RNA-seq reads. *Nature biotechnology* **33**, 290-5.

Phan NQ, Kim SJ, Bassham DC, 2008. Overexpression of Arabidopsis Sorting Nexin AtSNX2b Inhibits Endocytic Trafficking to the Vacuole. *Mol Plant* **1**, 961-76.

Raya-González J, Ortiz-Castro R, Ruíz-Herrera LF, Kazan K, López-Bucio J, 2014. PHYTOCHROME AND FLOWERING TIME1/MEDIATOR25 regulates lateral root formation via auxin signaling in Arabidopsis. *Plant Physiol* **165**, 880-94.

Samanta S, Thakur JK, 2015b. Importance of Mediator complex in the regulation and integration of diverse signaling pathways in plants. *Front Plant Sci* **6**, 757.

Samanta S, Thakur JK, 2015c. Role of Plant Mediator Complex in Stress Response. In: Pandey GK, ed. *Elucidation of Abiotic Stress Signaling in Plants: Functional Genomics Perspectives, Volume 2.* New York, NY: Springer New York, 3-28.

Schneider CA, Rasband WS, Eliceiri KW, 2012. NIH Image to ImageJ: 25 years of image analysis. *Nature methods* **9**, 671-5.

Schubert V, 2009. SMC proteins and their multiple functions in higher plants. *Cytogenetic and Genome Research* **124**, 202-14.

Schultz J, Milpetz F, Bork P, Ponting CP, 1998. SMART, a simple modular architecture research tool: identification of signaling domains. *Proceedings of the National Academy of Sciences* **95**, 5857-64.

Seguela-Arnaud M, Smith C, Uribe MC*, et al.*, 2015. The Mediator complex subunits MED25/PFT1 and MED8 are required for transcriptional responses to changes in cell wall arabinose composition and glucose treatment in Arabidopsis thaliana. *BMC plant biology* **15**, 1-13.

Shah J, Tsui F, Klessig DF, 1997. Characterization of a salicylic acid-insensitive mutant (*sai1*) of *Arabidopsis thaliana*, identified in a selective screen utilizing the SA-inducible expression of the *tms2* gene. *Molecular Plant-Microbe Interactions* **10**, 69-78.

Sheerin DJ, Menon C, Zur Oven-Krockhaus S*, et al.*, 2015. Light-activated phytochrome A and B interact with members of the SPA family to promote photomorphogenesis in Arabidopsis by reorganizing the COP1/SPA complex. *Plant Cell* **27**, 189-201.

Shin A-Y, Han Y-J, Baek A*, et al.*, 2016. Evidence that phytochrome functions as a protein kinase in plant light signalling. *Nat Commun* **7**, 1-13.

Spoel SH, Dong X, 2012. How do plants achieve immunity? Defence without specialized immune cells. *Nature reviews immunology* **12**, 89-100.

Sugano S, Jiang CJ, Miyazawa S*, et al.*, 2010. Role of OsNPR1 in rice defense program as revealed by genome-wide expression analysis. *Plant Mol Biol* **74**, 549-62.

Sun J, Chen Q, Qi L*, et al.*, 2011. Jasmonate modulates endocytosis and plasma membrane accumulation of the Arabidopsis PIN2 protein. *New Phytol* **191**, 360-75.

Takahashi H, Kasahara K, Kokubo T, 2009. Saccharomyces cerevisiae Med9 comprises two functionally distinct domains that play different roles in transcriptional regulation. *Genes Cells* **14**, 53-67.

Tao Y, Xie Z, Chen W*, et al.*, 2003. Quantitative nature of Arabidopsis responses during compatible and incompatible interactions with the bacterial pathogen *Pseudomonas syringae*. *Plant Cell* **15**, 317-30.

Tian D, Traw MB, Chen JQ, Kreitman M, Bergelson J, 2003. Fitness costs of R-gene-mediated resistance in Arabidopsis thaliana. *Nature* **423**, 74-7.

Tsuda K, Sato M, Stoddard T, Glazebrook J, Katagiri F, 2009. Network properties of robust immunity in plants. *PLoS Genet* **5**, e1000772.

Van Hulten M, Pelser M, Van Loon LC, Pieterse CM, Ton J, 2006. Costs and benefits of priming for defense in Arabidopsis. *Proceedings of the National Academy of Sciences of the United States of America* **103**, 5602-7.

Verboon JM, Sugumar B, Parkhurst SM, 2015. Wiskott-Aldrich syndrome proteins in the nucleus: aWASH with possibilities. *Nucleus* **6**, 349-59.

Wang C, Yao J, Du X*, et al.*, 2015. The Arabidopsis Mediator Complex Subunit16 Is a Key Component of Basal Resistance against the Necrotrophic Fungal Pathogen Sclerotinia sclerotiorum. *Plant Physiol* **169**, 856-72.

Weiser NE, Yang DX, Feng S*, et al.*, 2017. MORC-1 Integrates Nuclear RNAi and Transgenerational Chromatin Architecture to Promote Germline Immortality. *Dev Cell* **41**, 408-23 e7.

Xiang S, Wu S, Zhang H*, et al.*, 2020. The PIFs Redundantly Control Plant Defense Response against Botrytis cinerea in Arabidopsis. *Plants (Basel)* **9**.

Yang D, Seaton DD, Krahmer J, Halliday KJ, 2016. Photoreceptor effects on plant biomass, resource allocation, and metabolic state. *Proc Natl Acad Sci U S A* **113**, 7667-72.

Yang Y, Li L, Qu LJ, 2015. Plant Mediator complex and its critical functions in transcription regulation. *J Integr Plant Biol*.

Zhang X, Wang C, Zhang Y, Sun Y, Mou Z, 2012. The Arabidopsis mediator complex subunit16 positively regulates salicylate-mediated systemic acquired resistance and jasmonate/ethylene-induced defense pathways. *Plant Cell* **24**, 4294-309.

Zhang X, Yao J, Zhang Y, Sun Y, Mou Z, 2013. The Arabidopsis Mediator complex subunits MED14/SWP and MED16/SFR6/IEN1 differentially regulate defense gene expression in plant immune responses. *The Plant Journal* **75**, 484-97.

Zipfel C, Felix G, 2005. Plants and animals: a different taste for microbes? *Curr Opin Plant Biol* **8**, 353-60.

Zou J, Rodriguez-Zas S, Aldea M*, et al.*, 2005. Expression profiling soybean response to Pseudomonas syringae reveals new defense-related genes and rapid HR-specific downregulation of photosynthesis. *Mol Plant Microbe Interact* **18**, 1161-74.